University of Stavanger

Faculty of Science and Technology

MASTER'S THESIS

Study program/ Specialization: Petroleum Engineeringy/ Reservoir Engineering	Spring Semester 2016 Open
Writer: Tewodros Sebsibe Worku	..... Writer's Signature

Faculty Supervisor
Prof. Dag Chun Standnes

Second Supervisor
-

Title of Thesis

Numerical simulation of Spontaneous Imbibition of Smart Water into Preferentially oil-wet Carbonate using ECLIPSE 100

Credits (ECTS):
30

Key Words Spontaneous Imbibition Smart Water Wettability Simulation Eclipse	Pages: 73 + Enclosure: 57 Stavanger June 14, 2016

This page is intentionally left blank

Abstract

Spontaneous imbibition (SI) is the main recovery mechanism in low matrix permeability, naturally fractured reservoirs. However, for imbibition to occur, the reservoir rock should be preferentially water-wet. Several studies have indicated that smart water may increase the water-wetness of an oil-wet carbonate reservoirs. Published experimental data suggest that sulfate ion in the injected fluid can alter wetting state of the carbonate from preferentially oil-wet to water-wet.

Numerical and analytical models have been developed to describe SI process in carbonate reservoirs. The suggested models attempt to capture the complex interactions among different phases and species during SI process. In this study, using the already existing surfactant model of ECLIPSE 100 simulator, dynamic effect of adsorption of sulfate on wettability alteration in core scale is modelled. Wettability change option of the surfactant model is employed to capture change in wettability due to adsorption of sulfate ion. Using the procedure of weight factor, wettability of the core shifts dynamically from oil-wet to water-wet conditions proportional to the adsorbed amount of sulfate. Laboratory experiments have been matched with the established procedure.

The result showed that the wettability change option under surfactant model in ECLIPSE 100 is capable of modelling the change in wettability due to adsorption of sulfate ion. The model is able to predict experimental data using the procedure of weight factor. Moreover, a correlation between weight factor and Amott wettability index is established. The basic model that could be used for further investigations or upscaling to field scale is established.

This page is intentionally left blank

Acknowledgments

I am deeply indebted to my supervisor Professor Dag Chun Standnes, who has offered me excellent guidance and encouragement during the course of this thesis. It has been a period of intense learning for me, but would not have been possible without his unreserved support including on weekends and during his holidays.

I would also like to extend my gratitude to Associate Professor Skule Strand for providing me with the experimental data and outstanding suggestions.

Finally, I am thankful to my siblings, friends and classmates for being supportive and understanding.

This page is intentionally left blank

Contents

List of Figures

List of Tables

Nomenclature

Δt	time
δ_{OS}	Oil-Solid Interfacial tension
δ_{WO}	Water-Oil Interfacial tension
δ_{WS}	Water-Solid Interfacial tension
μ	viscosity
θ	Contant Angle
φ	Porosity
C_e	Concentration of solute remaining in the solution
C_{inj}	Injected concentration
$CA(C_{surf})$	he adsorption isotherm as a function of local surfactant concentration in solution
I_O	Amott oil index
I_W	Amott water index
K_f	Freundlich adsorption constant
L_c	Characteristic length
L_O	Length of capillary tube
m_{rock}	Rock mass
P_c	Capillary pressure
P_{cgw}	Gas water capillary pressure
q_e	Amount of solute adsorbed per unit mass of solid at equilibrium

SCN^-	Thiocyanate
t_D	Dimensionless time
AN	Acid Number
EOR	Enhanced Oil Recovery
Eq.	Equation
IFT	Interfacial tension
j(S_w)	Leverett j-function
LSWI	Low salinity water imbibition
MD	Mass density of the rock
OOIP	Original Oil in Place
PORV	Pore volume of the cell
q	Injection rate
SI	Spontaneous Imbibition
USBM	U.S Bureau of Mines

Chapter 1

Introduction

1.1 Background

Oil recovery by spontaneous imbibition of brine into reservoir rock is of special importance in fractured reservoirs. In particular, when the rock matrix has low permeability, spontaneous imbibition has been shown to be a major driving mechanism for oil recovery from fractured water-wet reservoirs [1].

Crain [2] defined *fracture* as a surface along which a loss of cohesion in the rock texture has taken place. It is mechanical breaks in rocks including cracks, discontinuities and openings. Fractures are commonly caused by stress due to tectonic forces, folds and faults exceeding the mechanical strength of the rock. Those are termed natural fractures, as opposed to induced fracture caused by drilling stress or by purposely fracturing reservoir by hydraulic pressure from the surface [2]. Thus, a fractured reservoir is one in which naturally occurring fractures either have or are predicted to have a significant effect on the reservoir fluid flow in the form of increased permeability, increased porosity, and/or increased anisotropy [3].

Fractured reservoirs are more common in carbonate rocks than sandstone rocks. They are characterized by highly permeable fracture and low permeability matrix. Significant amount of global proven reserve (more than 60% of oil and 40% of gas) is contained in fractured carbonate reservoirs. However, the ultimate oil recovery from carbonate reservoirs is generally less than 30%. This is mainly due to rock wettability that ranges from oil-wet to mixed wet, and low matrix permeability coupled with high fracture density. Water injection in these reservoirs results in low recovery due to water channeling in high permeability fractures and bypassing low permeability

matrix [4]. Consequently, several enhanced recovery methods have been suggested to improve oil recovery from carbonate reservoirs by overcoming the high negative capillary pressure that trapped the oil in place.

One of the proposed techniques for improved recovery in fractured carbonate reservoirs is wettability alteration from oil-wet to water wet; thereby promotes positive capillary pressure which in turn results in recovery through spontaneous imbibition into low permeability matrix. Most carbonate reservoirs are preferentially oil-wet. The wettability preference of a reservoir rock reflects the imbibition potential of the reservoir. Water imbibes into matrix block when the reservoir rock is water-wet.

In the presence of high permeability layers or fractures, injection water will tend to flow into the high permeability areas bypassing the low permeability zones. Therefore, the oil located in the low permeability parts would not be displaced. The differential pressure is limited as the result of the injected water prefers flowing in high permeable fracture. Thus, viscous force would be weak for oil production during waterflooding. As a result, spontaneous imbibition would be the main mechanism for oil production in fractured carbonate reservoir compared to viscous displacement [5].

However, spontaneous imbibition can be slow process, and consequently, oil recovery mainly dependent on spontaneous imbibition may be economically impractical. Spontaneous imbibition of water into matrix block and thereby oil recovery can be significantly increased by changing the wettability of the rock.

One of the novel techniques to alter wettability in carbonate reservoir is smart water injection; for example injection of low salinity water spiked with sulfate. Smart water is fundamentally injection water that ionic composition is adjusted in such a way that the crude oil/brine/rock (CBR) equilibrium is changed and results in modification of initial wetting of the rock. As a result, water imbibes into rock matrix faster and is able to displace the oil.

Smart water injection have several advantages compared to other EOR methods [6]. Among others:

- It can achieve higher ultimate oil recovery with minimal investment in current operations; assuming that a water-flooding infrastructure is already in place.
- It can be applied during the early life cycle of the reservoir.

- It is relatively a simple chemical EOR method, which makes it able to be used in conjunction with other EOR methods; for example mobility control processes.

Smart water as EOR fluid has been verified experimentally and there are also good indications that it has huge potential in the field. In sandstone core flood experiment, increases in oil recovery between 5% and 38% OOIP is observed. Incremental oil recovery up to 40% OOIP have been observed for carbonate core flooding experiments [7, 8]. Generally, incremental oil recovery from field tests are lower than core flood experiments. Nevertheless, incremental oil recovery up to 15% OOIP for sandstone has been achieved. For carbonate reservoirs, for example Ekofisk, increase of 50% OOIP is reported and smart water effect is believed to contribute to the total recovery increase observed [9, 10]. The Ekofisk field in the North Sea is a typical example of the success of seawater injection. The reservoir is highly fractured and mixed wet, which pointed against injection of water. However, after injection of SW, the recovery is now estimated to reach 50-55% of OOIP compared to 18% at the very beginning. Figure 1.1 shows tremendous increase in oil production since the start of SW injection in mid 1980s [11].

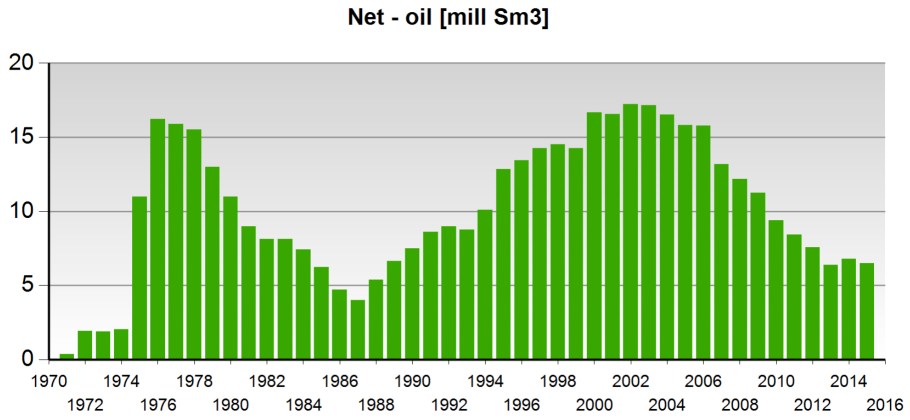

Figure 1.1: *Ekofisk field net oil production chart [12].*

Wettability alteration of the rock from oil wet to water wet has been suggested to be the primary mechanism for increased oil recovery during smart water flooding in carbonates. Core experiments have revealed that water-wetness of the chalk material increased with increasing temperature and concentration of sulphate in the seawater [9].

1.2 Problem Statement

Due to the complexity and uncertainty associated with fractured reservoirs, implementing a simulation and numerical analysis is primarily necessary to investigate the effect of key engineering parameters on ultimate reservoir performance. Yu et al. [13] presented one dimensional model of spontaneous imbibition of seawater (SW) into preferentially oil-wet chalk cores. Two capillary pressures curves, one for water-wet the other for oil-wet, are assumed. Depending on adsorption of sulfate on the rock surface, capillary pressures shifts dynamically from oil-wet to water-wet.

Andersen et al. [14] also suggested mathematical model to describe experimental work that involves measuring capillary pressure with porous disc method using different brines in the system. The model represents brine-dependent co-current spontaneous imbibition. The brine dependence has been expressed by interpolating between relative permeability and capillary pressure between sulfate of *0.0M or 0.37M* concentration. They assumed sulfate is the only wetting agent. The model gives a good match in the water-wet case but there is a significant discrepancy in the oil-wet case.

Brady [15] proposed a model using surface complexion reaction with reaction network relevant for sandstone and carbonates. Surface complexion models allow the charge on oil and reservoir surfaces to be modeled as a function of waterflood chemistry. However, the model doesn't involve multiphase flow and hence dynamic change of wettability can't be modelled.

Recently, Qiao et al. [16] developed a comprehensive mechanistic model for wettability alteration in carbonated due to smart water injection. Their model captures interactions among aqueous species (Ca^{2+}, Mg^{2+}, SO_4^{2-}), crude oil acidity, and solid surface properties. In this model, parameters are categorized into two types based on sensitivity. Type I are those responsible for ultimate recovery and wettability alteration. It includes reaction-equilibrium constants and crude-oil acid number. Type II are rate controlling agents that includes total surface sites of solid and the diffusion coefficient. The authors reported that the model is first of its kind to combine multiphase and multicomponent reactive transport model that explicitly takes into account wettability alteration from these geochemical interactions in carbonate reservoirs.

In spite of several core-scale laboratory researches on wettability alteration [17–19], it seems that more numerical and simulation works are required to understand mechanisms involved in larger-scale operations. However, most of the works have

developed new core scale mathematical model that couples multiphase flow and surface complexion. Generally, most of the developed models utilize Pennsim and Matlab as their simulating tools [13, 15, 20]. One of the advantages of Pennsim is that it is a multicomponent and multiphase simulator. Although these tools have proved acceptable performance on an academic level, they are not worldwide and convenient to use in comparison with other commercial software like ECLIPSE.

1.3 Objective

ECLISPE 100 simulator is industry standard and being able to model improved oil recovery by smart water injection using such simulator could be valuable. Obviously, the current version does not specifically describe the complex interactions among different phases and species involved in chemically tuned injection water. However, it is capable of giving acceptable result that is representative of the overall effect of smart water injection on wettability alteration and thereby enhanced oil recovery.

The main objective of this project is to model laboratory experiments enhancing the spontaneous imbibition process of so-called smart water into non water-wet carbonate rock samples using ECLIPSE 100. This allows for "dynamic" modelling of wettability alteration using the procedure of weight factors between a water and oil-wet case. Particularly we focus on:

- Modeling spontaneous imbibition into non water-wet carbonate rock using water-wet and oil-wet cases and capturing the effect of sulfate concentration in the imbibing water phase. Injected sulfate concentration and corresponding wettability alteration is investigated. Moreover, relations among adsorbed amount, weight factor and wettability index are investigated.
- Matching experimental data using the procedure of weight factors between a water-wet and oil-wet cases.

1.4 Scope

- Establish simplified procedure on how to simulate smart water imbibition taking into account sulfate concentration in the imbibing aqueous phase using ECLIPSE 100.
- Match laboratory experiments using the established approach.

1.5 Methodology

Smart water composition and impact on the capillary pressure should be modelled using the Surfactant Model. Wettability alteration due to adsorption of ion is part of modeling surfactant injection in ECLIPSE 100. The presence of surfactant can affect reservoir performance in three different ways [21]:

- The surfactant modifies the oil-water surface tension
- The surfactant can modify the water properties such as viscosity
- The adsorbed surfactant can affect the wettability of the rock

However, the objective of this thesis is to model wettability alteration due to smart water injection. Thus, the inputs parameters to account change in oil-water surface tension and property of the water due to surfactant injection are kept constant.

Cylindrical core of a total of 60x20x80 grid-blocks (96, 000 grid-blocks) is used. To mimic imbibition cell, the core sample represented by 40 grid blocks in r-direction, 20 in θ-direction, and 40 in z-direction is surrounded by grid blocks containing high porosity (0.99), high permeability (100,000 mD), and 100% water saturation. Relative permeability curves representing strongly oil-wet and water-wet cases are used. Initially, the outer boundary of the core sample is closed and water is injected to fill the surrounding grid blocks with 100% water saturation. Then restart file representing imbibition cell is generated. The spontaneous imbibition (no injection and production wells) is initiated by opening the core sample. Detail procedure is elaborated in section 3.1

Chapter 2

Theory

2.1 Wettability

2.1.1 Definition

Wettability can be defined as *"the tendency of one fluid to spread or adhere to a solid surface in the presence of other immiscible fluids"* [22]. It is a property that arises due to rock-fluid interaction. Wettability has significant impact on fluid distribution, trapping and multiphase flow in porous medium. Another closely related definition was given by Jerauld and Rathmell who stated that wettability is a tendency of one fluid of a fluid pair to coat a solid surface spontaneously [23].

Taking all the definitions into account, fundamentally, wettability refers to when a solid comes in contact with two immiscible fluids, one of the fluids has greater affinity towards the solid surface. Thus, fluid with the highest affinity for the solid surface is called the wetting phase while the other one is called non-wetting phase [24].

2.1.2 Classification of wettability

Wettability is a complex and continuous parameter; nevertheless, it can be broadly grouped into three categories: as water-wet, oil-wet and intermediate (or neutral) wet. In water-wet case, water is preferentially the wetting phase and it will be in contact with the rock surface while the oil resides in the middle of the larger pores. However, in oil-wet case, the oil will be in contact with the rock surface while the

water occupies the middle of the larger pores. Figure 2.1, illustrates microscopic view of water-wet and oil-wet rock. As indicated in the Figure 2.1, the non-wetting phase occupies the larger pores while the wetting phase attached to the rock surface in the pore throat or smaller pores. Intermediate or neutral-wet is a case where the rock surface shows no preference for either fluid.

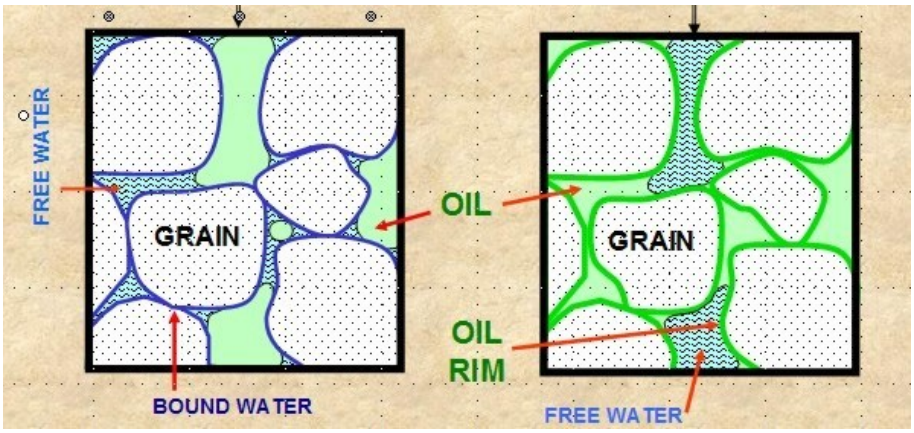

Figure 2.1: *Wettability and fluid distribution at pore level [2].*

Other wettability types are fractional wet and mixed wet. Fractional wet occurs due to heterogeneity of reservoir rocks where a portion of the rock is strongly water-wet and the other portion is strongly oil-wet. This occurs due to variation in composition and chemistry of the reservoir rock. In mixed wettability condition, smaller pores and fine grains would be preferentially water-wet, whereas the larger pores become strongly oil-wet and continuous. Consequently, the oil can easily be displaced from larger pores and hence no or little oil will be held by capillary forces in small pores. Thus, it results in low residual oil saturation [25].

2.1.3 Measurement of wettability

Several quantitative and qualitative methods have been developed to evaluate wettability of reservoir rocks. Among quantitative methods, contact angle, imbibition and forced displacement (Amott), and USBM method are common. Another approach is qualitative methods that includes imbibition rates, microscopic examination, relative permeability curves, permeability/saturation relationships, capillary pressure curves, displacement capillary pressure, and reservoir logs [26]. Qualitative methods are indirect methods in the sense that wettability is deduced from other measurements. For example, capillary pressure and relative permeability curves are useful to distinguish between strongly water-wet and strongly oil-wet. Some of the aforementioned methods are discussed below.

1. Quantitative Methods

i. Contact-Angle Method

When a drop of water is placed on the surface of a solid immersed in oil, an angle between the surface of the liquid and the solid is formed. The angle formed is referred to as contact angle and it ranges from 0° to 180° [26]. Thomas Young [27] proposed that the contact angle is the result of mechanical equilibrium of a drop on solid surface under the action of interfacial tension involved in Figure 2.2.

$$\delta_{OS} = \delta_{WS} + \delta_{OW} \cos\theta \tag{2.1}$$

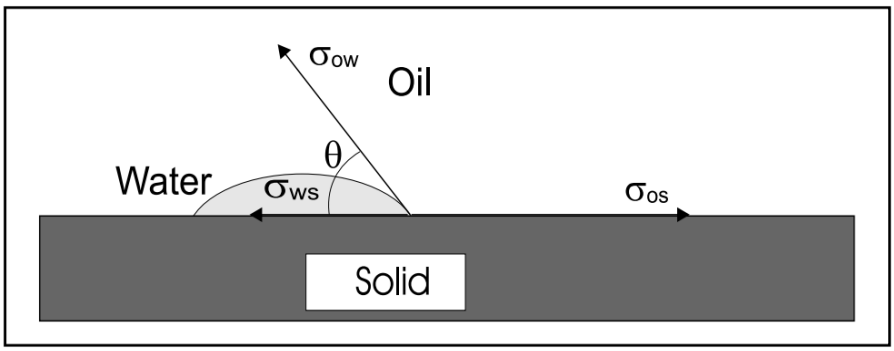

Figure 2.2: *Force balance at water-oil-solid interface defining contact-angle θ [28].*

By convention, the angle formed is measured through the water phase. Contact angle less than 90° indicates water-wetness while an angle greater than 90° indicates oil-wetness.

However, if both fluids have equal affinity towards the solid surface, a contact angle of 90° is formed and the system is called neutral-wet.
In Figure 2.3 (a), the water droplet is spreading, which indicates that water is the wetting phase and hence has higher affinity towards the solid. Thus, the contact angle is less than 90°. However, in (b), the droplet contracts and tries to minimize its contact area with the solid surface. Consequently, the contact angle through the water phase is greater than 90° indicating oil-wetness. In (c), both fluids have equal preference towards the solid surface indicating neutral-wetness.

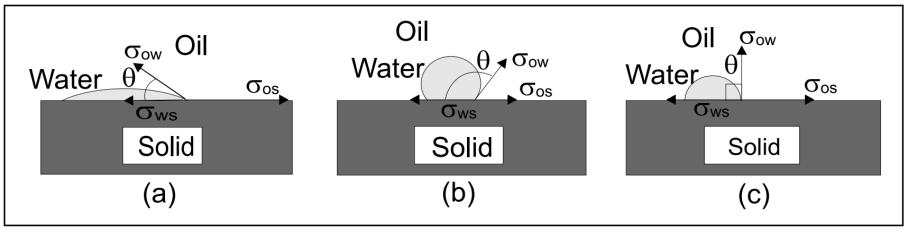

Figure 2.3: *Three surfaces with different wettability [24].*

(a) water-wet ($\theta < 90°$), (b) oil-wet ($\theta > 90°$), and (c) neutral-wet ($\theta = 90°$)

There are several methods of contact angle measurements, but the most common ones are sessile drop method and modified sessile drop method. Sessile drop method (Figure 2.2), involves placing liquid sample also called 'probe' liquid onto a surface by means of a syringe, which can then be analyzed by using a microscope to determine its contact angle.

Modified sessile methods uses two flat, polished mineral crystals that are mounted parallel to each other as shown in Figure 2.4. The cell containing the two mineral surfaces is filled with water (brine), afterwards an oil drop is placed between the two crystals.

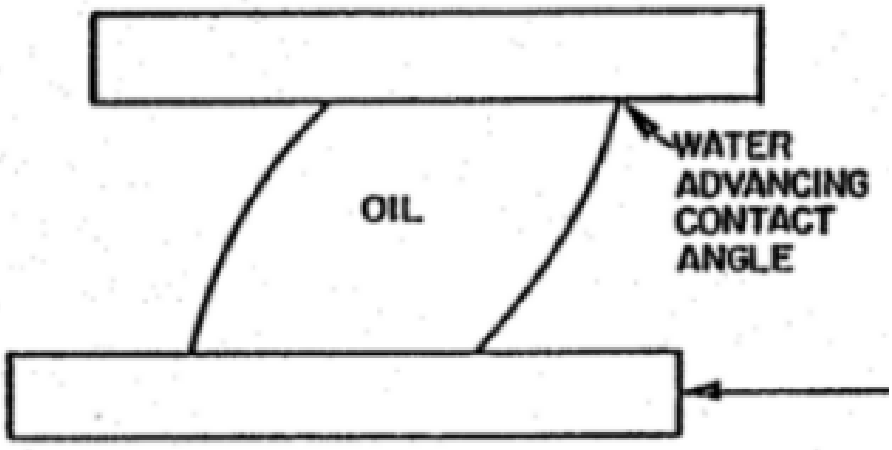

Figure 2.4: *Modified sessile method [26].*

The mobile plate is moved slowly allowing the brine to move over the portion of the surface previously covered with the oil, thus creating advancing contact angle. The angle measured in this way is called water-advancing contact angle.

The contact angle method is probably the simplest and cheapest method of quantifying wettability if it is applied on clean and smooth surface. It is also applicable for non-porous mediums. However, wettability measured in this way may not be representative of the actual reservoir rocks. Since polished mineral surfaces are used and reservoir heterogeneity, roughness and pore geometry are not taken into account. Raeesi et al. demonstrated that roughness and pore geometry have considerable impact on contact angle and hence wettability [28, 29]. The contact on the smooth side is fixed value, whereas on the rough side a range of contact angles is possible. Another limitation is hysteresis developed between the water-advancing and water-receding angles due to roughness, heterogeneity, and immobility in macromolecular scale [26].

ii. Amott method

Amott method test is the most widely used and preferred method of characterizing wettability of a porous medium [9]. It combines spontaneous and forced imbibition to measure the average core wettability. The steps involved in Amott test are summarized next.

1. A core sample at irreducible water saturation is placed in a water-filled tube so that water imbibes spontaneously (from S1 to S2 in Figure 2.5.)
2. Then the remaining oil in the core is displaced until the oil saturation reaches irreducible oil saturation (S2 to S4). The recovered oil (due to spontaneous imbibition and forced displacement) is noted.
3. The core is immersed in oil for about 20 hours and the amount of water displaced due to spontaneous imbibition of oil is noted (S4 to S3).
4. The sample is placed in flow cell and the remaining water is displaced by forcing oil through the sample (S3 to S1). A total amount of water displaced (both by spontaneous imbibition of oil and forced displacement) is noted.

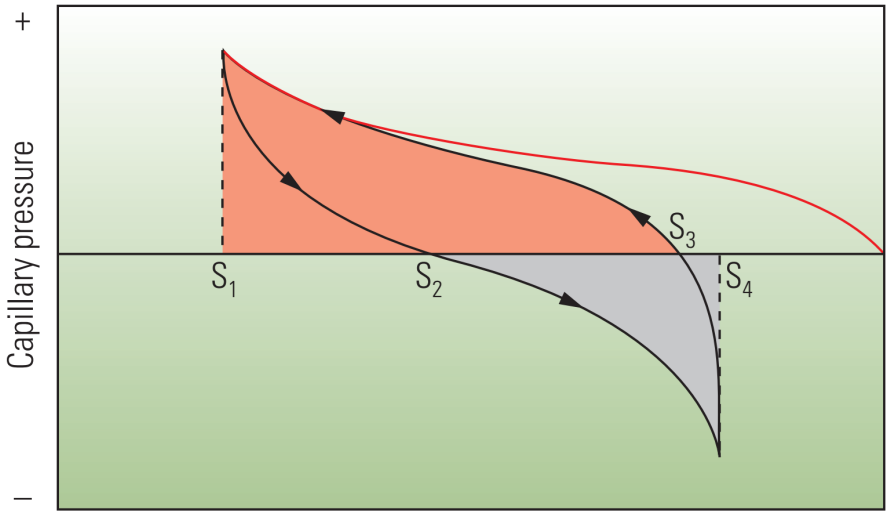

Figure 2.5: *Water saturation fraction [30].*

Amott water index I_W and oil index I_O are defined as spontaneous imbibition to total saturation change for water and oil respectively

$$I_W = \frac{(S_2 - S_1)}{(S_4 - S_1)} \tag{2.2}$$

$$I_O = \frac{(S_4 - S_3)}{(S_4 - S_1)} \tag{2.3}$$

For a strongly water-wet core, I_W is close to 1 while I_O is close to 0. Similarly, in a strongly oil-wet core, I_O is close to 1 whereas I_W will be close 0.

A modified method called Amott-Harvey index, denoted by I_{AH}, is a widely used to characterize wettability of a core sample. It is defined as the difference between I_W and I_O as shown in Eq. 2.4.

$$I_{AH} = I_W - I_O \tag{2.4}$$

The results ranges from +1 for strongly water-wet to -1 for strongly oil-wet. I_{AH} near zero indicates intermediate wetness [30]. This occurs when either $I_O = I_W = 0$ or $I_O = I_W = 1$.

iii. USBM method

USBM, developed by Donaldson et al. [31], is an alternative method for determining wettability index. USBM method uses the same data as Amott method, however, it considers the work done for one fluid to displace the other. The work done is proportional to the area under the capillary pressure curve as indicated in Figure 2.6. For example, for water-wet core, the area under the brine-drive capillary pressure curve (when the water displaces the oil) is smaller than the area under the capillary pressure curve for the reverse displacement. This method gives average wettability of the core sample [26].

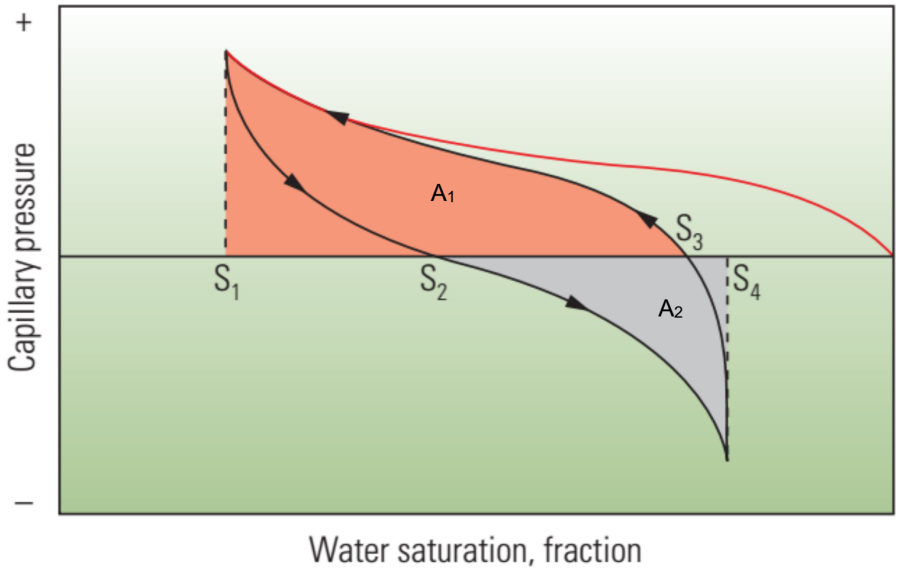

Figure 2.6: *USBM method [30].*

To quantify wettability, USBM method uses the ratio of the areas under the capillary pressure curve.

$$W_{USBM} = \log\left(\frac{A_1}{A_2}\right) \tag{2.5}$$

W_{USBM} greater than zero indicates water wetness, whereas W_{USBM} less than zero indicates oil wetness. An index of near zero indicates neutral wetness. Generally, large $|W_{USBM}|$ is indicative of the degree of preference for the respective fluid. USBM method is one of the commonly used methods in the industry. However, comparison with Amott test shows minimal correlation. Particularly, significant deviation occurs near neutral wettability. The Amott method is more sensitive in this area and could be a better indicator [32]. USBM method is a more descriptive of the natural phenomenon undergoing since it measures force to displace one fluid with another.

iv. Chromatographic Method

This is apparently new method of quantifying wettability in carbonate reservoirs. It is based on chromatographic separation between a tracer SCN^- and SO_4^{2-}. Due to opposite charge, SO_4^{2-} has great affinity to carbonate surface. The test could be conducted on a core with residual oil saturation or a core with 100% water saturation. The core sample is flooded with brine with no tracer and sulfate ion until residual oil saturation is reached. Then the core is flooded with brine containing SCN^- and SO_4^{2-}. The tracer is non-adsorbing agent and hence reaches breakthrough sooner than SO_4^{2-} which will be delayed due to adsorption. The effluent is collected and concentration of each species is determined. Finally relative concentration is plotted against injected pore volume. As illustrated in Figure 2.7, the area between the effluent curves depends on the wettability of the core sample [33].

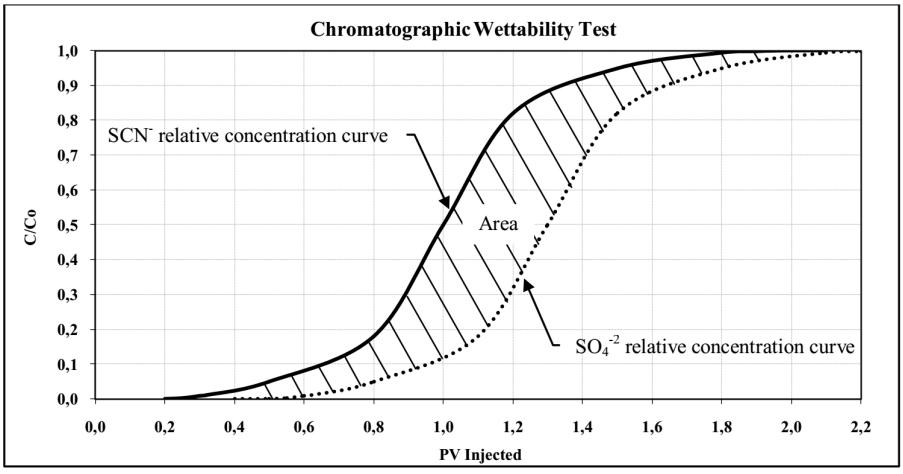

Figure 2.7: *Schematic illustration of the chromatographic wettability test separation between SCN^- and SO_4^{2-} [34].*

The area between the tracer and sulfate ion is proportional to the water-wet surface of the core. The new wettability index (WI_{New}), as shown in Eq. 2.6, is computed by dividing the area between the two effluent curves to the maximum reference area. The maximum separation between SCN^- and SO_4^{2-} is obtained by flooding a strongly water-wet core saturated with heptanes as an oil.

$$WI_{New} = \frac{A_{Wett}}{A_{Heptane}} \tag{2.6}$$

Values of WI_{New} ranges from 1 (strongly water-wet) to 0 which is strongly oil-wet. WI_{New} of 0.5 indicates neutral-wet core.
This method doesn't have limitations regarding its validity in certain wettability range compared to other traditional methods. In fact, it is observed that it gives excellent result close to neutral wetting conditions [33].

2. Qualitative Methods

Qualitative methods are based on visual inspection, rate of imbibition and shape of relative permeability curves. Generally, they are fast and effective to distinguish between completely water-wet and oil-wet conditions. Due to relevance to this document, imbibition and relative permeability methods are discussed here.

i. Imbibition method

Imbibition method is based on rate and volume of fluid imbibed in a core. If large volume of water imbibes rapidly, the core is strongly water-wet while lower rate and small volume indicate weakly water-wet condition. This applies for oil-wet core as well. If neither the oil nor the water imbibes, the core is neutrally wet. In some cases, both oil and water imbibe in the core indicating that the core is either fractional or mixed wettability [26]. Figure 2.8 shows spontaneous imbibition of brine into chalk cores with different oil type. In the case of Figure 2.8a, n-heptane is used and plateau is reached in around 30 minutes suggesting that it is strongly water-wet. However, in Figure 2.8b (b), an oil with AN of 0.5 is used and hence the core is no longer strongly water-wet. Consequently, it took almost 1000 minutes to reach plateau.

Limitation with imbibition method is that the rate is affected by other factors such as relative permeability, viscosity, IFT, pore structure, and initial saturation affects. However, dependence on other variables can be reduced if the measured imbibition value is compared with imbibition measured when the core is strongly water-wet.

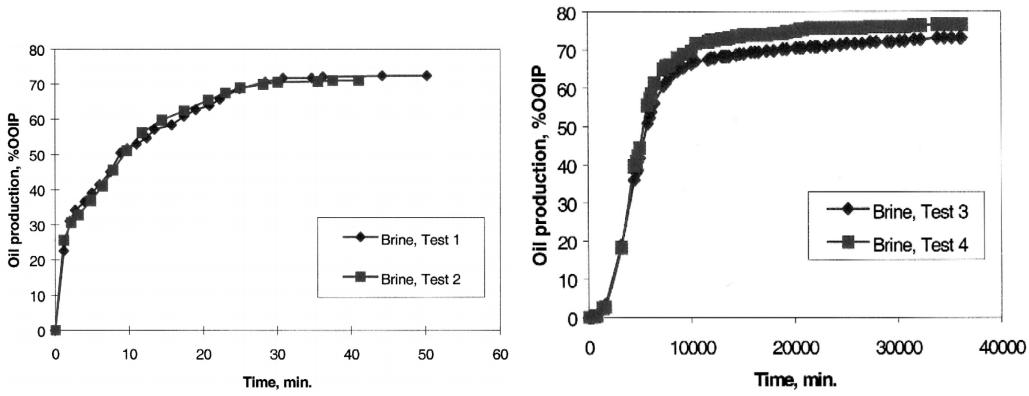

(a) Strongly water-wet core *(b) Moderately water-wet core*

Figure 2.8: *Spontaneous imbibition of brine into chalk core [18].*

(a) 100% n-heptane (b) oil with AN =0.5

ii. Relative Permeability method Wettability and relative permeability are interdependent parameters. As discussed in 2.1.1, wettability affects distribution of water and oil and their movement through pore spaces. Therefore, the effect of wettability on flow behavior of reservoir fluid is reflected on relative permeability. However, it is important to emphasize that relative permeability is used to discriminated strongly water-wet and strongly oil-wet cases. A minor change in wettability, for example, between strongly water-wet and moderately water-wet may not be noticed by this method [35]. Figure 2.9 shows typical relative permeability for strongly water-wet and strongly oil-wet cases.

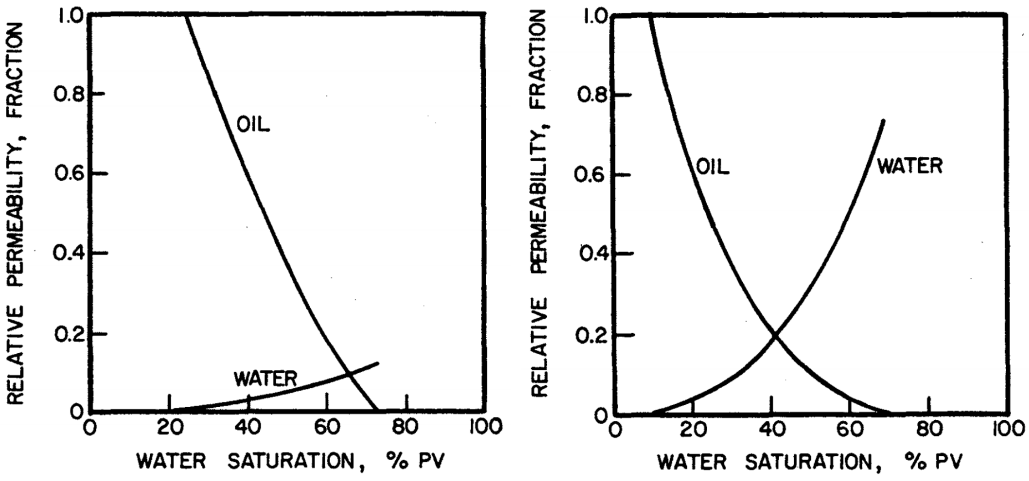

(a) Strongly water-wet *(b) Strongly oil-wet*

Figure 2.9: *Typical relative permeability curves [36].*

Relative permeability is unique property for each reservoir rock. Nevertheless, Craig [36] developed a rule of thumb to discriminate between water-wet and oil-wet conditions

1. Connate water saturation are usually greater than 20 to 25% PV in a water-wet rock, but less than 10% PV in an oil-wet rock.
2. Water saturation at which oil and water relative permeabilities are equal is generally greater than 50% for water-wet cores and less than 50% for oil-wet ones
3. The relative permeability to water at residual oil saturation is generally less than 30% in water-wet rocks, but from 50 to 100% in oil-wet ones.

Craig's rules of thumb generally give a good indication of the rock wettability even though there are some exceptions. Caudle et al. [37] pointed out that relative permeabilities measured on a water-wet sandstone are dependent on the initial water saturation. Thus, initial water saturations changes location and shape of the curves. However, Craig [36] stated that initial water saturation has significant effect on relative permeability curves measured on strongly water-wet rocks, but has little effect on curves measured on oil-wet rocks as long as the initial saturation is less than 20%.

2.1.4 Correlation Between Oil Recovery and Wettability index

Spontaneous imbibition of water into the matrix is believed to be the main mechanism for improved oil recovery in fractured carbonate rocks. As discussed in the theory part, SI depends on wettability of the rock. Thus, it is reasonable to expect relation between wettability index and maximum recovery. Zhang and Austad, as shown in Figure 2.10a, suggested correlation of plateau recovery with wettability index based on chromatographic wettability testing method (WI_{new}) [38]. In the experiment, SO_4^{2-} concentration is varied for three temperature values. Zhang and Austad also proposed relationship between Amott wettability index and WI_{new} that are shown in Figure 2.10b.

There is also a rule of thumb that agrees fairly well with the experimental correlation presented above. The rule of is used to roughly quantify wettability in chalk core sample based on maximum oil recovery. It is assumed that 75% recovery corresponds to Amott wettability index (I_w) of unity. Similarly, no oil production indicates completely oil-wet case and this corresponds to $I_w = 0$ while is I_O non-zero.

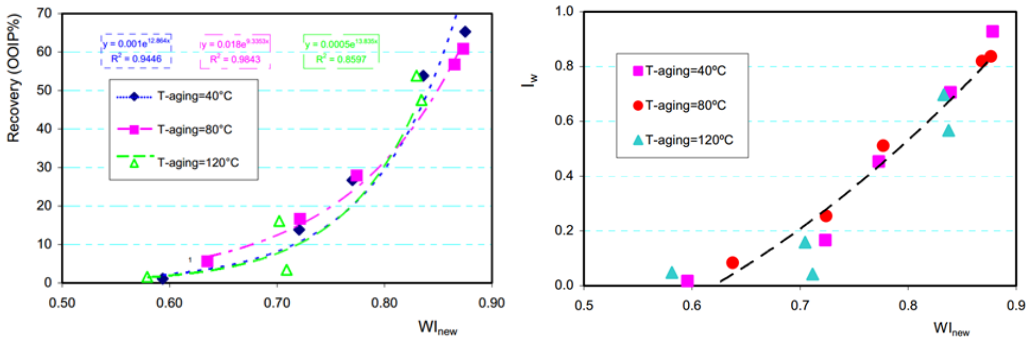

(a) Recovery vs WI_{new} *(b) I_w vs WI_{new}*

Figure 2.10: *Relationship between wettability index and maximum recovery [38, 39].*

The experimental correlation provided above enables conversion between I_w and WI_{new} given maximum recovery is available. Wettability index calculated in the methods specified above would be used to quantify wettability of the experimental data to be matched.

2.2 Fractured Reservoirs

Naturally fractured carbonate reservoirs are characterized by the presence of two distinct porous media : matrix and fracture. Usually, low porosity and low permeability matrix blocks is surrounded by a highly permeable, network of irregular cracks and fissures. The isolated matrix block acts as a source of hydrocarbon while overall fluid flow depends on the fractured networks. In fractured reservoir, the fracture has significant effect on overall property and performance of the reservoir. Thus, it can not be ignored in the conceptual model unlike most conventional reservoirs which are somewhat fractured but the fracture plays insignificant role regarding fluid flow. Figure 2.11 shows schematic illustration of fracture and grid model for numerical simulation.

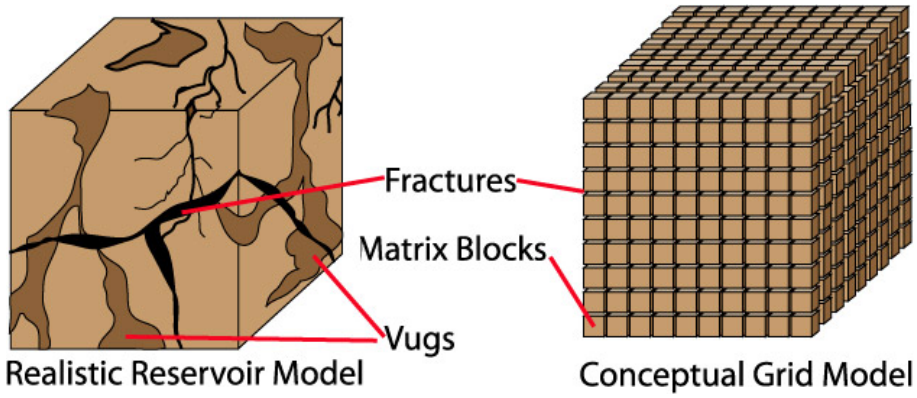

Figure 2.11: *Schematic illustration of naturally fractured reservoir [40].*

Based on the relationship between matrix and fracture properties, fractured reservoirs can be divided into four categories [41].

- Type I - little to no porosity and permeability in the matrix. Fractures provide essential porosity and permeability. Reserves is defined by fracture characteristics.
- Type II - low porosity and permeability in the matrix. Matrix provides some storage capacity and fractures provide pathways for the fluid flow. Fracture intensity and distribution dictates production.
- Type III - Characterized by high matrix porosity and low permeability. Fracture networks provide permeability and defines anisotropy.
- Type IV - high matrix porosity and permeability. Both storage and flow is dictated by matrix while fractures simply enhance permeability.

2.2.1 Recovery Mechanisms in Fractured Reservoirs

Recovery mechanisms in naturally fractured reservoirs are different to conventional reservoirs. Large contrast in capillary pressure between the matrix and the fractures is the main reason for the difference in recovery performance between fractured and conventional reservoirs [42].
The principal recovery mechanisms are :

i Spontaneous Imbibition

Spontaneous imbibition is an important recovery mechanism in fractured reservoirs. The water injected to maintain pressure will rapidly invade the fracture surrounding the matrix. Most of the flow is through the highly permeable fracture and this in turn limits the build up of large differential pressure across the reservoir. The limited viscous forces are negative for production. For example, during waterflooding, most of the water flows in the fracture only, and bypasses the oil in the matrix leading to poor sweep efficiency and low recoveries. Therefore, the dominant recovery mechanism is capillary imbibition rather than viscous displacement [41].

The amount and the rate of water that imbibes from the fracture to the rock matrix depends on the capillary pressure which in turn is mainly a function of wettability and pore structure of the rock.

ii Gravity Drainage

Gravity drainage is gas-oil displacement where gravity force is dominant over viscous and capillary forces. The height of the matrix block and the density difference between the gas in the fracture and the oil in the matrix dictates the efficiency of gravity drainage. If matrix block is tall, gravity drainage is important recovery mechanism otherwise capillary threshold pressure prevent the oil against flowing to the fracture.

iii Fluid Expansion

During primary recovery, the pressure will drop. Particularly, due to high transmissibility in the fracture, rapid drop is expected in the fracture than in the matrix. This implies that there is pressure difference between the matrix and the fracture. Consequently, this leads to flow of oil to the fracture as the fluids expand. Pressure drop below bubble point causes gas to evolve from the oil and results in further recovery. However, once the gas is connected in the system, only gas is produced leaving significant quantity of oil in the matrix. Moreover, due to high permeability of the fracture network, the pressure drop

around a producing well is lower than in conventional reservoirs. Thus, pressure drop does not play significant role in production from fractured reservoir [41].

2.3 Model For Spontaneous Imbibition

Several models with different approaches have been suggested for SI of water into a naturally fractured reservoir. Many traditional and recently presented SI models are derived based on Hagen-Poiseuille (H-P) flow in cylindrical capillaries. Usually, transfer functions are used to describe the rate by which oil is expelled from the matrix block. One of the limitations of the earliest models was that they are based on cylindrical capillaries. However, natural porous media are usually tortuous and non-circular [43]. Therefore, models based on cylindrical capillaries may not be a good representation of SI in natural porous media. Various investigators have developed SI model by considering some parameters that they assumed to dictate SI in porous media. Some of the models that take various geometrical shape and size into account are highlighted below.

2.3.1 Aronofsky Model

This model is the first approach to modeling SI and it is most widely used as basis for several other modifications of cylindrical capillaries methods [44]. The author noticed that oil recovery by SI can be modeled as exponential curve given in Eq. 2.7.

$$R = R_{max}(1 - e^{-\omega t}) \tag{2.7}$$

where R is oil recovery as a function of time, R_{max} is maximum oil recovery, and ω to be found empirically. Determining *omega* is time consuming [45]. Aronofsky model is simple model since only one parameter varies to match oil recovery. However, there are some limitations to this model. Firstly, ω is a function of petrophysical properties and geometry of a system. Secondly, obtaining an good value that takes into account variation of matrix block size and petrophysical properties is not always possible.
Thirdly, the value obtained in laboratory may not necessarily be applicable in actual reservoir [46]. Moreover, the model overestimates recovery in early time and underestimates in late time.

Ma et al. proposed a modified version of Aronofsky model introducing different definition of dimensionless time t_D and characteristic length L_c that takes into account shape factor and boundary conditions [47]. Their model is presented in Eq. 2.8.

$$\frac{R}{R_{max}} = (1 - e^{-\omega t_D}) \tag{2.8}$$

$$t_D = t\sqrt{\frac{k}{\phi}}\frac{\sigma}{\sqrt{\mu_w \mu_o}}\frac{1}{L_c^2} \tag{2.9}$$

$$L_c^2 = \frac{V_b}{\sum_{i=1}^{n}\frac{A_i}{l_{A_i}}} \tag{2.10}$$

where V_b is bulk volume of the core (m^3), L_i is distance from *i-th* imbibition surface to the no flow boundary(m) and A_i is *i-th* imbibition surfaces.

The modified method was tested by correlating ultimate oil recovery by SI from strongly water-wet core sample . Sample size, shape, and boundary conditions are taken into account. A close fit to experimental data was obtained by equation of decay with dimensionless time t_D as the only parameter varied. Moreover, it was suggested that, it is possible to assess wettability of non-strongly water-wet conditions by comparing the reduction in SI rate relative to results obtained for strongly water-wet case [47].

A single-parameter fit correlation based on solving Washburn equation was proposed by Standnes [44]. Washburn equation describes capillary flow in a bundle of parallel cylindrical horizontal tubes. The equation is also applicable to describe imbibition into porous media. Fries and Dreyer [48] suggested explicit solution of Washburn equation for vertical flow including gravity term with respect of height and a Lampbert's W function used to mathematical rearrangement. The explicit solution is given below.

$$h(t) = \frac{a}{b}[1 + W(-e^{-1-\frac{b^2 t}{a}})] \tag{2.11}$$

$$a = \frac{2\sigma cos\theta k}{\phi \mu_w} \tag{2.12}$$

$$b = \frac{\rho g k}{\phi \mu_w} \tag{2.13}$$

where W(x) is the Lambert's W function defined as inverse exponential function given by

$$x = W(x)e^{W(x)} \tag{2.14}$$

In Eq.(2.11), $\frac{a}{b}$ gives capillary rise to the gravity head as indicated in Eq. (2.15)

$$\frac{a}{b} = \frac{2\sigma cos\theta}{r}\frac{1}{\rho g} = \frac{P_c}{\rho g} \tag{2.15}$$

where L is the length of the capillary tube and therefore, dividing Eq. (2.11) by L gives the fraction of the tube imbibed. Thus, normalized oil recovery as a fraction of recoverable oil vs time is given by:

$$\frac{R(t)}{R_{max}} = 1 + W(-e^{-1-\frac{b^2 t}{a}}) \tag{2.16}$$

with introduction of pure fit parameter $\alpha = \frac{b^2}{a}$ in Eq. (2.16) we get

$$\frac{R(t)}{R_{max}} = 1 + W(-e^{-1-\alpha t}) \tag{2.17}$$

The correlation better fits to experimental data compared to the standard Aronofsky exponential decay correlation. It also preserves the simplicity of Aronofsky's model as it requires only adjusting one parameter to fit experimental SI data. As indicated in the Figure 2.12, discrepancies of Aronofsky's model at early and late time is improved in this correlation. Even though only one parameter is varied like Aronofsky model, the correlation fits SI date more accurately.

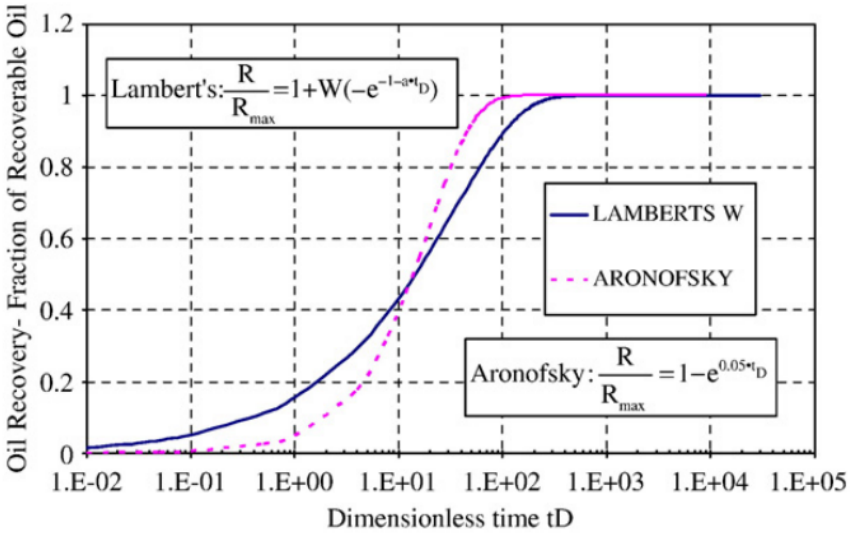

Figure 2.12: *The Aronofsky model and the improved correlation based on the Lambert's W function [44].*

2.3.2 Cai Model

Recently, Cai et al. [1] presented an analytical model for SI of a wetting fluid in porous media based on fractal geometry. Fractal characteristics is based on the assumption that natural porous media have self-similar over several length scale. In this model, early time imbibition weight is expressed as

$$M^2 = \frac{\sigma cos\theta}{2\mu\tau^2}\frac{2-D_f}{3-D_f}\frac{(A\phi\rho)^2 r_{max}}{1-\phi}t \tag{2.18}$$

where, r_{max} is the maximum pore radius and D_f is the pore fractal dimension which is $0 < D_f < 2$ for two dimensional space and $0 < D_f < 3$ in three-dimensional Euclidean space. I this model, it is assumed that porosities and pore diameters of homogeneous porous media are respectively equal in two and three dimensional spaces. In Eq. 2.18, τ is to take tortuosity of porous media into account and it is given by Eq. 2.19.

$$\tau = \frac{L_t}{L_O} \tag{2.19}$$

where L_t and L_O are the tortuous and straight representative length. Thus, for straight capillary, $\tau = 1$. The presented model indicates that the weight of wetting liquid imbibed into porous media is a function geometry of the porous media *(*A,ϕ,D_f, *and* τ), fluid properties (ρ, μ, σ) and fluid-solid interaction(θ). Furthermore, Eq. 2.18 can also be expressed as

$$M^2 = 2at \tag{2.20}$$

Eq. 2.20 denotes that the accumulated imbibed wight in the porous medium is proportional to $\sqrt{t}$ in early imbibition period. A model similar to Eq. 2.20 that considers the fractal character of tortuous stream-tubes in porous media has been verified experimentally [1]. The authors argue that model represented in Eq. 2.18 is in good agreement with experimental data.

2.3.3 Handy Model

Handy [49] derived a macroscopic imbibition model to predict water imbibition behavior in porous media. The main assumptions for the model are wetting liquid imbibition occurs in a piston-like manner, and pressure gradient in the gas phase ahead of the wetting liquid front can be ignored. Imbibition weight in Handy's model is presented in Eq. 2.21.

$$M^2 = \frac{2P_c k A^2 \rho^2 \phi S_{wf}}{\mu} t \tag{2.21}$$

where k is intrinsic permeability. Generally, in diffusion equation, the small capillaries fill first followed by larger capillaries. However, in piston-like displacement, all capillaries fill at the same time leaving a residual saturation behind. The capillary pressure is assumed to provide the driving force throughout the porous medium in which water is flowing. Handy has also conducted experimental works to verify the validation of the assumptions in deriving Eq. 2.21. The model is in good agreement with experimental data even though comparatively it is simple and more representative of the experimental data than equations based on phase continuity behind the front [49].

2.3.4 Generalized Model by Cai et al.

Cai et al. [43] derived a comprehensive model based on H-P equation that generalizes several previous models. This model was developed by considering the different the different sizes and shapes of pores, the tortuosity of imbibition streamlines in random porous media, and the initial wetting-phase saturation. Flow rate q in circular capillary is given by

$$q = \frac{\pi \lambda^4 \Delta P}{128 \mu L_O} \tag{2.22}$$

Eq. 2.22 applies only to a straight capillary tube with a circular cross-sectional shape. However, pore channels are seldom circular in natural porous media. Therefore, correction is required to include tortuous and noncircular nature of natural porous media. Pickard [50] proposed Eq. 2.23 that takes into account the aforementioned factors.

$$q = \frac{\pi D_h^4 \Delta P}{128 \mu L_O} \tag{2.23}$$

where D_h is hydraulic diameter, k is a geometry correction factor dependent on the shape of the capillary and its eccentricity with $k = 1$ for circular capillary. L-Y

capillary pressure equation is modified to account for irregular pore structure [51] and given by Eq. 2.24.

$$P_c = \frac{2B\sigma cos\theta}{r} = \frac{2\sigma cos\theta}{\frac{1}{B}r} \tag{2.24}$$

where $B = 1$ for cylindrical pores and $0 < B < 1$ for non-cylindrical pores. By combining modified H-P and L-Y equations, Cai et al. derived accumulated weight (M) of imbibed liquid for laminar flow in tortuous capillaries with noncircular cross-sectional shapes given by:

$$M = \frac{\rho^2 A^2 \phi^2 (S_{wf} - S_{wi})^2 \alpha^3 r_{ae} \sigma cos\theta}{2\mu\tau^2} t \tag{2.25}$$

where r_{ae} is effective/average radius. α is dimensionless geometry correction factor and $\alpha > 1$, with $\alpha = 1$ for circular cross-section, and $\alpha = 1.094$ for a square, and $\alpha = 1.186$ for an equilateral triangle.

Eq. 2.25 is only valid for early imbibition times and has primarily has two limitations. The fist one is gravity effect neglected. The second is as time goes to infinity, accumulated weight of imbibed fluid also goes to infinity and this is not physically realistic. Gravity effect increases as height/time of the imbibed fluid increases. Therefore, Cai et al. employed new scaling group suggested by Standnes [44] to derive an analytical model for entire imbibition process considering the gravity force. Explicit analytical equation is given below

$$M(t) = \frac{a}{b}[1 + W(-e^{-1-\frac{b^2 t}{a}})] \tag{2.26}$$

Eq. 2.26 is similar to Eq. 2.11 except that in this case a and b have different values as indicated below.

$$a = \frac{\rho^2 A^2 \phi^2 (S_{wf} - S_{wi})^2 \alpha^3 r_{ae} \sigma cos\theta}{4\mu\tau^2} \tag{2.27}$$

$$b = \frac{\rho^2 A \phi (S_{wf} - S_{wi})^2 \alpha^4 r_{ae}^2 g}{8\mu\tau^2} \tag{2.28}$$

The authors argue that this model considers almost all of parameters that control SI in porous media such as fluid properties, porous media properties and properties that arise due to solid-fluid interactions. Models presented in the previous sections can be obtained with mathematical manipulation of the generalized model. As indicated in Figure 2.13, results obtained by fitting experimental data show that the presented generalized expression can describe SI for many wetting liquids in natural and artificial porous media.

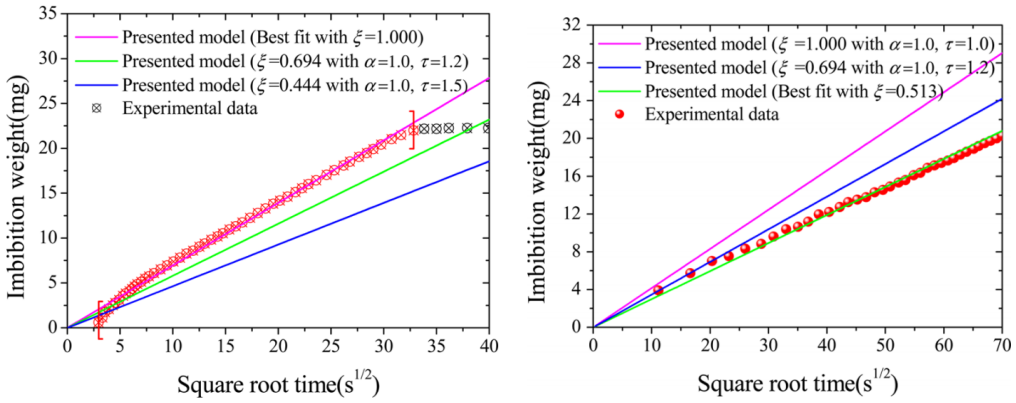

(a) Decanol as wetting liquid *(b) n-hexadecane as wetting liquid*

Figure 2.13: *Comparison of experimental data and prediction by the model [43].*

In the Figure 2.13, $\xi = \frac{\alpha^3}{\tau^2}$ is a composite parameter that includes influences of both shape and streamline tortuosity on SI. It is evident from the figure that the model gives best fit to the experimental data. Particularly an accurate match for circular porous media.

2.4 Mechanisms of Smart Water

Crude oil is a complex mixture of thousands of different compounds such as liquid fraction, asphatenes, and resins which are rich in polar components. It is indicated that crude oil components that mainly affect wettability of the rock are polar organic bases ($R_3NH^+ \rightleftharpoons H^+ + R_3N$), organic acids ($RCOOH \rightleftharpoons H^+ + RCOO^-$), and heteroatoms like nitrogen, sulfur and oxygen (NSO). The polar components in crude oil adhere to the surface of the rock depending surface charge of the rock. The mechanisms they adhere to the rock surface depend on asphaltene content, AN, base number, and brine composition. AN is measured in *mgKOH/g oil*.

The four interaction mechanisms between crude oil and rock surface have been identified are *polar binding*, *surface interaction*, *acid-base interactions*, and *ion-binding interactions* [52]. Polar binding occurs between mineral surfaces and polar heteroatoms in crude oil in absence of water. However, if an oil is a poor solvent for its asphaltenes, surface precipitation can occur and hence the precipitates adhere to the rock surface making it oil-wet. Acid-base interactions occur between sites of opposite charge, and this interaction is pH dependent adhesion. Ion-binding interactions take place when divalent or multivalent ions in the brine present. They bind both to the mineral surface and oil-water interface creating bridge.

It has been observed that the water-wetting condition of carbonate reservoirs increases as the temperature of the reservoir increases. The reservoir temperature is important factor because the acid number in the actual crude oil decreases as the temperature increases [53].

Suggested mechanisms of smart water that are pertinent to carbonates are discussed next.

2.4.1 Mechanisms of Smart Water in Carbonates rocks

Carbonate reservoirs are generally characterized as mixed-wet to preferentially oil-wet system with heterogeneity. They are observed to be positively charged at basic conditions (pH$<$ 9.5) and therefore, are able to attract negatively charged acidic components in crude oil. Thus, the AN of the crude oil has been shown to be a crucial factor for the wetting state of carbonates. Furthermore, it was observed that the water wetness decreases as the AN increases [54]. For example, smart water is verified to increase the water wetness of carbonate rocks by a symbiotic interaction

between potential determining active ions and the mixed-wet calcite surface. The potential determining ions are calcium (Ca^{2+}), magnesium (Mg^{2+}), and sulfate (SO_4^{2-}) [55].

The mechanism for wettability alteration was suggested to be an interaction between the cationic surfactant monomers and adsorbed negatively charged carboxylic material, forming a cat-anionic complex, which is released from the surface. Figure 2.14 depicts surface interactions undergoing during wettability alteration of carbonate from oil-wet to water-wet. As stated previously, initially, the rock is positively

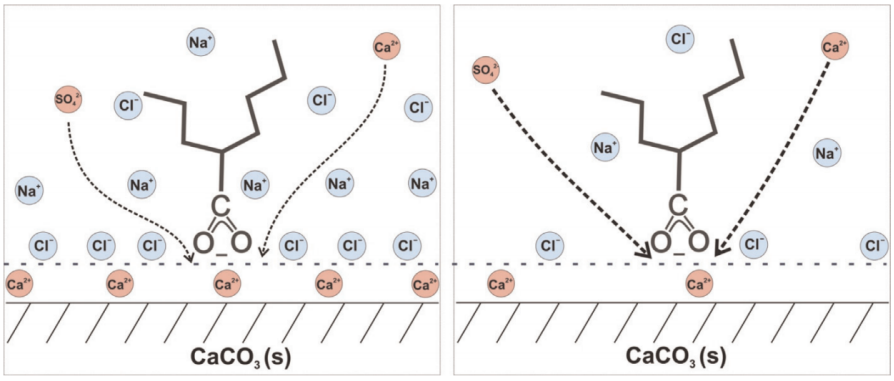

Figure 2.14: *Wettability alteration mechanism at carbonate surfaces [56].*

charged due to a pH < 9.5 and high concentration of Ca^{2+} and possible Mg^{2+} in the formation water. Sulfate ion from the injected water will adsorb onto the positively charged surface and lower the positive charge which leads to less electrostatic repulsion. As a result, the concentration of Ca^{2+} close to the surface is increased. Calcium ion can bind to the negatively charged carboxylic group and releases it from the surface. At higher temperature, ion activity of Mg^{2+} increases and it is able to displace Ca^{2+} and even the Ca^{2+}- carboxylate complex from the surface. The process is illustrated in Eq. 2.29. However, spiking the injected water with SO_4^{2-} is not advisable due to precipitation of anhydride ($CaSO_4$) at higher temperature.

$$CaCO_3(s) + Mg^{2+} \rightleftharpoons MgCO_3(s) + Ca^{2+} \tag{2.29}$$

2.5 Smart Water Implementation in ECLIPSE 100

One of the suggested mechanisms of smart water is wettability alteration. Wettability change option is under Surfactant Model in ECLIPSE 100. This is due to the assumption that wettability change occurs when surfactants adsorbs on the surface of the rock. Furthermore, ECLIPSE 100 has Low Salinity Option (LSO) to model low salinity effect [57–59]. As stated before, low salinity water is a smart water which salinity is adjusted to a desired level. LSO allows one to modify saturation and relative permeability end points, and water-oil capillary pressure as a function of salt concentration rather than adsorption. The surfactant option allows dynamic modelling of wettability alteration effect of smart water. The wettability change option in Surfactant Model can be improvised to model wettability alteration by smart water by considering sulfate ion as surfactant. In this thesis, wettability change option is employed to model spontaneous imbibition due to wettability alteration.

2.6 Modeling Wettability Change due to Surfactant Adsorption

Huge amount of oil remains in the reservoir even after WF due to either it is bypassed by WF or immobile due to zero relative permeability at that saturation. Surfactants are surface active agents and hence lowers oil-water surface tension that held the oil trapped due to capillary pressure. Low surface tension enables the water to displace the oil more easily. Due to electrostatic attraction, surfactants have a tendency to be adsorbed on the surface of the rock. The adsorbed surfactant can affect the wettability of the reservoir rock.

The surfactant flooding model is activated by using *SURFACT* keyword in *RUNSPEC* section. The surfactant is assumed to exist only in the water phase, and therefore, distribution of injected surfactant is modeled by solving a conservation equation for surfactant within the water phase. The input to the reservoir is specified as a concentration at a water injector. The Surfactant Model is also able to model changes in the rock wettability due to the accumulation of surfactant by adsorption. The option to model change in wettability is activated by specifying the *SURFACTW* keyword, which also activates the Surfactant Model (*SURFACT* keyword) by defualt if it is not activated already.

At least two saturations tables, oil-wet and water-wet, have to be provided to model wettability alteration due to adsorption of surfactant. The *SATNUM* and *SURFWNUM* keywords are used to define the oil-wet and water-wet immiscible saturation regions respectively and hence the associated saturation tables. If miscibility is also to be considered, the keyword *SURFNUM* is used to define the miscible saturation regions. The immiscible saturation regions is for high IFT region while miscible saturation is for low IFT region. However, in thesis model miscibility is not expected, thus only immiscible saturation regions are used. Given two sets of saturation functions, one for immiscible oil-wet and one for immiscible water-wet, the immiscible water and oil table saturation end-points are interpolated firstly according to:

$$\begin{aligned} S_{wco}^{imm} &= F_4 S_{wco}^{ow} + (1 - F_4) S_{wco}^{ww} \\ S_{wcr}^{imm} &= F_4 S_{wcr}^{ow} + (1 - F_4) S_{wcr}^{ww} \\ S_{wmax}^{imm} &= F_4 S_{wmax}^{ow} + (1 - F_4) S_{wmax}^{ww} \\ S_{owcr}^{imm} &= F_4 S_{owcr}^{ow} + (1 - F_4) S_{owcr}^{ww} \end{aligned} \tag{2.30}$$

where F_4 is tabulated as a function of the adsorbed surfactant concentration and corresponds to the second column of the *SURFADDW* keyword. F_4 has maximum value of 1 and minimum value of 0. $F_4 = 1$ implies only the oil-wet saturation function is used whereas value of $F_4 = 0$ implies only the water-wet saturation function is used. The interpolated end-point values in Eq. 2.30 are then combined with the miscible table saturation end-points according to:

$$\begin{aligned} S_{wco}^{i} &= F_3 S_{wco}^{mis} + (1 - F_3) S_{wco}^{imm} \\ S_{wcr}^{i} &= F_3 S_{wcr}^{mis} + (1 - F_3) S_{wcr}^{imm} \\ S_{wmax}^{i} &= F_3 S_{wmax}^{mis} + (1 - F_3) S_{wmax}^{imm} \\ S_{owcr}^{i} &= F_3 S_{owcr}^{mis} + (1 - F_3) S_{owcr}^{imm} \end{aligned} \tag{2.31}$$

where F_3 is a function of the capillary number (expressed in terms of its logarithm base ten) and corresponds to the second column of the *SURFCAPD* keyword. A value of *0* implies immiscible conditions and a value of *1* is for miscible conditions. It should be emphasized that in smart water injection, there is no significant miscibility between the oil and injected fluid. Therefore, $F_3 = 0$ is used and this is in line with the objective of this study. As shown in Eq. 2.32, the immiscible oil-wet and water-wet capillary pressures and relative permeabilities are looked up in the immiscible oil-wet and water-wet saturation tables by applying two-point saturation (horizontal) end-point scaling using the interpolated saturation end-points.

$$\begin{aligned} P_c^{jw} &= f(S_w, S_{wco}^{i}, S_{wmax}^{i}, P_{cowmax}^{jw}) \\ k_r^{jw} &= f(S_w, S_{wcr}^{i}, S_{wmax}^{i}, k_{rmax}^{jw}) \end{aligned} \tag{2.32}$$

where j stands for o *and* w, k_r stands for k_{rw} and k_{ro}. In addition, miscible relative permeabilities are also looked up in miscible table applying end point scaling using interpolated saturation end points as shown in Eq. 2.33.

$$k_r^{mis} = f(S_w, S_{wcr}^i, S_{wmax}^i, k_{rmax}^{mis}) \tag{2.33}$$

The water-oil capillary pressure is only interpolated between the immiscible oil-wet and immiscible water-wet values [21]. The method is the same if we have three phase except that the gas relative permeability and gas-oil capillary pressure are assumed to exhibit no dependence upon surfactant concentration or surfactant adsorption. Summary of the keywords required for modeling wettability alteration in surfactant flooding is listed in appendix (ECLIPSE 100 KEYWORDS).

2.6.1 Capillary Pressure

As concentration of the surfactant increases water-oil capillary pressure will reduces. This in turn leads to reduction of residual oil saturation. The oil-water capillary pressure is give by

$$P_{cow} = P_{cow}(S_w)\frac{ST(C_{surf})}{ST(C_{surf} = 0)} \tag{2.34}$$

where $ST(C_{surf})$ is the surface tension at the present surfactant concentration, $ST(C_{surf} = 0)$ is the surface tension at zero concentration. However, in the case of smart water injection, there is no significant IFT change. Thus, P_C is rather interpolated between immiscible water-wet and immiscible oil-wet based on the weighing function as shown in Eq 2.32.

2.6.2 Water PVT Properties

The surfactant modifies the viscosity of the pure water phase. The viscosity of the water (at reference pressure) is given as input as a function of surfactant concentration. In modeling wettability alteration due to smart water, viscosity of the surfactant solution is considered to be equal to viscosity of the water.

2.6.3 Adsorption Isotherms

The adsorption of surfactant is assumed to be instantaneous, and the quantity adsorbed is a function of the surfactant concentration. It is required to supply an adsorption isotherm as a function of surfactant concentration under *SURFADS* keyword. The quantity of surfactant adsorbed on to the rock is given by:

$$Mass\ of\ adsorbed\ surfactant = PORV.\frac{1-\phi}{\phi}MD.CA(C_{surf}) \tag{2.35}$$

There are two adsorption models that can be selected, using the first argument of SURFROCK. The first model ensures that each grid block retraces the adsorption isotherm as the surfactant concentration falls in the cell. The second model assumes that the adsorbed surfactant concentration on the rock may not decrease with time and hence does not allow for any de-adsorption. In the current version of ECLIPSE 100, the adsorption concentrations are updated explicitly for the surfactant concentration.
The most common adsorption isotherms used are highlighted below.

i. Linear Isotherm
Linear isotherm is simple assumption that the adsorbed quantity directly proportional to the concentration of injected solution as shown in Figure 2.15a [60]. Linear isotherm is defined by:

$$q_e = KC_e \tag{2.36}$$

The linear isotherm is a special case of the Freundlich isotherm where the Freundlich exponent n is equal to 1 as shown in Eq. 2.37

ii. Freundlich Adsorption Isotherm
In 1909, Freundlich suggested an empirical expression representing the isothermal variation of adsorption of a quantity of gas adsorbed by unit mass of solid adsorbent with pressure. This equation is referred to as Freundlich Isotherm [60]. Mathematically expressed as:

$$q_e = K_f C_e^{1/n} \tag{2.37}$$

where K_f and n are constants whose values depend on adsorbent and gas at particular temperature. As indicated in Figure 2.15, $1/n$ indicates the intensity of adsorption.

Limitation of Freundlich Isotherm is that even though it established the relationship of adsorption with pressure at lower values correctly, it failed to predict value of adsorption at higher pressure [60].
Figure 2.15 indicates the relationship between adsorbed amount and concentration of injected solution for linear and Freundlich isotherms.

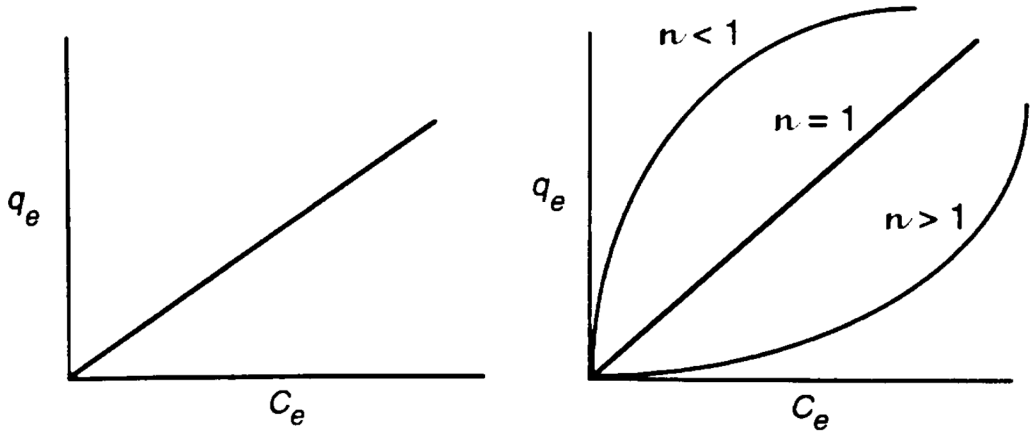

(a) Linear Isotherm *(b) Freundlich Isotherm*

Figure 2.15: *Linear and Freundlich Isotherm [61].*

iii. Langmuir Isotherm

In 1916, Langmuir proposed an adsorption isotherm known as Langmuir Adsorption Isotherm (LAI) which is based on the assumption that there exists equilibrium between adsorbed gas molecules and free gas molecules. LAI is given by Eq. 2.38.

$$x = \frac{x_m K_l C_e}{1 + K_l C_e} \tag{2.38}$$

where x and x_m are amount adsorbed and maximum amount adsorbed per unit mass, respectively. K_l Langmuir adsorption constant.
LAI is based on some reasonable assumptions which are mostly valid under low pressure [62]. The assumptions are:

- Fixed number of vacant or adsorption sites are available on the surface of solid.
- A uniform surface
- A single layer of adsorbed molecules and constant temperature

LAI works pretty well at low pressure. However, it deviates at high pressure. This is due to the assumptions made in deriving the equation.

For example, it does not account surface roughness and variation in affinity, it ignores interaction between adsorbents and adsorption is monolayer [63]. Figure 2.16 depicts adsorbed amount as a function concentration of solute for Langmuir and BET isotherms.

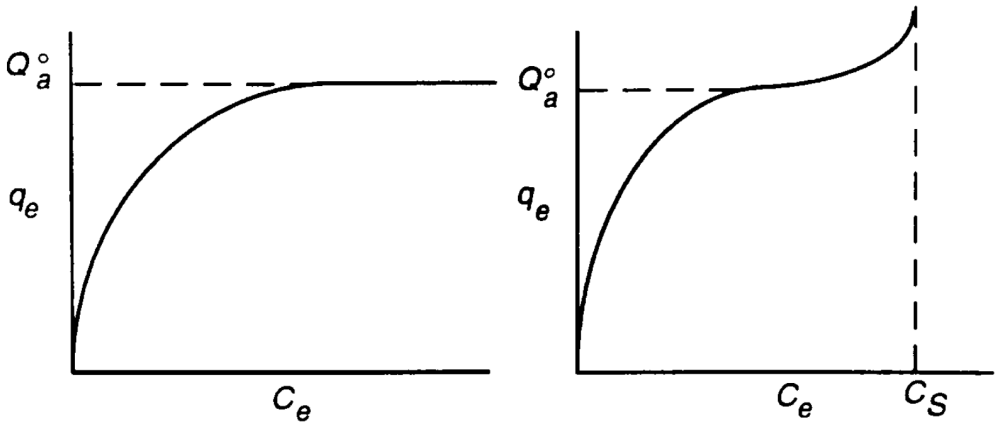

(a) Langmuir Isotherm *(b) BET Isotherm*

Figure 2.16: *Langmuir and BET Isotherm [61].*

iv. BET Isotherm

This a more general multilayer model. BET isotherm is basically extension of LAI which is, as pointed out previously, is monolayer isotherm. BET isotherm assumes that molecules physically adsorb on a solid in layers infinitely; no lateral interaction between each adsorption layer. However, LI applies for each layer. The resulting relation is expressed by Eq. 2.39.

$$q_e = \frac{K_B C_e Q^o}{(C_s - C_e)[1 + (K_B - 1)(\frac{C_e}{C_s})]} \tag{2.39}$$

where Q^o is maximum adsorption capacity for a single layer. Note that in 2.39, when $C_e << C_s$ and $KB >> 1$ and $K_{ad} = \frac{K_B}{C_s}$, BET isotherm approaches LAI. Moreover, many unusual isotherms are fitted well by BET as there are three coefficients to manipulate [61].

2.6.4 Capillary Pressure Correlations and Models

Capillary pressure (P_c) is an important parameter in modeling reservoir flow behavior. Usually, it is measured in core analysis laboratories. However, conventional techniques to measure P_c are expensive and time consuming.

Thus, a number of correlation models have been suggested to calculate P_c and some of them are highlighted as follows. The models are used to fit measured data and summarize the data with a small set of parameters.

i. Leverett j-function

Leverett proposed the following correlation based on gas/water of P_c data for drainage and imbibition.

$$P_{cgw} = \sigma_{gw}\sqrt{\frac{\Phi}{k}}j(S_w) \tag{2.40}$$

The function j(S_w) is referred to as Leverett j-function or simply j-function. It is used to correlate P_c of cores with different permeability but similar porosity and wettability. It is obtained by plotting $\frac{P_{cgw}}{\sigma_{gw}}\sqrt{\frac{\Phi}{k}}$ against S_w.

The j-function has been used for correlating capillary pressure data for rocks with similar pore types and wettability but with different permeabilities. This model was developed to obtain a dimensionless function to average core P_c curves to obtain the most representative curve for a field . The restrictions on the model is that particularly good results are obtained only in unconsolidated sands and from the same formation [64].

ii. Thomeer Model

Thomeer developed the following empirical model based on P_c profile from core sample.

$$\frac{P_c}{P_{ct}} = e^{\frac{-G}{\ln\left(\frac{S_{HG}}{S_{HG\infty}}\right)}} \tag{2.41}$$

where S_{HG} mercury saturation. Thomeer model has in addition three parameters; threshold pressure (P_{ct}), pore geometric factor (G) and mercury saturation at infinite capillary pressure ($S_{HG\infty}$). Low values of G indicate well sorted pore throats whereas high values indicate poorly sorted pore throats and this associates capillary pressure to the pore throat distribution. However, it is not always easy to estimate G; particularly for shally reservoirs and tight rocks with low permeability [65, 66].

iii. Brooks and Corey Model

Brooks and Corey developed an empirical correlation based on the concept of threshold pressure (P_d). The threshold pressure indicates that pressure reached a maximum value to form a continuous network across the sample. Left side of Eq. 2.42 indicates effective saturation.

The variable lambda (λ) describes pore size distribution on the core samples. λ is dimensionless parameter which depends on fitting parameters (a,b) and effective porosity as shown in Eq. 2.43.

$$\frac{S_w - S_{wr}}{1 - S_{wr}} = \left(\frac{P_d}{P_c}\right)^{\lambda} \tag{2.42}$$

$$\lambda = e^{(a+b\ln(\frac{\phi_e}{100})} \tag{2.43}$$

iv. Bentsen and Anli

Bentsen and Anli postulated a drainage capillary pressure model in which a core initially saturated with water is invaded by an oil. The expression is given by Eq. 2.44.

$$P_{cow} = P_{ct} - P_{cs}\ln\left(\frac{S_w - S_{wi}}{1 - S_{wi}}\right) \tag{2.44}$$

where P_{cs} is a parameter with pressure units for controlling the shape of the capillary pressure function. The authors suggested that the model overcomes some of the limitations of *j-function*. Moreover, it involves three parameters to be obtained experimentally. Range of parameters for several rock/oil/water systems were suggested but the means to obtain those parameters are not reported [66, 67].

v. S.M. Skjæveland Correlation

Skjævland et al. developed P_c correlation for mixed wet reservoirs that covers primary drainage, imbibition, secondary drainage, and hysteresis scanning loops [68]. The expression is given by:

$$P_c = \frac{c_w}{\left(\frac{S_w - Swr}{1 - Swr}\right)^{a_w}} + \frac{c_o}{\left(\frac{S_o - Sor}{1 - Sor}\right)^{a_o}} \tag{2.45}$$

where a and c are constants and there is one set for imbibition and another for drainage. Most of the correlations mentioned before are applicable for water-wet reservoirs and besides, they are limited to primary drainage and capillary pressure. However, it is indicated that most reservoirs are at wettability condition other than completely water-wet. [69]. Therefore, this model offers representative capillary pressure curves for numerical modeling with varying wettability [68].

Chapter 3

Numerical Model

3.1 Methodology

As indicated in section 1.3, the objective is modelling spontaneous imbibition of smart water into non water-wet carbonate core by using water-wet and oil-wet cases and capture the effect of sulfate concentration in the imbibing fluid. Sulfate concentration is varied in the injected fluid and corresponding wettability alteration is investigated. Using the approach established, experimental data will be matched by using the procedure of weight factor between a water-wet and oil-wet cases. Furthermore, relation between wettability index and ECLIPSE 100 weight factor will investigated. Relation between adsorbed sulfate and weight factor is described.

The workflow is described as follows.

i. The outermost grid blocks surround the core sample is filled with imbibing water in the *BASE.DATA* file. The core is isolated from the surrounding water by closing the boundary as shown below.

EQUALS

- -	multiplier	i		j		k	
MULTR	*0*	*40*	*40*	*1*	*20*	*19*	*58 /*
MULTZ	*0*	*1*	*40*	*1*	*20*	*18*	*18 /*
MULTZ	*0*	*1*	*40*	*1*	*20*	*58*	*58 /*

/

ii. Sulfate concentration in the imbibing water is varied. In the *BASE.DATA* file there is *WSURFACT* keyword which sets surfactant concentration in the injection well. Desired sulfate concentration is inserted under this keyword.

iii. Restart file*(BASE_RST.UNRST)* is obtained from the *BASE.DATA* file run.

iv. In the *BASE_RST.DATA)* file, spontaneous imbibition (no injection and production wells) is initiated by opening up the core in so that water imbibes freely as indicated in the grid model.

EQUALS

- -	multiplier	i		j		k	
MULTR	*1*	*40*	*40*	*1*	*20*	*19*	*58/*
MULTZ	*1*	*1*	*40*	*1*	*20*	*18*	*18/*
MULTZ	*1*	*1*	*40*	*1*	*20*	*58*	*58/*

/

However, the procedures mentioned above can be automated to reduce time and avoid repetitions by creating a BATCH file. A BATCH file is created with names of the *BASE* file and *BASE_RST* and saved in a *.BAT* file
Assuming the two files are in the same folder and desired sulfate concentration adjusted in the *BASE* file, the *.BAT* file can then be run by double clicking it.

The reference concentration is seawater sulfate concentration which is $24mM$. Concentration is varied from no sulfate concentration ($0S$) to four times seawater sulfate concentration ($4S$). The experimental data that will be matched in the end is also conducted in the same procedure.

As explained in the mechanism of smart water (section 2.4), during imbibition, sulfate ion from the imbibing water is attached to the surface of the rock releasing crude oil components. Thus, based on the amount of sulfate ion adsorbed, wettability of the rock is altered. Weighting of oil-wet to water-wet saturation function is referred to as *Weight Factor* (WF) in ECLIPSE 100. It is tabulated as a function of the adsorbed surfactant concentration. Weight factor is provided in the second column of *SURFADDW* keyword. The experimental data is matched by adjusting the sulfate concentration and WF (also denoted by F_4 in ECLIPSE 100 manual).

3.2 Input Parameters

3.2.1 Grid Model

The numerical model contains a total of 96,000 blocks in cylindrical coordinates ($60x20x80$ in r, θ and z-direction respectively). The core sample was represented by 40 grid blocks in r-direction, 20 in θ-direction, and 40 in z-direction. In order to mimic imbibition cell, the core sample is surrounded by a 100%water saturated outermost grid blocks as shown in Figure 3.1. The outermost grid blocks is represented by 41-60 in r-direction, 1-18 from the top and 59-80 from bottom in z-direction.

Table 3.1: *Grid properties*

	r	θ	z	ϕ	k(mD)	S_{wi}	S_{or}
Core	$1-40$	$1-20$	$19-58$	0.49	2	0.09	0.12
Outermost block	$41-60$	$1-20$	$1-18/59-80$	0.99	100.0000	1	0

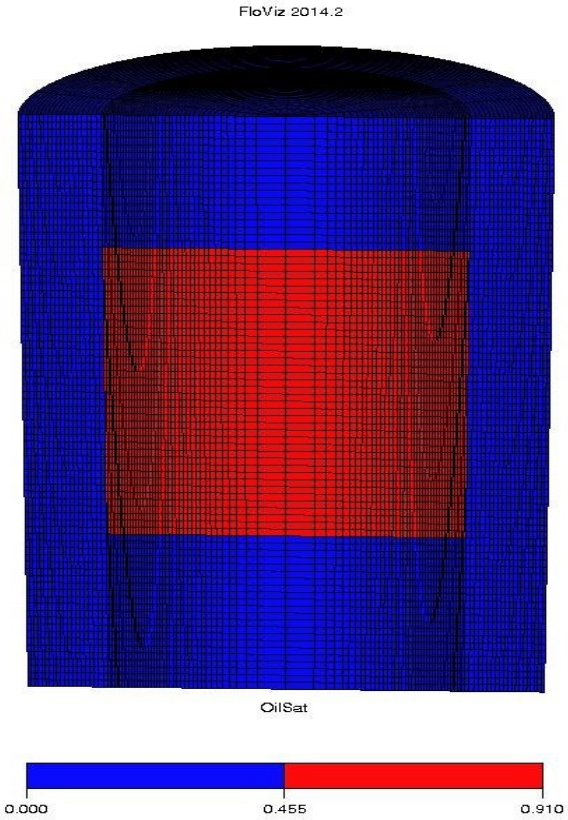

Figure 3.1: *Grid mode used in the simulation (red for the core)*

3.2.2 Fluid property

Fluid properties at the temperature and pressure the laboratory experiment conducted (90 ^oC and 10 bar respectively). Note that some of fluid parameters are estimated from closely related fluid at similar conditions.

Table 3.2: *Fluid properties*

	Density(g/cc)	Viscosity (cP)	B_w,B_o	AN	IFT(dynes/cm)
Water	0.9847	0.35	1	-	20
Oil	0.7834	0.65	-	0.5	

3.2.3 Relative Permeabilities

Two saturation tables should be provided; immiscible water-wet and immiscible oil-wet. The two saturations tables are used for oil-wet and water-wet region defined under *SATNUM* and *SURFWNUM* keywords respectively. The third saturation table for miscible region (*SURFNUM*), which is important in surfactant model, is ignored by providing the same saturation table as in the immiscible oil-wet region. The reason is that miscibility is not expected in smart water injection. As sulfate adsorbed on the surface of the rock, wettability is altered and that is reflected in the weight factor under *SURFADDW* keyword. A value of 1 implies only the oil-wet saturation function is used and a value of 0 implies purely water-wet saturation function is used. The value shouldn't be greater than 1 or less than 0.

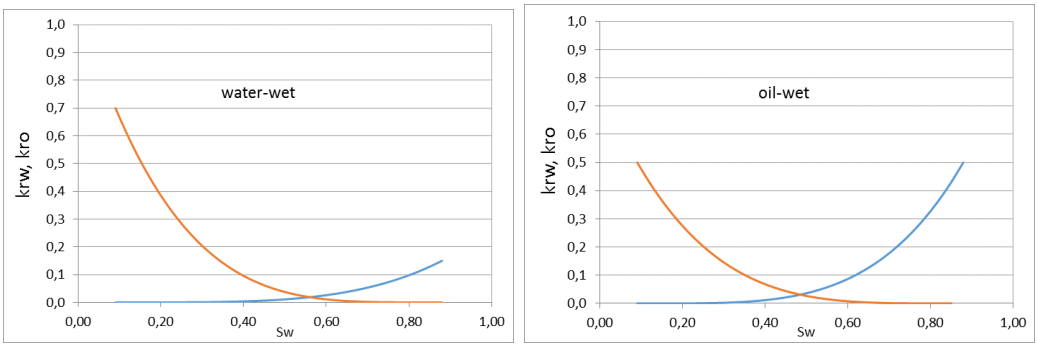

(a) Water-wet *(b) Oil-wet*

Figure 3.2: *Water-wet and oil-wet relative permeability curve modified from [20].*

Relative permeability for the outermost grid blocks surrounding the core is simply linear. Grid blocks out side of the core is filled with injected water initially. Thus, the water saturation is unity.The relative permeability curves for both water and oil varies linearly. Moreover, the capillary pressure is zero for all saturations value.

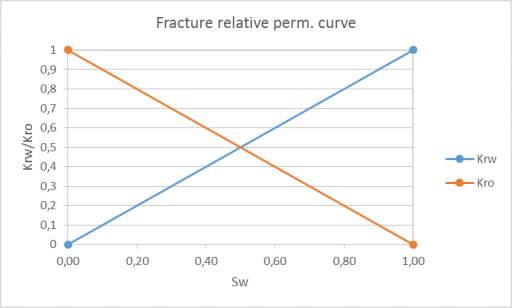

Figure 3.3: *Outermost block relative permeability curve [30].*

3.2.4 Capillary Pressure

Capillary pressure used in the simulation for water-wet and oil-wet cases are shown below. Maximum gravity head for the core sample is *115 Pa* and the oil wet P_c is adjusted in such a way that gravity effect is eliminated. Gravity influence will be discussed later.

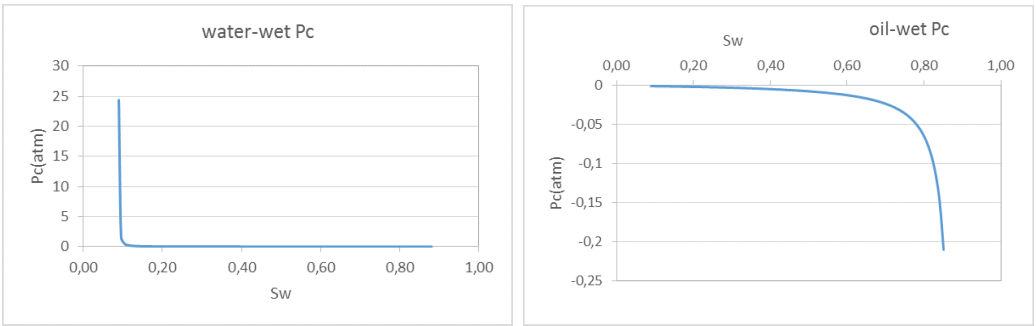

(a) Water-wet capillary pressure *(b) Oil-wet capillary pressure*

Figure 3.4: *Water-wet and oil-wet capillary pressure modified from [16].*

3.2.5 Adsorption Isotherm

Linear isotherm is assumed and the maximum adsorbed amount, *R(g/g)* is determined from the relation 3.1. The adsorbed amount is limited by the adsorbent surface available for adsorption and injected concentration. In this experiment, 4 times SW sulfate concentration is the optimum sulfate concentration in the imbibing fluid. Injecting much higher sulfate concentration would not produce any extra oil due the fact that it is higher than the adsorption capacity of the core. Moreover, sulfate concentration higher than 4 times SW suggested to result in precipitation of $CaSO_4$. Normally, lower amount of potential determining ions such as Ca^{2+} is injected. The reason is formation water supplies extra Ca^{2+}. Thus, higher SO_4^{2-} concentration than required leads to shortage of Ca^{2+}. This affects SI process which is the result of a temperature dependent and symbiotic effect of SO_4^{2-} and Ca^{2+} [70].

$$R(g/g) = \frac{C_{inj} q \Delta t}{m_{rock}} \tag{3.1}$$

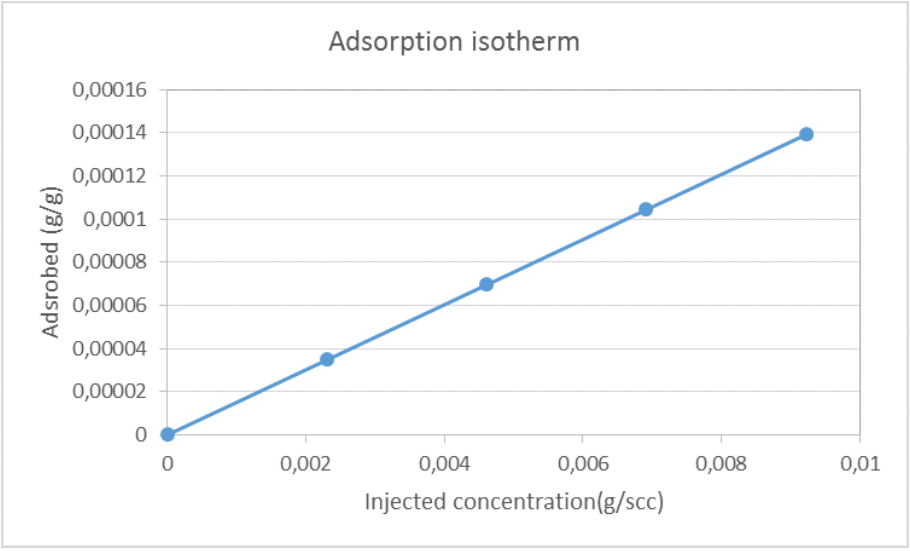

Figure 3.5: *Linear adsorption isotherm.*

Chapter 4

Results and Discussions

The methodology has also been outlined in section 3.1. The basic input data required has been presented in section 3.2. In this section, results from the simulation and history matching are presented.

4.1 Spontaneous imbibition in water-wet and oil-wet cases

As stated in the objective of this thesis, by using water-wet and oil-wet cases, SI into non water-wet core is modelled. Establishing SI for the two extreme cases (water-wet and oil-wet) is the first step. The result for water-wet and oil-wet cases is shown in Figure 4.1. As indicated in the figure, there no recovery for both cases from 0 to 7 days. During this period, imbibing fluid is injected in the outermost grid blocks surrounding the core. Then, as shown in section 3.1, the core boundary is opened so that the water imbibes freely.

No SI and hence no oil recovery is observed for oil-wet case. However, for water-wet case, SI initiated almost instantly. It is discussed in the theory part that, oil recovery in fractured carbonate rocks mainly depends on SI. However, SI is insignificant in oil-wet core and this is reflected in the results obtained. Influence of gravity is discussed in history matching phase.

The *SURFADDW* entry is shown in Table 4.1. The first column is the adsorbed amount(g/g) while the second column is weight factor for corresponding cases.

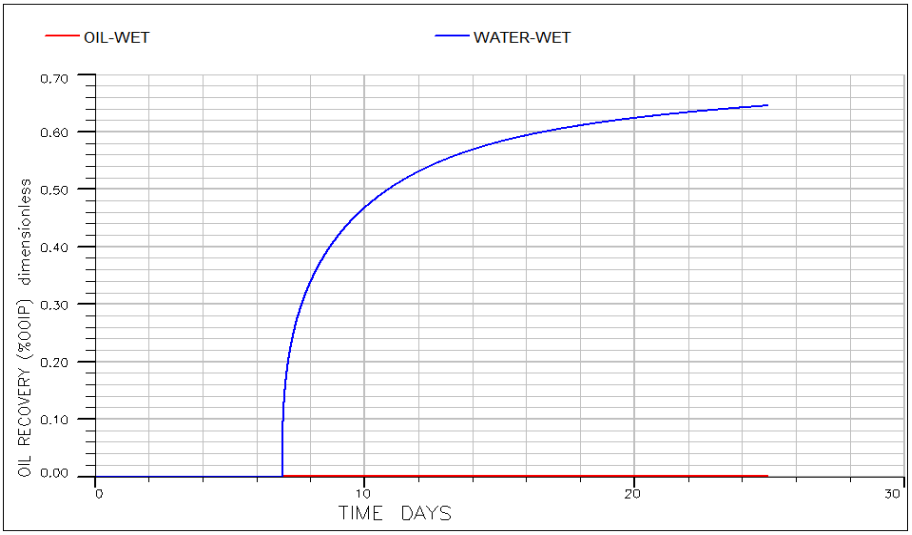

Figure 4.1: *Recovery efficiency for water-wet and oil-wet.*

Table 4.1: *SURFADDW keyword*

SURFADDW		
First column	Second column	
Adsorption(g/g)	water-wet	oil-wet
0.000000000	0	1
0.000034799	0	1
0.000069598	0	1
0.000104397	0	1
0.000139196	0	1

The second column of *SURFADDW* is the weight factor (WF). WF = 0 for all entry in first column corresponds to water-wet case whereas WF = 1 for all entry in first column is for oil-wet case. For any wetting state between the extremes, the WF starts from initial wetting state to maximum achieved wetting state that corresponds to maximum adsorption.

Maximum recovery achieved in carbonate core sample can be correlated to wettability index as discussed in section 2.1.4. Moreover, the rule of thumb discussed in section 2.1.4 is employed here to calculate the *'calculated wettability index'* listed in the subsequent discussions. In the Figure 4.1, 65% recovery is achieved for water-wet case. This corresponds to $I_w = 87\%$. Similarly, the oil-wet case corresponds to $I_w = 0$ which is oil-wet.

4.2 History Matching

The experimental data to be matched in the established procedure is presented below [56]. The experiment was conducted on chalk core. Fluid and core properties are listed in the input section 3.2. Moreover, the experiment was carried out at 90 ^oC and hence, fluid expansion is expected. Thermal expansion should be taken into account. Thermal coefficient of the oil is $0.001/^oC$. An increase of 70 ^oC from room temperature gives recovery of 7%. Therefore, the experimental date corrected for thermal expansion is provided below.

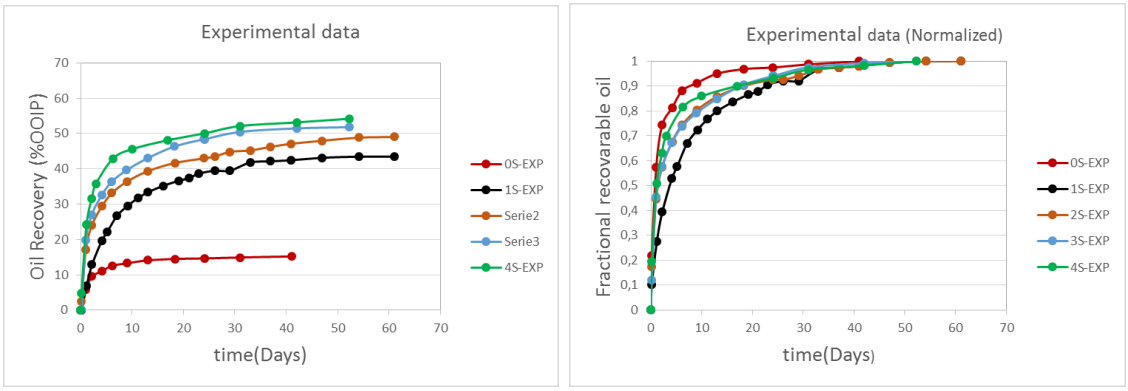

(a) Experimental data (recovery vs time) *(b) Normalized*

Figure 4.2: *Experimental data to be matched [56].*

The imbibing fluid used in the laboratory experiment is presented in Table 4.2. In the laboratory experiment, modified seawater depleted in $NaCl$ and spiked with different amount of SO_4^{2-} is used. Ordinary SW has $24mM$ sulfate concentration. Five imbibing fluids have been used for SI experiment. They are denoted as 'XS' where 'X' stands for "X times the SO_4^{2-} concentration of ordinary SW ". For example 0S implies no sulfate concentration and 4S signifies four times SW SO_4^{2-} concentration.

Table 4.2: *Ionic composition(mM) of imbibing fluid*

Smart water used					
Ions(mM)	0S	1S	2S	3S	4S
Na^+	2	50	98.1	146	194.1
Ca^{2+}	13	13	13	13	13
Mg^{2+}	45.5	45-5	45.5	45.5	45.5
Cl^-	125	125	125	125	125
SO_4^{2-}	0	24	48	72	92
HCO_3^-	2	2	2	2	2
TDS(g/l)	6.6	10.1	13.42	16.83	20.24
IS(mol/L	0.18	0.26	0.33	0.40	0.47

I. 0S

As shown in Figure 4.3, oil recovery of 15% is achieved by imbibing with seawater depleted in $NaCl$ and no sulfate concentration. The imbibing fluid (0S) contains no wettability altering agent as it has no SO_4^{2-}. Thus, it represents the initial wetting of the core. If it were completely oil-wet, there would be no recovery due to SI. Normalized simulated and experimental recovery data are presented below.

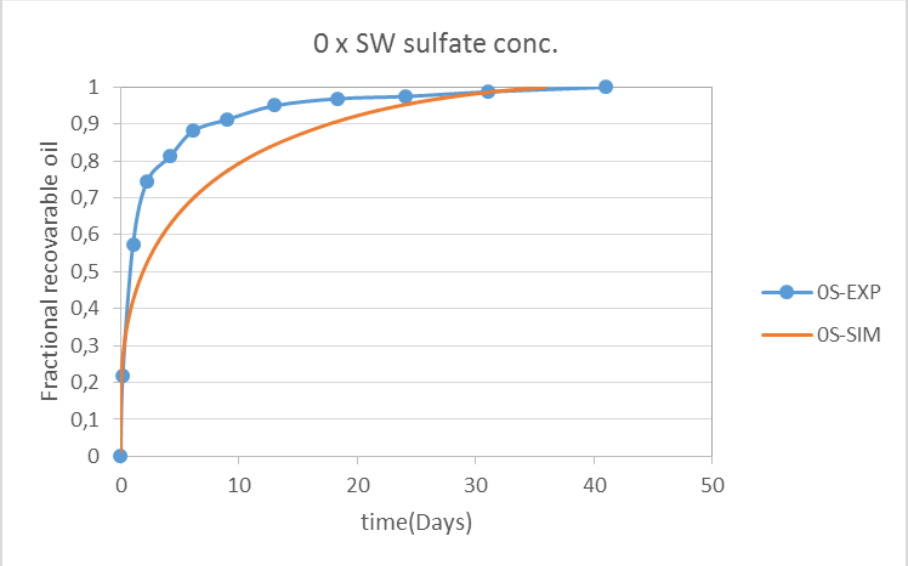

Figure 4.3: *Spontaneous Imbibition with 0S.*

Wettability index calculated in using the correlation presented in section 2.1.4 is $I_w = 0.2$. The wettability index calculated based on a rule of thumb gives the same result. The weight factor that matched the recovery is also shown with the in Table 4.3. In the experimental data, 0S reaches plateau in a bit shorter time compared to other curves shown in Figure 4.2. This is in line with the suggested mechanism of smart water. There is no adsorption and desorption process which might be slower process compared to recovery due to initial wetting state of the core. However, the simulated data is slow to reach plateau compared to the experimental data. This is due to gravity effect which is particularly noticeable in slightly water-wet cases.

Table 4.3: *0S, Weight factor and I_w*

SURFADDW		Calculated	Maximum Oil Recovered (%)
Adsorbed (g/g)	Weight factor	Wettability index	15
0.000000000	0.88	0.20	

Saturation function and capillary pressure used to generate the simulated curve are shown below. ECLISPE 100 uses WF to generate respective curves. It is hardly possible to read the capillary (Pc) values, therefore tabulated values are found in the appendix B.1.

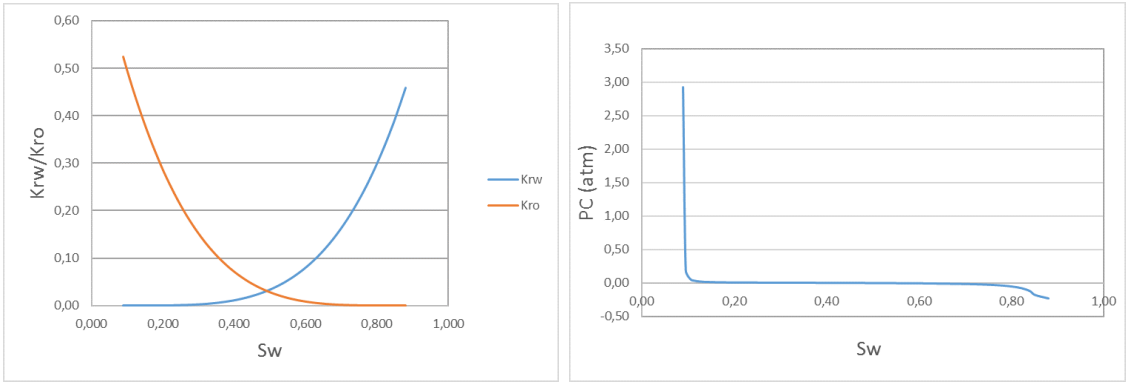

(a) Saturation curve for 0S *(b) Pc curve for 0S*

Figure 4.4: *Saturation and capillary pressure curve for 0S.*

II. 1S

When the sulfate concentration is increased to seawater sulfate concentration which is $24mM$, recovery increased to 44%. The only significant difference between 0S and 1S fluid is the concentration of SO_4^{2-}. Thus, it is reasonable to attribute the higher recovery jump to wettability alteration due to adsorption of SO_4^{2-}. Moreover, the simulated data is a bit faster than the experimental data to reach plateau. This trend applies also for other imbibing fluid concentrations discussed below. Normalized simulated and experimental recovery data are presented in Figure 4.5.

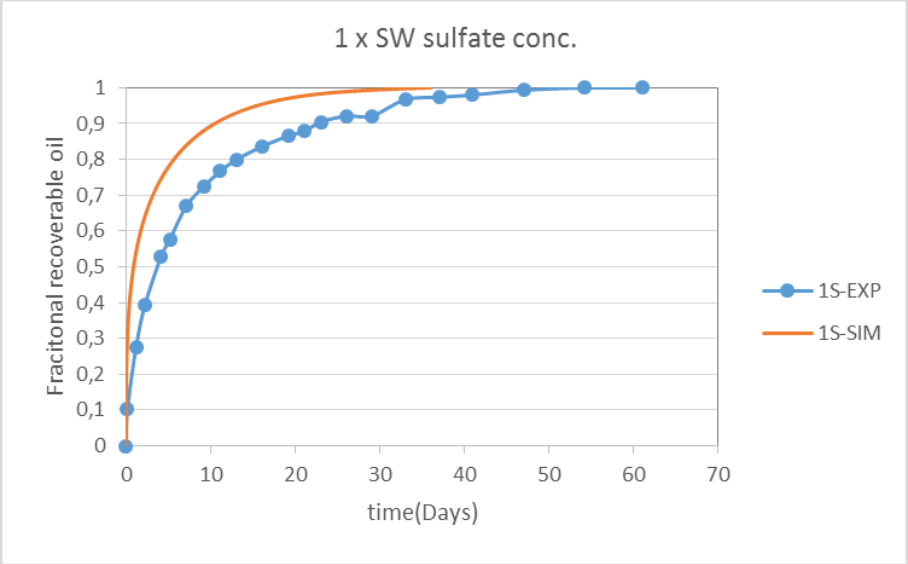

Figure 4.5: *Spontaneous Imbibition with 1S.*

Table 4.4 shows maximum adsorbed amount and corresponding WF. For any adsorbed value between the maximum and minimum (0.0 in this case), ECLIPSE 100 applies linear interpolations.

Table 4.4: *1S, Weight factor and* I_w

SURFADDW		Calculated	Maximum Oil Recovered (%)
Adsorbed (g/g)	Weight factor	Wettability index	44
0.000000000	0.88	0.2	
0.000034799	0.27	0.59	

Compared to 0S, recovery increased from 15% to 44% OOIP. However, this is a big jump compared to recovery increase achieved by other concentrations as indicated in ***III ,IV ,V*** below. This is due to initial wetting of the core which is related to the low AN (0.5) of the injected oil. Table 4.4 indicates that the initial wetting of the core sample is slightly water-wet. A similar experiment conducted in slightly higher temperature and oil with high AN (2.07) shows relatively a uniform increase in recovery as SO_4^{2-} concentration increases. As discussed in the section 2.4, a higher AN implies a less water-wet condition. Therefore, it requires more adsorption of SO_4^{2-}. Generally, the result shows that modification of wettability at the waterfront is able to create capillary forces strong enough to displace oil from very low permeable matrix blocks.

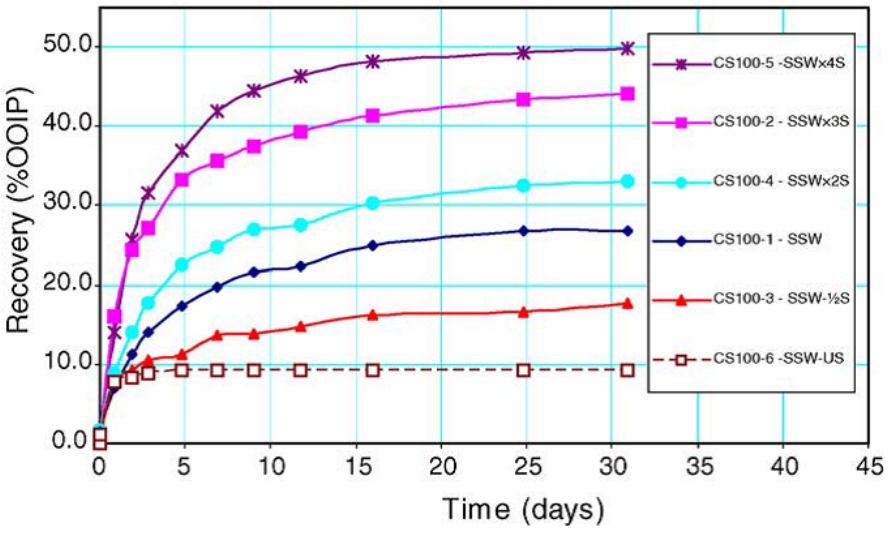

Figure 4.6: *SI using chalk core varying SO_4^{2-} concentration [71]*

Conducted at 100 ^oC, (AN = 2.07 mgKOH/g)

Saturation function and capillary pressure used to generate the simulated curve are shown Figure 4.7a and 4.7b respectively.

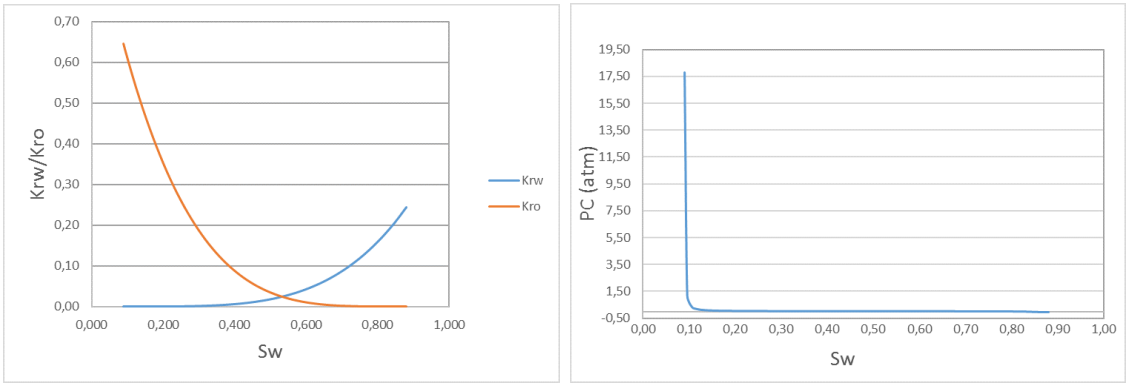

(a) Saturation curve for 1S *(b) Pc curve for 1S*

Figure 4.7: *Saturation and capillary pressure curve for 1S.*

III. 2S

Spontaneous imbibition with 2S has increased recovery from 44% in 1S to 49%. However, it could be said that it is minimal increase compared to the increase from zero sulfate to one times seawater sulfate concentration. Based on Figure 4.8 one can say, relatively, a close match is observed between the simulated and experimental data suggesting that the model matches better as water wetness increases.

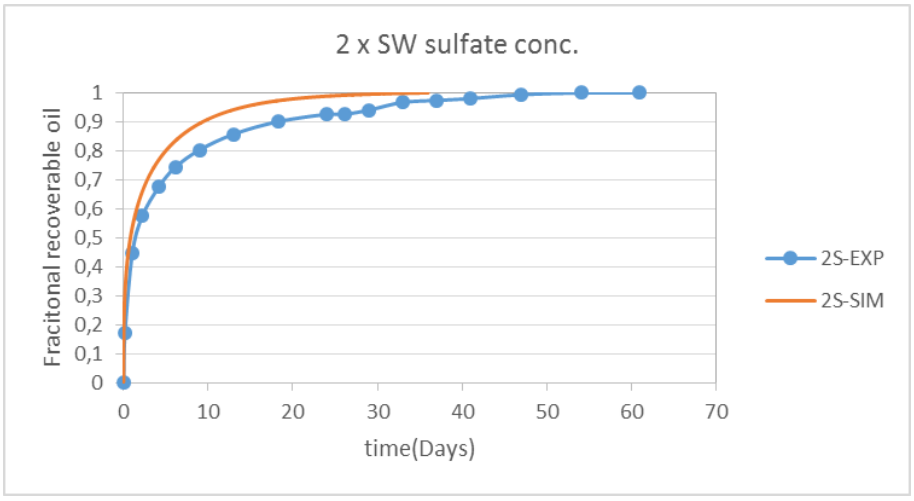

Figure 4.8: *Spontaneous Imbibition with 2S.*

Adsorbed amount and WF, and calculated wettability index is shown in Table 4.5.

Table 4.5: *2S, Weight factor and I_w*

SURFADDW		Calculated	Maximum Oil Recovered (%)
Adsorbed (g/g)	Weight factor	Wettability index	
0.000000000	0.88	0.2	
0.000034799	0.27	0.59	49
0.000069598	0.265	0.65	

Saturation function and capillary pressure used to generate the simulated curve are shown Figure 4.9a and 4.9b respectively.

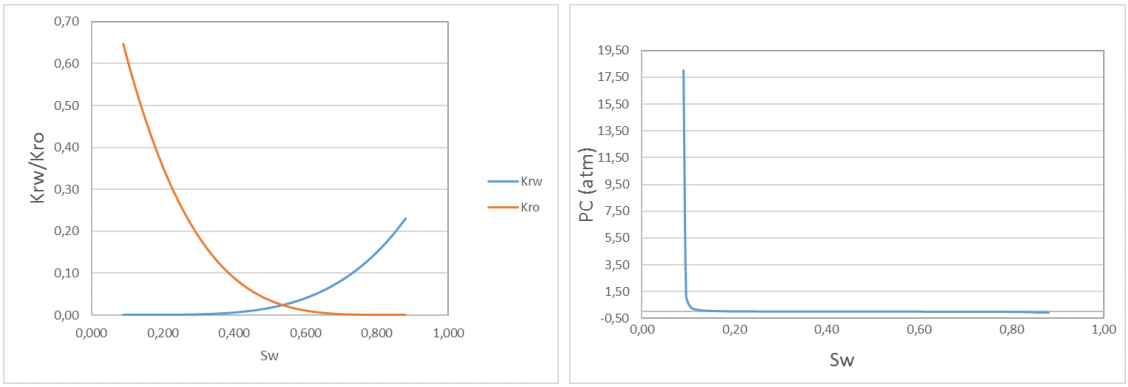

(a) Saturation curve for 2S *(b) Pc curve for 2S*

Figure 4.9: *Saturation and capillary pressure curve for 0S.*

IV. 3S

With imbibing fluid of 3S only only a slight increase in oil recovery is observed. It could be said that there is excellent match between the simulated and experimental data. Even though minor increase is observed compared to ***2S***, as indicated in Figure 4.10, considerable improvement in terms of capturing features of the experimental curve. High sulfate concentration results in dominance of the water-wet curve which in turn leads to relatively accelerated and high recovery. Corresponding weight factor and wettability index is shown in Table 4.6.

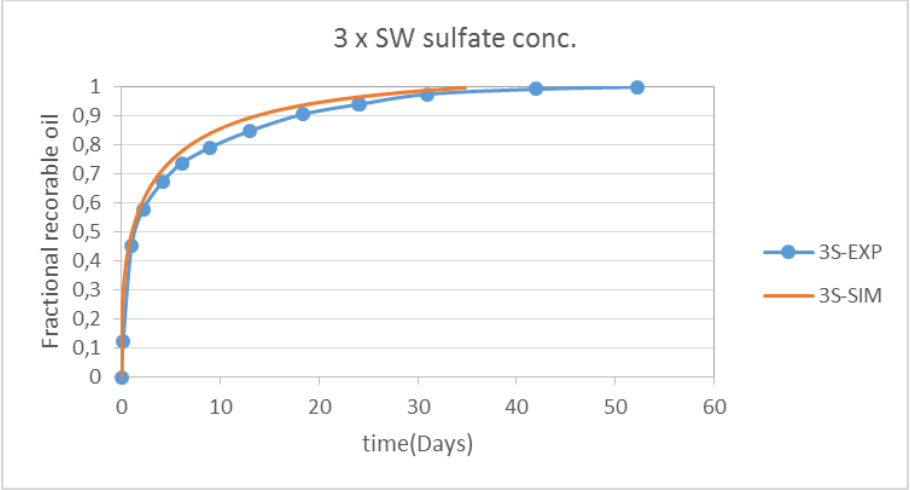

Figure 4.10: *Spontaneous Imbibition with 3S.*

Table 4.6: *3S, Weight factor and* I_w

SURFADDW		Calculated	Maximum Oil Recovered (%)
Adsorbed (g/g)	Weight factor	Wettability index	
0.000000000	0.88	0.2	
0.000034799	0.27	0.59	51
0.000069598	0.265	0.65	
0.000104397	0.22	0.68	

Saturation function and capillary pressure used to generate the simulated curve are shown Figure 4.11a and 4.11b, respectively.

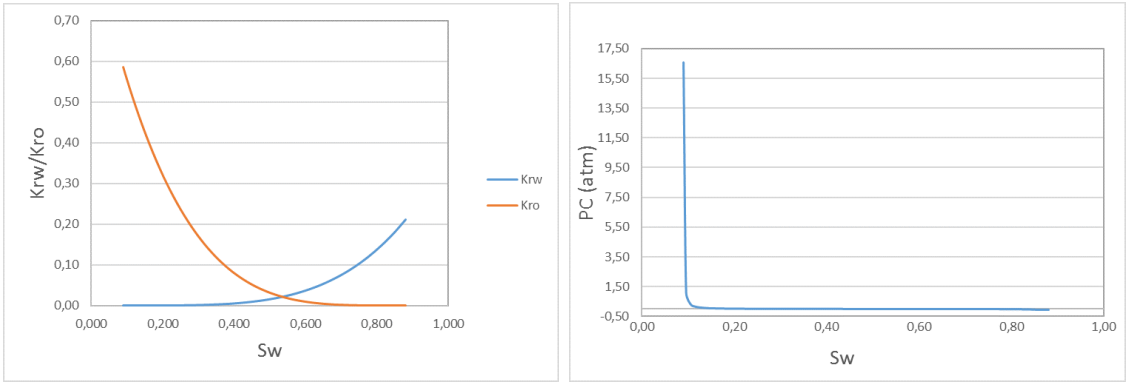

(a) Saturation curve for 3S *(b) Pc curve for 3S*

Figure 4.11: *Saturation and capillary pressure curve for 3S.*

V. 4S

Spontaneous imbibition with 4S gave the maximum recovery. It is also evident from Figure 4.12 that the simulated curve is almost identical to the experimental data. This confirms the suggestion that the model matches better as water wetness increases. In terms of maximum recovery, there is an increase compared to 3S. Moreover, one can notice that 4S not only gave maximum recovery but also relatively shorter time to reach plateau. This is indication that as sulfate concentration increases water wetness increases and this results higher and accelerated recovery.

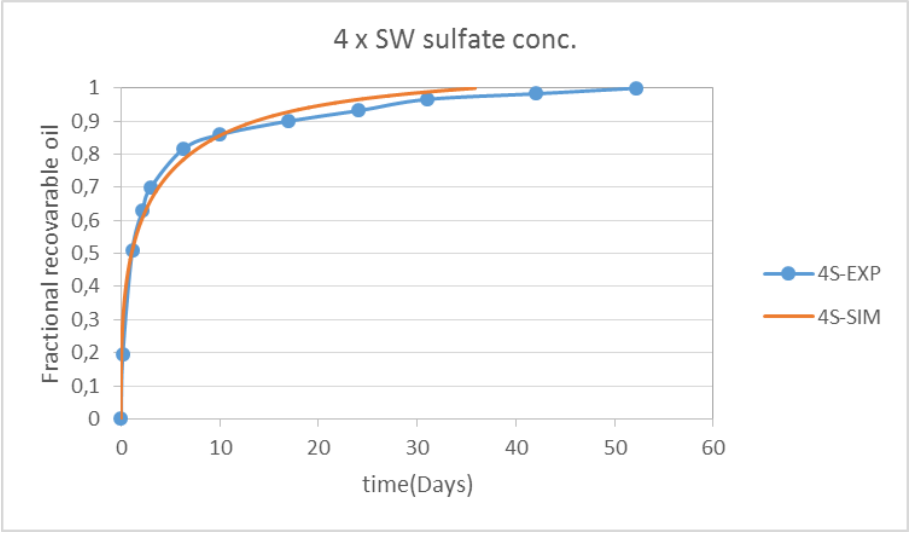

Figure 4.12: *Spontaneous Imbibition with 4S.*

Table 4.7 indicates adsorption during imbibition of 4S and corresponding WF and wettability index. Note that one curve is matched after the other and hence curve for 4S is the last one to be matched. The maximum adsorbed amount occurs during imbibition of 4S as evidenced by highest recovery and fastest curve relatively.

Table 4.7: *4S, Weight factor and* I_w

SURFADDW		Calculated	Maximum Oil Recovered (%)
Adsorbed (g/g)	Weight factor	Wettability index	
0.000000000	0.88	0.2	
0.000034799	0.27	0.59	
0.000069598	0.265	0.65	55
0.000104397	0.22	0.68	
0.000139196	0.19	0.73	

Saturation function and capillary pressure used to generate the simulated curve are shown Figure 4.13a and 4.13b respectively.

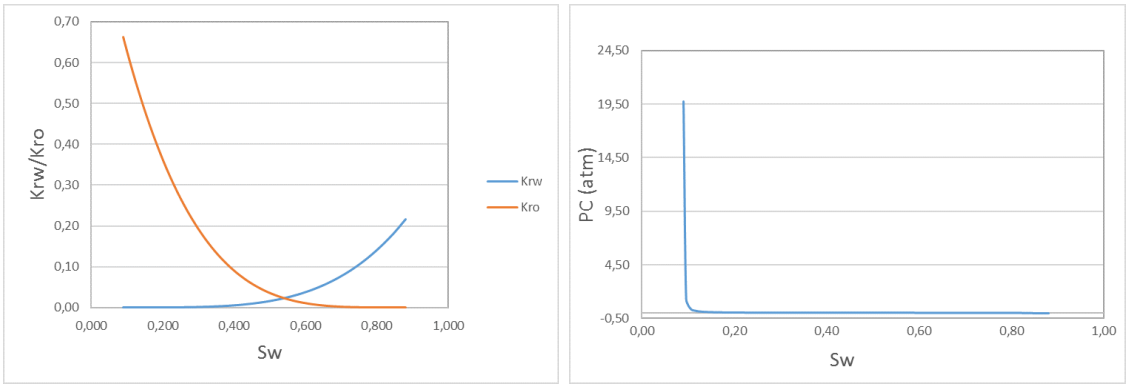

(a) Saturation curve for 4S *(b) Pc curve for 4S*

Figure 4.13: *Saturation and capillary pressure curve for 4S.*

ECLIPSE plot indicating recovery for all imbibing fluids is shown in Figure 4.14. No recovery is observed until 7 days. This is because the grid blocks surrounding the core is filled with imbibing fluid during this period. Thus, as mentioned in methodology (section 3.1), the core sample is isolated by closing the boundary until the restart file is created.

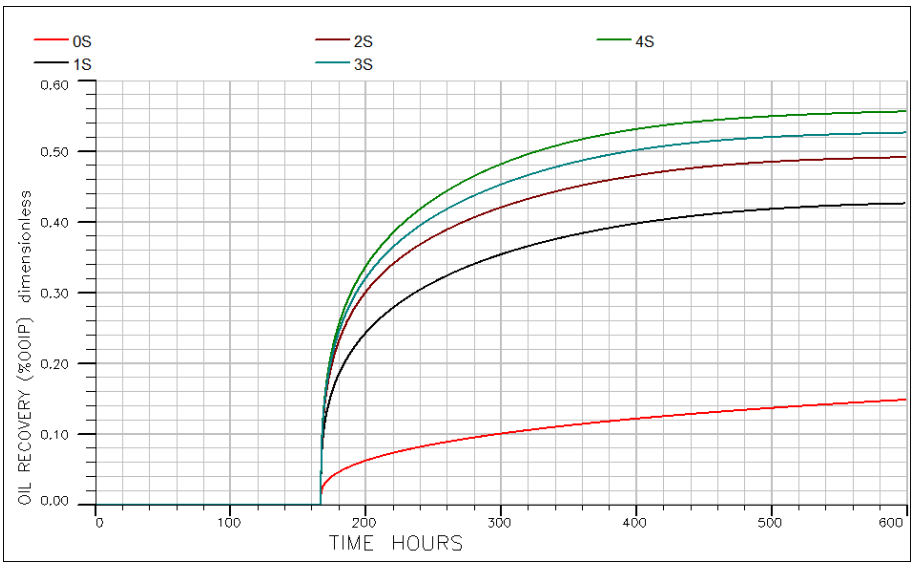

Figure 4.14: *Spontaneous Imbibition with 0S, 1S, 2S, 3S and 4S.*

4.2.1 Summary of History Matching

Based on the history matching presented above one can draw the following conclusions:

- The simulated curves, for the most part, are able to capture the most important features of the experimental data. Recovery during imbibition of 0S represent initial state of the core whereas recovery during imbibition of ***1S***, ***2S***, ***3S*** and ***4S*** represent dynamic alteration of wettability due adsorption of sulfate.
- From the normalized experimental data, there is a slight difference in the time it takes to reach plateau. A similar trend is observed in the simulated value also except the case of ***0S*** which could be due to gravity effect however small it is. However, in the experimental data (normalized), ***0S*** is in fact the fastest one. This is due to the initial wetting of the core sample unlike other cases which the increase in water wetness is due to adsorption of sulfate. The adsorption and desorption process could take some time. Thus, the simulated curve for ***0S*** could not exactly capture the features observed in the corresponding experimental curve.
- Generally, the simulated curves are faster than the experimental curves. Nevertheless, the overall match between experimental and simulated data is very good. Obviously, one can notice that the model better fits the experimental data as final water wetness increases. This is particularly true for the cases of ***2S***, ***3S*** and ***4S***.

4.3 Correlation between Adsorption and Weight Factor

History matching by using weight factor (WF) has been shown in section 4.2. Overall adsorption and WF used in the history matching is presented below. It is good to note that in ECLIPSE 100, *WF = 1* signifies oil-wet whereas *WF= 0* represents water-wet.

Table 4.8: *Adsorption and Weight Factor*

Adsorption (g/g)	WF
0.000000000	0.88
0.000034799	0.27
0.000069598	0.265
0.000104397	0.22
0.000139196	0.19

The water wetness of the core increases as more sulfate adsorbs on the surface of the core. This implies that there is opposite trend between WF and wettability index. Figure 4.15 shows overall correlation between adsorption and WF.

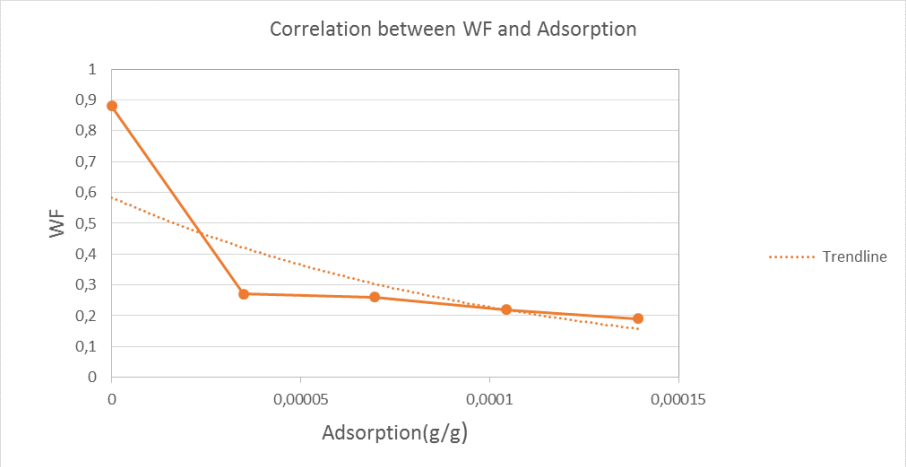

Figure 4.15: *Correlation between Adsorption(g/g) and WF*

4.4 Correlation between Weighing Factor and Wettability Index

The experimental data has been matched by controlling weighting factor in *SURFADDW* keyword in the *BASE_RST.DATA* file. It is interesting to investigate if there is any correlation between weight factor (*WF*) used and the wettability index *(I_w)* for each sulfate concentration in the imbibing fluid. Weight factor and corresponding wettability index is presented in Table 4.9.

Table 4.9: *Weight factor and Wettability index*

Weight Factor	Wettability Index
0.88	0.2
0.27	0.59
0.265	0.65
0.22	0.68
0.19	0.73

As shown in the Table 4.9, when adsorption increases WF decreases. However, I_w seem to show opposite trend.

Figure 4.16 depicts WF against calculated I_w and the corresponding trendline is also shown. One can conclude that there is positive correlation between WF and I_w. The implication with this is that given the maximum recovery, one can estimate the WF from the correlation. WF describes the oil wet-to water-wet ration that is dependent on the adsorption of the surfactant injected (sulfate in this case). I_w describes the maximum achieved recovery which in turn depends on wettability. The two parameters are inherently describe wettability but from different perspective.

As shown in history matching section, there is a big gap between recovery based 0S and 1S as imbibing fluid. That gap is reflected in Figure 4.16. Unfortunately there is no imbibition at $\frac{1}{2}$S in the experimental data provided. It would have given insight how the curves behave between 0S and 1S.

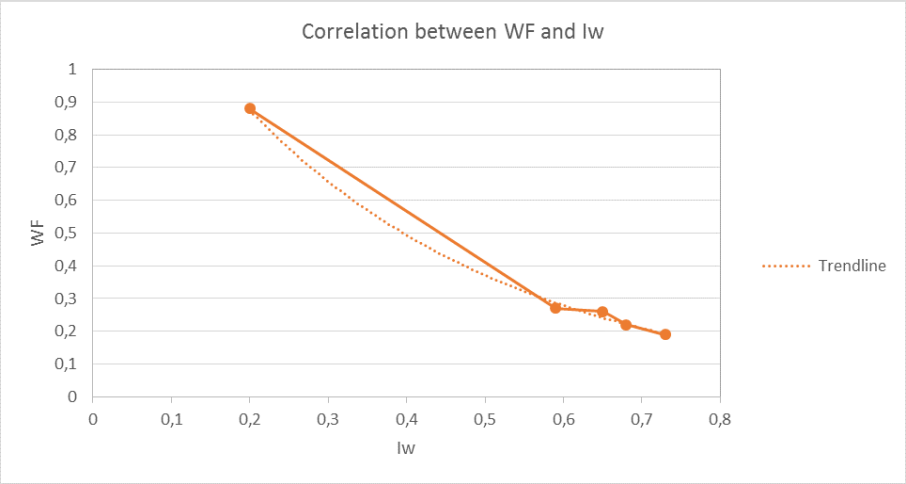

Figure 4.16: *Correlation between WF and* I_w

4.5 Gravity Influence

Gravity plays significant role in expelling the oil from the matrix block on field basis. In laboratory scale as well, particularly when the height of the core increases, gravity effect is clearly observed. However, for the core height used in this model which is 4cm, recovery due to gravity is minimal and thus recovery is dominated by SI. Besides, maximum gravity head including the outermost grid blocks is calculated to be *115Pa* and capillary pressure is adjusted to take this into account. Figure 4.17 , indicates recovery solely due to gravity. In order to investigate recovery purely due to gravity, zero capillary pressure is assumed. Moreover, zero sulfate concentration is injected. Recovery due to gravity is characterized by slow but steady recovery. It is reasonable to conclude that the recovery is rather dominated by spontaneous imbibition due to wettability alteration.

Høgnesen [72], used similar grid block dimensions and investigated the effect of gravity. He concluded that recovery due to gravity becomes dominant especially if core height is over *1m*. He demonstrated that, horizontal extension has also some effect on recovery. Increase in horizontal dimension causes depletion of SO_4^{2-} from the waterfront due adsorption and hence as water saturation increases capillary force decreases. Moreover, gravity effect becomes dominant as horizontal extension of the cores increases. Capillary pressure induced by sulfate could contribute significantly even though the size of the core is increased to D=*3.5m* and H = *6.91m* [72]

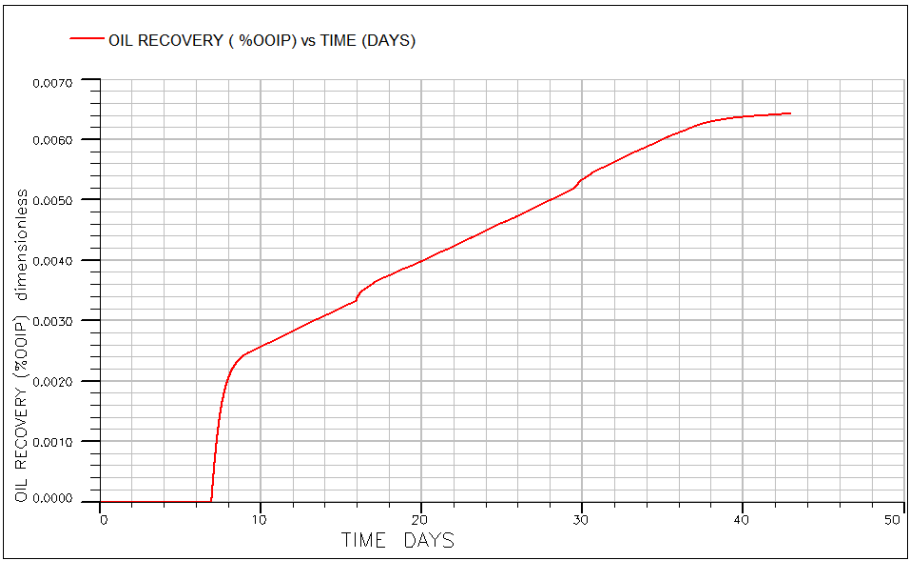

Figure 4.17: *Recovery due to gravity*

4.6 Sensitivity analysis

4.6.1 Numerical Dispersion Error

To investigate the error due to numerical dispersion, simulation run with three types of grid blocks is carried out. A fine grid consisting of 80x50x90 in r-direction, *θ-direction* and *z-direction* respectively. A coarse grid of 30x20x40 is used. The 4S imbibing fluid is used for this investigation. As indicated in Figure 4.18, the curve based on the coarse grid is faster than the the two fine grids. This is due to the waterfront becoming smeared in coarse grid. Curves based on the two fine grids blocks superimposed on one another. They also seem slower than the coarse grid curve. A more sharp front is expected in the fine grid blocks than the coarse grid.

All simulations presented in this paper are run with 60x40x80 as indicated in the section 3.2 (Input parameters). Based on the simulation run, one can conclude that there is not significant numerical error that is caused by grid dimension on the results presented in this study. The grid can be refined further at a cost of increased runtime but no significant difference would be observed. Thus, the grid block dimension used this study provides acceptable results regarding numerical dispersion.

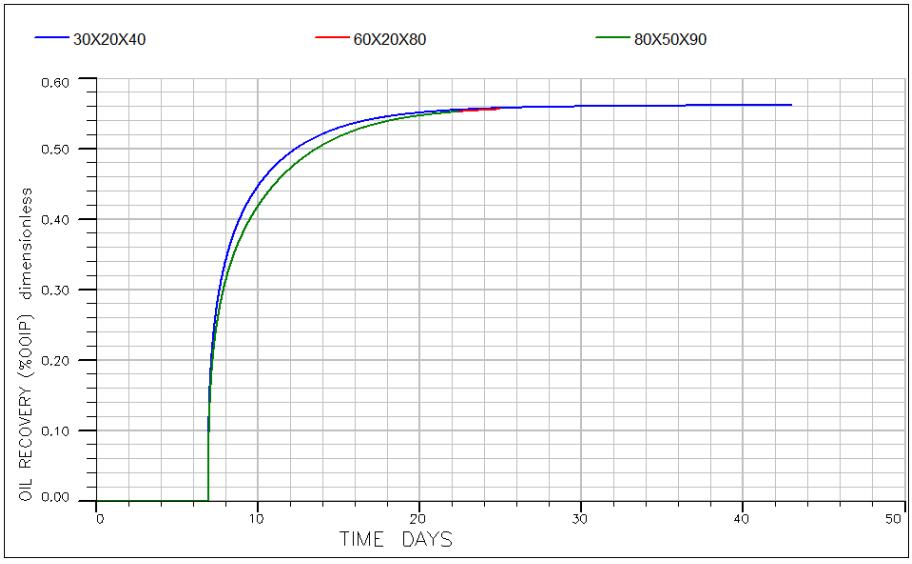

Figure 4.18: *Oil Recovery (%OOIP) vs Time (Days) using fine and coarse grid- 4S*

4.6.2 Effect of Weight Factor

In the history matching section, WF has been used to match the experimental data. It is also pointed out that as water wetness increases WF decreases. In order to investigate how significant WF is on the model. Analysis of the effect of WF on the model is carried out using 4S as imbibing fluid. The WF used in each case is presented in Table 4.10.

Table 4.10: *Effect of Weight Factor*

Adsorption(g/g)	WF1	WF2	WF3
0.000000000	0.88	0.98	0.78
0.000034799	0.27	0.37	0.17
0.000069598	0.265	0.365	0.165
0.000104397	0.22	0.32	0.12
0.000139196	0.19	0.29	0.09

WF1 is weight factor used in the history matching procedure for 4S as imbibing fluid. For the same adsorption, WF3 < WF1 < WF2 as indicated in Table 4.10. Based on Figure 4.19, it is clear that the model is sensitive to WF. Consequently, the WF is a function of adsorption and hence maximum recovery depends on the WF used.

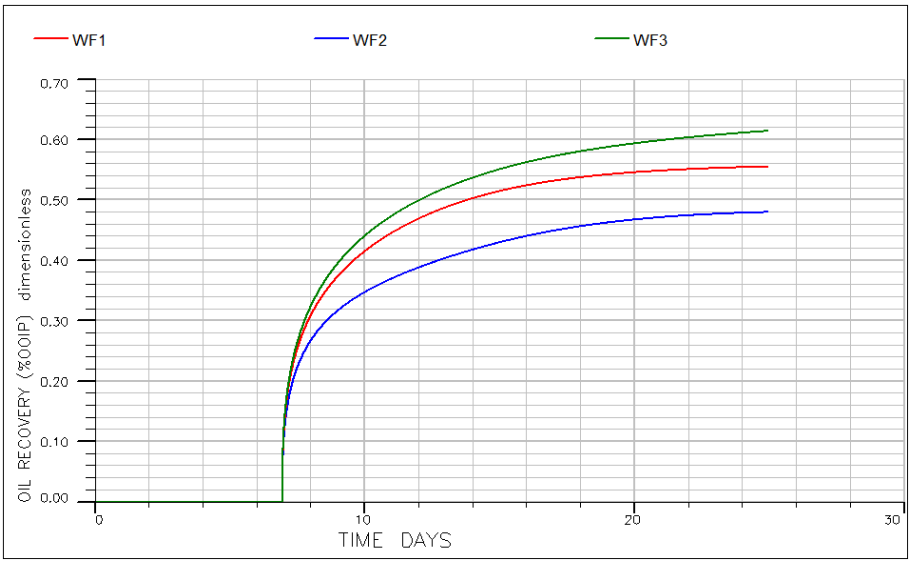

Figure 4.19: *Effect of Weight Factor- 4S as imbibing fluid.*

4.6.3 Effect of Capillary Pressure

Capillary pressure has huge impact on efficiency of smart water in releasing trapped oil. Oil displacement process depends, among other parameters, on capillary pressure which in turn depends on wettability of the reservoir rock. Thus, the alteration of wettability from oil-wet to water-wet changes the capillary pressure from negative to positive and thereby initiates spontaneous imbibition [35, 73]. Figure 4.20 indicates the effect of capillary pressure during imbibition of 4S with different Pc. When Pc is increased twice, recovery increased from 55% to 65% OOIP. However, when Pc in reduced by half recovery reduced from 55% to 44% OOIP. It is apparent that the model is sensitive to Pc. Thus, the input Pc value has significant role on the maximum recovery achieved.

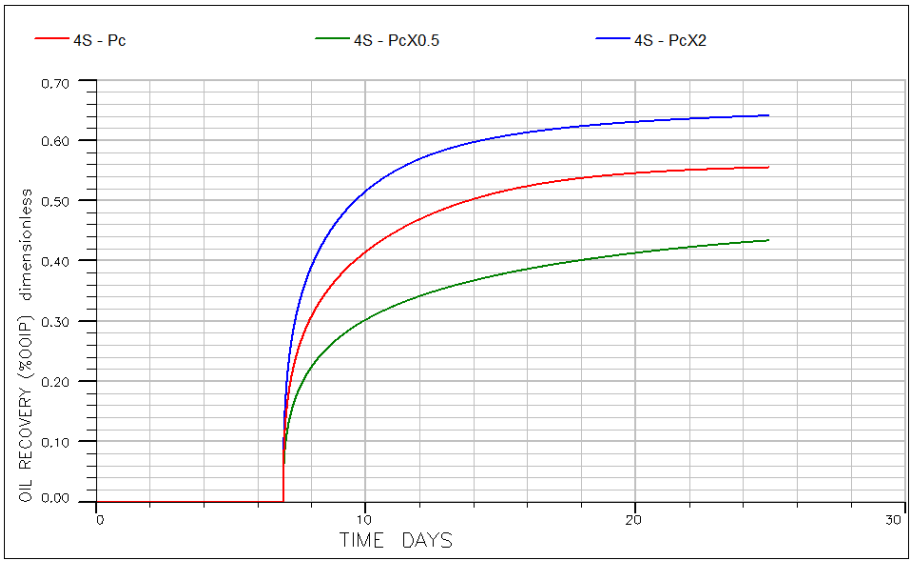

Figure 4.20: *Capillary pressure effect using 4S as imbibing fluid*

Chapter 5

Summary and Conclusion

The main objective of this study was dynamic modeling of wettability alteration due to spontaneous imbibition of smart water into preferentially oil-wet core using water-wet and oil-wet cases. Using the established model and weight factor, the model is tested by history matching laboratory data. Moreover, investigating if there exists correlation between parameters such as WF, adsorption and wettability index has been done. Based on the results observed in this study one can draw the following conclusions:

1. ECLIPSE 100 black oil Surfactant Model simulator is able to model dynamic wettability alteration of spontaneous imbibition of smart water into preferentially oil-wet carbonate. Nevertheless, it should be emphasized that the model does not capture detailed chemistry of wettability alteration, but rather the overall effect of smart water injection in wettability alteration that could be extended to field scale.

2. Generally, the simulated curves are faster than the experimental curves. However, the overall match between experimental and simulated data is very good. Obviously, one can notice that the model better fits the experimental data as final water wetness increases. This is particularly true for the cases of ***2S***, ***3S*** and ***4S***.

3. There seems to be a correlation between adsorbed amount and weight factor and furthermore, a correlation between WF and wettability index is also observed.

4. The basic model that could be used for further investigations or upscaling to field scale is established.

In this study, there is no adsorption isotherm relevant to core samples which the laboratory experiment conducted; therefore, linear adsorption isotherm is assumed. Moreover, as stated in 3.2, fluid properties such as density and viscosity are not provided at conditions the laboratory experiment conducted. Nevertheless, properties of a closely related fluid measured at the same temperature and pressure is used. Probably, this can introduce some uncertainty in the results observed. Nevertheless, some parameters can be estimated without affecting the overall results.

The model could be improved with precise fluid and core input parameters that are obtained at the conditions intended to model. In the sensitivity studies, it is observed that the model is sensitive to grid block dimension, weight factor and capillary pressure. Furthermore, parameters such as adsorption, saturations functions have obviously considerable effect on the results obtained. Generally, accuracy of such model rests upon the accuracy of the input parameters. Therefore, for further investigation and upscaling of a similar model, it is recommended to be aware of the impact of the accuracy of the aforementioned input parameters.

ECLIPSE 100 is industry standard and most widely used simulator. Certainly, the current version does not specifically describe the complex interactions among different phases and species involved in chemically tuned injection water. Sulfate is considered to be the main wettability alteration agent in smart water. On the other hand, other potential determining ions such as Ca^2+ and Mga^2+ have a role to play in the adsorption of sulfate and desorption of polar components. ECLIPSE 100 do not has the facility to account for the effect of other ions. However, it offers dynamic modeling capability that is representative of the overall effect of smart water injection.

Bibliography

[1] J. Cai, X. Hu, D. C. Standnes, and L. You, "An analytical model for spontaneous imbibition in fractal porous media including gravity," *Colloids and Surfaces A: Physicochemical and Engineering Aspects*, vol. 414, pp. 228–233, 2012.

[2] "Crain's petrophysical handbook - wettability of porous rocks," https://www.spec2000.net/09-wettability.htm, (Accessed on 04/04/2016).

[3] R. Nelson, in *Geologic Analysis of Naturally Fractured Reservoirs*, second edition ed. Gulf Professional Publishing, 2001. ISBN: 978-0-88415-317-7. [Online]. Available: http://www.sciencedirect.com/science/article/pii/B9780884153177500002

[4] E. W. Al-Shalabi, K. Sepehrnoori, and G. A. Pope, "Modeling the combined effect of injecting low salinity water and carbon dioxide on oil recovery from carbonate cores," in *International Petroleum Technology Conference, IPTC-17862-MS*. International Petroleum Technology Conference, 2014.

[5] M. Seyyedi and M. Sohrabi, "Enhancing water imbibition rate and oil recovery by carbonated water in carbonate and sandstone rocks," *Energy & Fuels*, vol. 30, no. 1, pp. 285–293, 2015.

[6] K. Sunil and A. AL-Kabab, "Enhanced oil recovery:challenges and opportunities ,p64-69_kokal-al_kaabi.pdf," http://www.world-petroleum.org/docs/docs/publications/2010yearbook/P64-69_Kokal-Al_Kaabi.pdf, (Accessed on 04/18/2016).

[7] A. A. Yousef, S. Al-Saleh, A. U. Al-Kaabi, and M. S. Al-Jawfi, "Laboratory investigation of novel oil recovery method for carbonate reservoirs," in *Canadian Unconventional Resources and International Petroleum Conference*. SPE-137634-MS, Society of Petroleum Engineers, 2010.

[8] A. Lager, K. Webb, C. Black, M. Singleton, and K. Sorbie, "Low salinity oil recovery-an experimental investigation1," *Petrophysics*, vol. 49, no. 01, 2008.

[9] T. Austad, S. Strand, M. V. Madland, T. Puntervold, and R. I. Korsnes, "Seawater in chalk: An EOR and compaction fluid," in *International Petroleum Technology Conference, SPE-118431-PA*. International Petroleum Technology Conference, 2007.

[10] A. A. Yousef, S. Al-Saleh, and M. S. Al-Jawfi, "The impact of the injection water chemistry on oil recovery from carbonate reservoirs," in *SPE EOR Conference at Oil and Gas West Asia, SPE-154077-MS*. Society of Petroleum Engineers, 2012.

[11] T. Austad, S. Strand, E. Høgnesen, and P. Zhang, "Seawater as IOR fluid in fractured chalk," in *SPE International Symposium on Oilfield Chemistry, SPE-93000-MS*. Society of Petroleum Engineers, 2005.

[12] "Factpages - norwegian petroleum directorate," http://factpages.npd.no/FactPages/default.aspx?nav1=field&nav2=PageView%7CAll&nav3=43506, (Accessed on 04/18/2016).

[13] L. Yu, S. Evje, H. Kleppe, T. Kårstad, I. Fjelde, and S. Skjaeveland, "Spontaneous imbibition of seawater into preferentially oil-wet chalk cores—experiments and simulations," *Journal of Petroleum Science and Engineering*, vol. 66, no. 3, pp. 171–179, 2009.

[14] P. O. Andersen, R. Ahsan, S. Evje, F. Bratteli, M. V. Madland, and A. Hiorth, "A model for brine-dependent spontaneous imbibition experiments with porous plate," in *EAGE Annual Conference & Exhibition incorporating, SPE Europec, SPE-164901-MS*. Society of Petroleum Engineers, 2013.

[15] P. V. Brady and J. L. Krumhansl, "A surface complexation model of oil-brine-sandstone interfaces at 100 ^{o}C: Low salinity waterflooding," *SPE-163053-PA, Journal of Petroleum Science and Engineering*, vol. 81, pp. 171–176, 2012.

[16] C. Qiao, L. Li, R. T. Johns, and J. Xu, "A mechanistic model for wettability alteration by chemically tuned waterflooding in carbonate reservoirs," *SPE Journal, SPE-170966-MS*, 2015.

[17] D. C. Standnes and T. Austad, "Wettability alteration in carbonates: Interaction between cationic surfactant and carboxylates as a key factor in wettability alteration from oil-wet to water-wet conditions," *Colloids and Surfaces A: Physicochemical and Engineering Aspects*, vol. 216, no. 1, pp. 243–259, 2003.

[18] D. C. Standnes and T. Austad, "Wettability alteration in chalk: 1. preparation of core material and oil properties," *Journal of Petroleum Science and Engineering*, vol. 28, no. 3, pp. 111–121, 2000.

[19] R. Gupta and K. K. Mohanty, "Wettability alteration of fractured carbonate reservoirs," in *SPE Symposium on Improved Oil Recovery, SPE-113407-MS*. Society of Petroleum Engineers, 2008.

[20] C. Qiao, R. Johns, L. Li, and J. Xu, "Modeling low salinity waterflooding in mineralogically different carbonates," in *SPE Annual Technical Conference and Exhibition, SPE-175018-MS*. Society of Petroleum Engineers, 2015.

[21] Schlumberger, *Eclipse Technical Description.* Schlumberger, 2014.

[22] W. G. Anderson, "Wettability literature survey- part 1: Rock/oil/brine interactions and the effects of core handling on wettability, SPE-13932-PA, Society of Petroleum Engineers," 1986.

[23] G. Jerauld and J. Rathmell, "Wettability and relative permeability of Prudhoe bay: a case study in mixed-wet reservoirs," *SPE Reservoir Engineering*, vol. 12, no. 01, pp. 58–65, 1997.

[24] D. C. Standnes, "Enhanced oil recovery from oil-wet carbonate rock by spontaneous imbibition of aqueous surfactant solutions." 2001, University of Stavanger, PhD Thesis.

[25] R. Salathiel, "Oil recovery by surface film drainage in mixed-wettability rocks," *Journal of Petroleum Technology*, vol. 25, no. 10, pp. 1–216, 1973.

[26] W. Anderson, "Wettability literature survey-part 2: Wettability measurement," *Journal of Petroleum Technology*, vol. 38, no. 11, pp. 1–246, 1986.

[27] T. Young, "An essay on the cohesion of fluids," *Philosophical Transactions of the Royal Society of London*, vol. 95, pp. 65–87, 1805.

[28] B. Raeesi, N. R. Morrow, and G. Mason, "Effect of surface roughness on wettability and displacement curvature in tubes of uniform cross-section," *Colloids and Surfaces A: Physicochemical and Engineering Aspects*, vol. 436, pp. 392–401, 2013.

[29] C. S. Vijapurapu, D. N. Rao, and L. Kun, "The effect of rock surface characteristics on reservoir wettability," in *SPE/DOE Improved Oil Recovery Symposium, SPE-75211-MS.* Society of Petroleum Engineers, 2002.

[30] W. Abdallah, J. S. Buckley, A. Carnegie, J. Edwards, B. Herold, E. Fordham, A. Graue, T. Habashy, N. Seleznev, and C. Signer, "Fundamentals of wettability," *Technology*, vol. 38, no. 1125-1144, p. 268, 1986.

[31] E. C. Donaldson, R. D. Thomas, and P. B. Lorenz, "Wettability determination and its effect on recovery efficiency," *Society of Petroleum Engineers Journal*, vol. 9, no. 01, pp. 13–20, 1969.

[32] M. Crocker and L. Marchin, "Evaluation and determination of cross correlations between wettability methods. status report," National Inst. for Petroleum and Energy Research, Bartlesville, OK (USA), Tech. Rep., 1986.

[33] S. Strand, D. Standnes, and T. Austad, "New wettability test for chalk based on chromatographic separation of SCN- and SO_4^{2-}," *Journal of Petroleum Science and Engineering*, vol. 52, no. 1, pp. 187–197, 2006.

[34] H. Aksulu, "Effect of core cleaning solvents on wettability restoration and oil recovery by spontaneous imbibition in surface reactive, low permeable limestone reservoir cores," 2010, University of Stavanger, MSc Thesis.

[35] W. Anderson, "Wettability literature survey-part 4: Effects of wettability on capillary pressure," *Journal of Petroleum Technology*, vol. 39, no. 10, pp. 1–283, 1987.

[36] F. Craig, "The reservoir engineering aspect of waterflooding," *SPE Monograph Series*, vol. 3, 1971.

[37] B. Caudle, R. Slobod, and E. Brownscombe, "Further developments in the laboratory determination of relative permeability," *Journal of Petroleum Technology*, vol. 3, no. 05, pp. 145–150, 1951.

[38] P. Zhang and T. Austad, "Waterflooding in chalk–relationship between oil recovery, new wettability index, brine composition and cationic wettability modifier (SPE94209)," in *67th EAGE Conference & Exhibition*, 2005.

[39] P. Zhang and T. Austad, "The relative effects of acid number and temperature on chalk wettability," in *SPE International Symposium on Oilfield Chemistry, SPE-92999-MS*. Society of Petroleum Engineers, 2005.

[40] S. Ali, "Characterization of naturally fractured reservoirs through well test analysis," http://emaze.com/finalpresentation, (Accessed on 04/19/2016).

[41] M. A. Fernø, *Enhanced Oil Recovery in Fractured Reservoirs*, ser. Department of

Physics and Technology, University of Bergen Norway. INTECH Open Access Publisher, http://www.intechopen.com, DOI= 10.5772/34732, 2012.

[42] Å. Haugen, "Fluid flow in fractured carbonates: wettability effects and enhanced oil recovery," 2010, University of Bergen, ISBN: 9788230815496.

[43] J. Cai, E. Perfect, C. Cheng, and X. Hu, "Generalized modeling of spontaneous imbibition based on hagen–poiseuille flow in tortuous capillaries with variably shaped apertures," *Langmuir*, vol. 30, no. 18, pp. 5142–5151, 2014.

[44] D. C. Standnes, "A single-parameter fit correlation for estimation of oil recovery from fractured water-wet reservoirs," *Journal of Petroleum Science and Engineering*, vol. 71, no. 1, pp. 19–22, 2010.

[45] J. C. Reis and M. Cil, "A model for oil expulsion by counter-current water imbibition in rocks: one-dimensional geometry," *Journal of Petroleum Science and Engineering*, vol. 10, no. 2, pp. 97–107, 1993.

[46] R. Iffly, D. Rousselet, and J. Vermeulen, "Fundamental study of imbibition in fissured oil fields." in *Annual Technical Conference, Dallas, Texas, USA, SPE-4102-MS*, 1972.

[47] M. Shouxiang, N. R. Morrow, and X. Zhang, "Generalized scaling of spontaneous imbibition data for strongly water-wet systems," *Journal of Petroleum Science and Engineering*, vol. 18, no. 3, pp. 165–178, 1997.

[48] N. Fries and M. Dreyer, "An analytic solution of capillary rise restrained by gravity," *Journal of Colloid and Interface Science*, vol. 320, no. 1, pp. 259–263, 2008.

[49] L. Handy, "Determination of effective capillary pressures for porous media from imbibition data," *Trans. AIME*, vol. 219, pp. 75–80, 1960.

[50] W. F. Pickard, "The ascent of sap in plants," *Progress in Biophysics and Molecular Biology*, vol. 37, pp. 181–229, 1981.

[51] A. Franken, J. Nolten, M. Mulder, D. Bargeman, and C. Smolders, "Wetting criteria for the applicability of membrane distillation," *Journal of Membrane Science*, vol. 33, no. 3, pp. 315–328, 1987.

[52] J. Buckley, Y. Liu, and S. Monsterleet, "Mechanisms of wetting alteration by crude oils," *SPE journal*, vol. 3, no. 01, pp. 54–61, 1998.

[53] S. J. Fathi, T. Austad, and S. Strand, "Water-based enhanced oil recovery

(EOR) by" Smart Water" in carbonate reservoirs," in *SPE EOR Conference at Oil and Gas West Asia, SPE-154570-MS*. Society of Petroleum Engineers, 2012.

[54] T. Austad and D. C. Standnes, "Spontaneous imbibition of water into oil-wet carbonates," *Journal of Petroleum Science and Engineering*, vol. 39, no. 3, pp. 363–376, 2003.

[55] S. J. Fathi, T. Austad, and S. Strand, ""Smart Water" as a wettability modifier in chalk: The effect of salinity and ionic composition," *Energy & Fuels*, vol. 24, no. 4, pp. 2514–2519, 2010.

[56] T. Puntervold, S. Strand, R. Ellouz, and T. Austad, "Modified seawater as a smart EOR fluid in chalk," *Journal of Petroleum Science and Engineering*, vol. 133, pp. 440–443, 2015.

[57] T. Austad, S. Shariatpanahi, S. Strand, C. Black, and K. Webb, "Conditions for a low-salinity enhanced oil recovery (EOR) effect in carbonate oil reservoirs," *Energy & Fuels*, vol. 26, no. 1, pp. 569–575, 2011.

[58] T. Hassenkam, A. C. Mitchell, C. S. Pedersen, L. Skovbjerg, N. Bovet, and S. L. S. Stipp, "The low salinity effect observed on sandstone model surfaces," *Colloids and Surfaces A: Physicochemical and Engineering Aspects*, vol. 403, pp. 79–86, 2012.

[59] N. Morrow and J. Buckley, "Improved oil recovery by low-salinity waterflooding," *Journal of Petroleum Technology*, vol. 63, no. 05, pp. 106–112, 2011.

[60] "Adsorption isotherm and its types — chemistry learning," http://www.chemistrylearning.com/adsorption-isotherm/, (Accessed on 05/06/2016).

[61] "Adsorption equilibria," http://mimoza.marmara.edu.tr/~zehra.can/ENVE401/3.%20Adsorption%20Equilibria.pdf, (Accessed on 05/06/2016).

[62] S. Brunauer, P. H. Emmett, and E. Teller, "Adsorption of gases in multimolecular layers," *Journal of the American Chemical Society*, vol. 60, no. 2, pp. 309–319, 1938.

[63] A. Mittal, L. Kurup, and J. Mittal, "Freundlich and Langmuir adsorption isotherms and kinetics for the removal of tartrazine from aqueous solutions using hen feathers," *Journal of Hazardous Materials*, vol. 146, no. 1, pp. 243–248, 2007.

[64] M. C. Leverett, "Flow of oil-water mixtures through unconsolidated sands," *Transactions of the AIME*, vol. 132, no. 01, pp. 149–171, 1939.

[65] J. Thomeer, "Introduction of a pore geometrical factor defined by the capillary pressure curve," *Journal of Petroleum Technology*, vol. 12, no. 03, pp. 73–77, 1960.

[66] "Capillary pressure models -," http://petrowiki.org/Capillary_pressure_models, (Accessed on 05/08/2016).

[67] R. G. Bentsen and J. Anli, "A new displacement capillary pressure model," *Journal of Canadian Petroleum Technology*, vol. 15, no. 03, 1976.

[68] S. Skjaeveland, L. Siqveland, A. Kjosavik, W. Hammervold, and G. Virnovsky, "Capillary pressure correlation for mixed-wet reservoirs," in *SPE India Oil and Gas Conference and Exhibition, SPE-60900-PA*. Society of Petroleum Engineers, 1998.

[69] N. R. Morrow, "Wettability and its effect on oil recovery," *Journal of Petroleum Technology*, vol. 42, no. 12, pp. 1–476, 1990.

[70] P. Zhang, M. T. Tweheyo, and T. Austad, "Wettability alteration and improved oil recovery in chalk: The effect of calcium in the presence of sulfate," *Energy & Fuels*, vol. 20, no. 5, pp. 2056–2062, 2006.

[71] P. Zhang and T. Austad, "Wettability and oil recovery from carbonates: Effects of temperature and potential determining ions," *Colloids and Surfaces A: Physicochemical and Engineering Aspects*, vol. 279, no. 1–3, pp. 179 – 187, 2006. [Online]. Available: http://www.sciencedirect.com/science/article/pii/S0927775706000148

[72] E. Høgnesen, D. Standnes, and T. Austad, "Experimental and numerical investigation of high temperature imbibition into preferential oil-wet chalk," *Journal of Petroleum Science and Engineering*, vol. 53, no. 1, pp. 100–112, 2006.

[73] E. C. Donaldson and W. Alam, *Wettability*. ISBN: 9781933762296, Gulf Publishing Company, Chap. 1, 1–55, 2008.

Appendix A

ECLIPSE FILE

A.1 BASE.DATA

- -THE BASE.DATA STARTS HERE.
(THIS IS A TWO COLUMN PAGE)

- - SPONTANEOUS IMBIBITION OF SMART WATER INTO POROUS MEDIA
- - ==========
RUNSPEC
TITLE
SI OF SMART WATER ONTO CHALK CORES
DIMENS
60 20 80 /
RADIAL
START
01 'OCT' 2015 /
OIL
WATER
SURFACTW
LAB
EQLDIMS
2 100 20 1 20 /
TABDIMS
6 2 100 21 3 12 /
WELLDIMS
2 50 2 2/
NUPCOL
4 /
NSTACK
50 /
UNIFOUT
UNIFIN
ENDSCALE
/
GRIDOPTS
YES /
GRID ==========
NOECHO
INCLUDE

```
grid.DATA /
DTHETA
96000*18
/ DZ
96000*0.1
/
COORDSYS
1 80 COMP /
BOX
1 60 1 20 1 80 /
PERMR
96000*100000 /
PERMTHT
96000*100000 /
PERMZ
96000*100000 /
BOX
1 40 1 20 19 58 /
PERMR
32000*2 /
PERMTHT
32000*2 /
PERMZ
32000*2 /
ENDBOX
PORO
96000*0.99 /
BOX
1 40 1 20 19 58 /
PORO
32000*0.49 /
ENDBOX
BOX 1 60 1 20 1 1 /
TOPS
1200*0
/
ENDBOX
INIT
EQUALS
MULTR 0 40 40 1 20 19 58 /
MULTZ 0 1 40 1 20 18 18 /
MULTZ 0 1 40 1 20 58 58 /
/
BOX
41 60 1 20 19 58 /
MULTPV
16000*1000 /
BOX
1 60 1 20 1 18 /
MULTPV
21600*1000 /
BOX
1 60 1 20 59 80 /
MULTPV
26400*1000 /
PROPS ======================
```

SWOF

- -Oil-Wet table (Corresponds to SATNUM number)

Sw	Krw	Kro	Pc(atm)
0.090	0.000000000	0.50000	-0.000759
0.096	0.000000001	0.48545	-0.0007641
0.105	0.000000074	0.46192	-0.00081
0.115	0.000000516	0.43925	-0.0008395
0.125	0.000001896	0.41742	-0.0009168
0.135	0.000005053	0.39642	-0.0009964
0.144	0.000011099	0.37622	-0.0010782
0.154	0.000021415	0.35680	-0.0011624
0.164	0.000037652	0.33815	-0.0012491
0.173	0.000061734	0.32023	-0.0013384
0.183	0.000095856	0.30304	-0.0014303
0.193	0.000142481	0.28655	-0.0015251
0.202	0.000204345	0.27074	-0.0016229
0.212	0.000284456	0.25559	-0.0017237
0.222	0.000386090	0.24109	-0.0018278
0.231	0.000512795	0.22722	-0.0019352
0.241	0.000668392	0.21395	-0.0020462
0.251	0.000856969	0.20127	-0.0021609
0.260	0.001082888	0.18916	-0.0022795
0.270	0.001350780	0.17761	-0.0024021
0.280	0.001665548	0.16660	-0.0025291
0.289	0.002032365	0.15611	-0.0026605
0.299	0.002456675	0.14612	-0.0027968
0.309	0.002944195	0.13661	-0.002938
0.319	0.003500909	0.12758	-0.0030845
0.328	0.004133074	0.11901	-0.0032365
0.338	0.004847219	0.11087	-0.0033944
0.348	0.005650141	0.10316	-0.0035586
0.357	0.006548911	0.09586	-0.0037293
0.367	0.007550869	0.08895	-0.0039069
0.377	0.008663624	0.08242	-0.0040919
0.386	0.009895061	0.07626	-0.0042848
0.396	0.011253331	0.07045	-0.0044859

0.406	0.012746859	0.06498	-0.004696
0.415	0.014384338	0.05983	-0.0049154
0.425	0.016174735	0.05500	-0.0051449
0.435	0.018127285	0.05047	-0.0053851
0.444	0.020251496	0.04622	-0.0056368
0.454	0.022557146	0.04224	-0.0059009
0.464	0.025054284	0.03853	-0.0061781
0.473	0.027753229	0.03507	-0.0064694
0.483	0.030664572	0.03184	-0.0067761
0.493	0.033799175	0.02885	-0.0070992
0.503	0.037168169	0.02607	-0.0074401
0.512	0.040782959	0.02349	-0.0078002
0.522	0.044655218	0.02112	-0.0081811
0.532	0.048796890	0.01892	-0.0085847
0.541	0.053220193	0.01691	-0.009013
0.551	0.057937611	0.01505	-0.0094683
0.561	0.062961904	0.01336	-0.0099531
0.570	0.068306099	0.01181	-0.0104703
0.580	0.073983495	0.01040	-0.0110231
0.590	0.080007663	0.00912	-0.01162
0.599	0.086392442	0.00797	-0.01225
0.609	0.093151947	0.00692	-0.01294
0.619	0.100300557	0.00598	-0.01367
0.628	0.107852929	0.00515	-0.01447
0.638	0.115823984	0.00440	-0.01534
0.648	0.124228920	0.00373	-0.01628
0.657	0.133083202	0.00315	-0.01731
0.667	0.142402566	0.00264	-0.01845
0.677	0.152203021	0.00219	-0.01969
0.686	0.162500845	0.00180	-0.02107
0.696	0.173312588	0.00147	-0.02260
0.706	0.184655071	0.00118	-0.02432
0.716	0.196545384	0.00094	-0.02624
0.725	0.209000889	0.00074	-0.02843
0.735	0.222039220	0.00057	-0.03092
0.745	0.235678280	0.00043	-0.03379
0.754	0.249936244	0.00032	-0.03713

0.764	0.264831557	0.00023	-0.04106
0.774	0.280382937	0.00016	-0.04575
0.783	0.296609369	0.00011	-0.05144
0.793	0.313530113	0.00007	-0.05846
0.803	0.331164697	0.00005	-0.06735
0.812	0.349532920	0.00003	-0.07894
0.822	0.368654855	0.00001	-0.09462
0.832	0.388550842	0.00001	-0.11698
0.841	0.409241493	0.00000	-0.15125
0.851	0.430747693	0.00000	-0.20991
0.880	0.500000000	0.00000	-0.26857 /

The table above is repeated here (no misicibility)

- -Oil-Wet table (Corresponds to SURFNUM number)

Sw	Krw	Kro	Pc(atm)
0.090	0.000000000	0.50000	-0.000759
0.096	0.000000001	0.48545	-0.0007641
0.105	0.000000074	0.46192	-0.00081
0.115	0.000000516	0.43925	-0.0008395
0.125	0.000001896	0.41742	-0.0009168
0.135	0.000005053	0.39642	-0.0009964
0.144	0.000011099	0.37622	-0.0010782
0.154	0.000021415	0.35680	-0.0011624
0.164	0.000037652	0.33815	-0.0012491
0.173	0.000061734	0.32023	-0.0013384
0.183	0.000095856	0.30304	-0.0014303
0.193	0.000142481	0.28655	-0.0015251
0.202	0.000204345	0.27074	-0.0016229
0.212	0.000284456	0.25559	-0.0017237
0.222	0.000386090	0.24109	-0.0018278
0.231	0.000512795	0.22722	-0.0019352
0.241	0.000668392	0.21395	-0.0020462
0.251	0.000856969	0.20127	-0.0021609
0.260	0.001082888	0.18916	-0.0022795
0.270	0.001350780	0.17761	-0.0024021
0.280	0.001665548	0.16660	-0.0025291
0.289	0.002032365	0.15611	-0.0026605

0.299	0.002456675	0.14612	-0.0027968
0.309	0.002944195	0.13661	-0.002938
0.319	0.003500909	0.12758	-0.0030845
0.328	0.004133074	0.11901	-0.0032365
0.338	0.004847219	0.11087	-0.0033944
0.348	0.005650141	0.10316	-0.0035586
0.357	0.006548911	0.09586	-0.0037293
0.367	0.007550869	0.08895	-0.0039069
0.377	0.008663624	0.08242	-0.0040919
0.386	0.009895061	0.07626	-0.0042848
0.396	0.011253331	0.07045	-0.0044859
0.406	0.012746859	0.06498	-0.004696
0.415	0.014384338	0.05983	-0.0049154
0.425	0.016174735	0.05500	-0.0051449
0.435	0.018127285	0.05047	-0.0053851
0.444	0.020251496	0.04622	-0.0056368
0.454	0.022557146	0.04224	-0.0059009
0.464	0.025054284	0.03853	-0.0061781
0.473	0.027753229	0.03507	-0.0064694
0.483	0.030664572	0.03184	-0.0067761
0.493	0.033799175	0.02885	-0.0070992
0.503	0.037168169	0.02607	-0.0074401
0.512	0.040782959	0.02349	-0.0078002
0.522	0.044655218	0.02112	-0.0081811
0.532	0.048796890	0.01892	-0.0085847
0.541	0.053220193	0.01691	-0.009013
0.551	0.057937611	0.01505	-0.0094683
0.561	0.062961904	0.01336	-0.0099531
0.570	0.068306099	0.01181	-0.0104703
0.580	0.073983495	0.01040	-0.0110231
0.590	0.080007663	0.00912	-0.01162
0.599	0.086392442	0.00797	-0.01225
0.609	0.093151947	0.00692	-0.01294
0.619	0.100300557	0.00598	-0.01367
0.628	0.107852929	0.00515	-0.01447
0.638	0.115823984	0.00440	-0.01534
0.648	0.124228920	0.00373	-0.01628

0.657	0.133083202	0.00315	-0.01731
0.667	0.142402566	0.00264	-0.01845
0.677	0.152203021	0.00219	-0.01969
0.686	0.162500845	0.00180	-0.02107
0.696	0.173312588	0.00147	-0.02260
0.706	0.184655071	0.00118	-0.02432
0.716	0.196545384	0.00094	-0.02624
0.725	0.209000889	0.00074	-0.02843
0.735	0.222039220	0.00057	-0.03092
0.745	0.235678280	0.00043	-0.03379
0.754	0.249936244	0.00032	-0.03713
0.764	0.264831557	0.00023	-0.04106
0.774	0.280382937	0.00016	-0.04575
0.783	0.296609369	0.00011	-0.05144
0.793	0.313530113	0.00007	-0.05846
0.803	0.331164697	0.00005	-0.06735
0.812	0.349532920	0.00003	-0.07894
0.822	0.368654855	0.00001	-0.09462
0.832	0.388550842	0.00001	-0.11698
0.841	0.409241493	0.00000	-0.15125
0.851	0.430747693	0.00000	-0.20991
0.880	0.500000000	0.00000	-0.26857 /

- -Water-Wet table (Corresponds to SURFWNUM number)

Sw	Krw	Kro	Pc(atm)
0.090	0.0000000000	0.70000	24.37791
0.096	0.0000000004	0.67963	1.599039
0.105	0.0000000222	0.64668	0.461709
0.115	0.0000001547	0.61494	0.241595
0.125	0.0000005687	0.58439	0.155423
0.135	0.0000015160	0.55498	0.111188
0.144	0.0000033297	0.52671	0.084873
0.154	0.0000064244	0.49952	0.067685
0.164	0.0000112956	0.47340	0.055707
0.173	0.0000185203	0.44832	0.046954
0.183	0.0000287567	0.42425	0.04032
0.193	0.0000427442	0.40116	0.035145
0.202	0.0000613036	0.37903	0.031012
0.212	0.0000853368	0.35783	0.027648
0.222	0.0001158270	0.33753	0.024865
0.231	0.0001538386	0.31810	0.02253
0.241	0.0002005176	0.29953	0.020546
0.251	0.0002570907	0.28178	0.018845
0.260	0.0003248663	0.26483	0.017371
0.270	0.0004052339	0.24866	0.016085
0.280	0.0004996643	0.23324	0.014954
0.289	0.0006097094	0.21855	0.013952
0.299	0.0007370026	0.20456	0.01306
0.309	0.0008832584	0.19126	0.012262
0.319	0.0010502726	0.17861	0.011544
0.328	0.0012399223	0.16661	0.010895
0.338	0.0014541657	0.15522	0.010306
0.348	0.0016950424	0.14442	0.00977
0.357	0.0019646734	0.13420	0.00928
0.367	0.0022652606	0.12453	0.00883
0.377	0.0025990873	0.11539	0.008417
0.386	0.0029685183	0.10676	0.008035
0.396	0.0033759994	0.09863	0.007683
0.406	0.0038240576	0.09097	0.007356
0.415	0.0043153015	0.08377	0.007052

0.425	0.0048524205	0.07700	0.006769
0.435	0.0054381856	0.07065	0.006505
0.444	0.0060754489	0.06470	0.006258
0.454	0.0067671439	0.05914	0.006027
0.464	0.0075162852	0.05394	0.00581
0.473	0.0083259687	0.04909	0.005606
0.483	0.0091993717	0.04458	0.005415
0.493	0.0101397525	0.04039	0.005234
0.503	0.0111504508	0.03650	0.005063
0.512	0.0122348877	0.03289	0.004901
0.522	0.0133965653	0.02956	0.004749
0.532	0.0146390671	0.02649	0.004604
0.541	0.0159660578	0.02367	0.004466
0.551	0.0173812834	0.02108	0.004336
0.561	0.0188885712	0.01870	0.004212
0.570	0.0204918296	0.01654	0.004094
0.580	0.0221950485	0.01456	0.003981
0.590	0.0240022988	0.01277	0.003874
0.599	0.0259177327	0.01115	0.003771
0.609	0.0279455840	0.00969	0.003673
0.619	0.0300901672	0.00838	0.003579
0.628	0.0323558786	0.00720	0.00349
0.638	0.0347471953	0.00616	0.003404
0.648	0.0372686760	0.00523	0.003322
0.657	0.0399249605	0.00441	0.003243
0.667	0.0427207698	0.00369	0.003167
0.677	0.0456609063	0.00306	0.003094
0.686	0.0487502536	0.00252	0.003024
0.696	0.0519937765	0.00205	0.002957
0.706	0.0553965213	0.00165	0.002892
0.716	0.0589636151	0.00131	0.00283
0.725	0.0627002667	0.00103	0.00277
0.735	0.0666117659	0.00080	0.002712
0.745	0.0707034839	0.00060	0.002656
0.754	0.0749808731	0.00045	0.002602
0.764	0.0794494672	0.00033	0.00255
0.774	0.0841148810	0.00023	0.002499

```
0.783     0.0889828107  0.00016  0.002451
0.793     0.0940590338  0.00010  0.002404
0.803     0.0993494090  0.00006  0.002358
0.812     0.1048598761  0.00004  0.002314
0.822     0.1105964565  0.00002  0.002271
0.832     0.1165652526  0.00001  0.00223
0.841     0.1227724480  0.00000  0.00219
0.851     0.1292243079  0.00000  0.002151
0.880     0.1500000000  0.00000  0 /
      - - Outermost blocks
0.00000   0.00000       1.0000   0.00000
1.00000   1.00000       0.0000   0.00000 /
0.00000   0.00000       1.0000   0.00000
1.00000   1.00000       0.0000   0.00000/
0.00000   0.00000       1.0000   0.00000
1.00000   1.00000       0.0000   0.00000 /
/
```

This is a two column page

```
RSCONST
0 0.1 /
PVTW
10 1 4.4D-5 0.35 0 /
/
ROCK
10 4.2D-5 /
/
DENSITY
0.7834 0.9847 0.0097 /
/ PVDO
1.0 1.0 0.65
10 0.9 0.65 /
/
SURFST
0.00000000 20
0.00230544 20
0.00268968 20
0.00691632 20
0.00922176 20 /
/
SURFVISC
0.00000000 0.35
0.00230544 0.35
0.00268968 0.35
0.00691632 0.35
0.00922176 0.35/
/
SURFADS
0.00000000      0.000000000
0.00230544      0.000034799
0.00461088      0.000069598
0.00691632      0.000104397
0.00922176      0.000139196/

0.00000000      0.000000000
0.00230544      0.000034799
0.00461088      0.000069598
0.00691632      0.000104397
0.00922176      0.000139196/

0.00000000      0.000000000
0.00230544      0.000034799
0.00461088      0.000069598
0.00691632      0.000104397
0.00922176      0.000139196/

0.00000000      0.000000000
0.00230544      0.000034799
0.00461088      0.000069598
0.00691632      0.000104397
0.00922176      0.000139196/

SURFADDW
0.000000000     1
0.000034799     1
0.000069598     1
0.000104397     1
0.000139196     1/
```

```
0.000000000     1
0.000034799     1
0.000069598     1
0.000104397     1
0.000139196     1/

0.000000000     1
0.000034799     1
0.000069598     1
0.000104397     1
0.000139196     1/

0.000000000     1
0.000034799     1
0.000069598     1
0.000104397     1
0.000139196     1/

SURFCAPD
-8      0
-7      0
-6      0
-5.09       0
-4.74       0
-4.16       0
-3.9        0 /
-8      0
-7      0
-6      0
-5.09       0
-4.74       0
```

```
0.000000000     0.91
0.000034799     0.23
0.000069598     0.25
0.000104397     0.19
0.000139196     0.09/

-4.16       0
-3.9        0 /
-8      0
-7      0
-6      0
-5.09       0
-4.74       0
-4.16       0
-3.9        0 /
-8      0
-7      0
-6      0
-5.09       0
-4.74       0
-4.16       0
-3.9        0 /
-8      0
-7      0
-6      0
-5.09       0
-4.74       0
-4.16       0
-3.9        0 /
-8      0
-7      0
-6      0
-5.09       0
-4.74       0
-4.16       0
-3.9        0 /
EQUALS
```

```
FIPNUM 1 1 40 1 20 19 58 /
SATNUM 1 1 40 1 20 19 58 /
SURFNUM 2 1 40 1 20 19 58 /
SURFWNUM 3 1 40 1 20 19 58 /
FIPNUM 2 1 60 1 20 1 18 /
FIPNUM 2 1 60 1 20 59 80 /
FIPNUM 2 41 60 1 20 19 58 /
SATNUM 4 1 60 1 20 1 18 /
SATNUM 4 1 60 1 20 59 80 /
SATNUM 4 41 60 1 20 19 58 /
SURFNUM 5 1 60 1 20 1 18 /
SURFNUM 5 1 60 1 20 59 80 /
SURFNUM 5 41 60 1 20 19 58 /
SURFWNUM 6 1 60 1 20 1 18 /
SURFWNUM 6 1 60 1 20 59 80 /
SURFWNUM 6 41 60 1 20 19 58 /
SOLUTION ========================
SWAT
96000*1.00 /
BOX
1 40 1 20 19 58 /
SWAT
32000*0.09 /

ENDBOX
PRESSURE
96000*10.00 /
RPTSOL
RESTART=2 SOIL SWAT PRESSURE
/
RPTRST
BASIC=3 FREQ=5 PCOW /
SUMMARY ==============
ROEIW
1 /
ROE
1 /
ROFT
1 2 /
/
RWFT
1 2 /
/
FPR
FWIR
FWIT
FWPR
FWPT
FOPR
FOPT
FTPRSUR
FTPTSUR
FTIRSUR
FTITSUR
FTADSUR
FTIPTSUR
WTPRSUR
/
WTPTSUR
/
WTIRSUR
/
WTITSUR
/
RUNSUM
EXCEL
SCHEDULE ===============
RPTRST
BASIC=2 /
MESSAGES
9* 10000 2* /
DRSDT
0 /
TUNING
```

```
0.001 0.25 0.005 0.005 /
/
50 1* 400 /
MESSAGES
9* 100000 100000 100000 /
TSTEP
1*0.01 /
WELSPECS
WINJ1 I 1 1 1* WATER 3* NO /
PROD1 P 1 1 1* OIL 3* NO /
/
COMPDAT
WINJ1 1 1 1 17 OPEN 2* 0.001 3* Z /
PROD1 1 1 60 80 OPEN 2* 0.001 3* Z /
/
WCONINJE
WINJ1 WATER OPEN RATE 50000 /
/
WCONPROD
PROD1 OPEN LRAT 3* 50000 /
/
WSURFACT
WINJ1 0.00922176 /
/
TSTEP
50*0.01 /
TSTEP
50*0.01 /
TSTEP
50*0.01 /
TSTEP
50*0.01 /
TSTEP
50*0.1 /
TSTEP
50*0.1 /
TSTEP
50*0.1 /
TSTEP
50*1 /
TSTEP
50*1 /
WCONINJE
WINJ1 WATER SHUT RATE 0 /
/
WCONPROD
PROD1 SHUT LRAT 3* 0 /
/
TSTEP
50*1 /
END
```

END OF THE BASE FILE

A.2 BASE_RST.DATA

THE BASE_RST.DATA STARTS HERE.
(THIS IS A TWO COLUMN PAGE)

```
- - SPONTANEOUS IMBIBITION OF SMART WATER INTO POROUS MEDIA
- - ====================
RUNSPEC
TITLE
SI OF SMART WATER ONTO CHALK CORES
DIMENS
60 20 80 /
RADIAL
START
01 'OCT' 2015 /
OIL
WATER
SURFACTW
LAB
EQLDIMS
2 100 20 1 20 /
TABDIMS
6 2 100 21 3 12 /
WELLDIMS
2 50 2 2/
NUPCOL
4 /
NSTACK
50 /
UNIFOUT
UNIFIN
ENDSCALE
/
GRIDOPTS
YES /
GRID ================
NOECHO
INCLUDE
grid.DATA /
DTHETA
96000*18
/ DZ
96000*0.1
/
COORDSYS
1 80 COMP /
BOX
1 60 1 20 1 80 /
PERMR
96000*100000 /
PERMTHT
96000*100000 /
PERMZ
96000*100000 /
BOX
1 40 1 20 19 58 /
PERMR
32000*2 /
PERMTHT
32000*2 /
PERMZ
32000*2 /
ENDBOX
PORO
96000*0.99 /
BOX
```

```
1 40 1 20 19 58 /
PORO
32000*0.49 /
ENDBOX
BOX 1 60 1 20 1 1 /
TOPS
1200*0
/
ENDBOX
INIT
EQUALS
MULTR 1 40 40 1 20 19 58 /
MULTZ 1 1 40 1 20 18 18 /
MULTZ 1 1 40 1 20 58 58 /
/

SWOF
BOX
41 60 1 20 19 58 /
MULTPV
16000*1000 /
BOX
1 60 1 20 1 18 /
MULTPV
21600*1000 /
BOX
1 60 1 20 59 80 /
MULTPV
26400*1000 /
PROPS ======================
```

- -Oil-Wet table (Corresponds to SATNUM number)

Sw	Krw	Kro	Pc(atm)
0.090	0.000000000	0.50000	-0.000759
0.096	0.000000001	0.48545	-0.0007641
0.105	0.000000074	0.46192	-0.00081
0.115	0.000000516	0.43925	-0.0008395
0.125	0.000001896	0.41742	-0.0009168
0.135	0.000005053	0.39642	-0.0009964
0.144	0.000011099	0.37622	-0.0010782
0.154	0.000021415	0.35680	-0.0011624
0.164	0.000037652	0.33815	-0.0012491
0.173	0.000061734	0.32023	-0.0013384
0.183	0.000095856	0.30304	-0.0014303
0.193	0.000142481	0.28655	-0.0015251
0.202	0.000204345	0.27074	-0.0016229
0.212	0.000284456	0.25559	-0.0017237
0.222	0.000386090	0.24109	-0.0018278
0.231	0.000512795	0.22722	-0.0019352
0.241	0.000668392	0.21395	-0.0020462
0.251	0.000856969	0.20127	-0.0021609
0.260	0.001082888	0.18916	-0.0022795
0.270	0.001350780	0.17761	-0.0024021
0.280	0.001665548	0.16660	-0.0025291
0.289	0.002032365	0.15611	-0.0026605
0.299	0.002456675	0.14612	-0.0027968
0.309	0.002944195	0.13661	-0.002938
0.319	0.003500909	0.12758	-0.0030845
0.328	0.004133074	0.11901	-0.0032365
0.338	0.004847219	0.11087	-0.0033944
0.348	0.005650141	0.10316	-0.0035586
0.357	0.006548911	0.09586	-0.0037293
0.367	0.007550869	0.08895	-0.0039069
0.377	0.008663624	0.08242	-0.0040919
0.386	0.009895061	0.07626	-0.0042848
0.396	0.011253331	0.07045	-0.0044859
0.406	0.012746859	0.06498	-0.004696
0.415	0.014384338	0.05983	-0.0049154

0.425	0.016174735	0.05500	-0.0051449
0.435	0.018127285	0.05047	-0.0053851
0.444	0.020251496	0.04622	-0.0056368
0.454	0.022557146	0.04224	-0.0059009
0.464	0.025054284	0.03853	-0.0061781
0.473	0.027753229	0.03507	-0.0064694
0.483	0.030664572	0.03184	-0.0067761
0.493	0.033799175	0.02885	-0.0070992
0.503	0.037168169	0.02607	-0.0074401
0.512	0.040782959	0.02349	-0.0078002
0.522	0.044655218	0.02112	-0.0081811
0.532	0.048796890	0.01892	-0.0085847
0.541	0.053220193	0.01691	-0.009013
0.551	0.057937611	0.01505	-0.0094683
0.561	0.062961904	0.01336	-0.0099531
0.570	0.068306099	0.01181	-0.0104703
0.580	0.073983495	0.01040	-0.0110231
0.590	0.080007663	0.00912	-0.01162
0.599	0.086392442	0.00797	-0.01225
0.609	0.093151947	0.00692	-0.01294
0.619	0.100300557	0.00598	-0.01367
0.628	0.107852929	0.00515	-0.01447
0.638	0.115823984	0.00440	-0.01534
0.648	0.124228920	0.00373	-0.01628
0.657	0.133083202	0.00315	-0.01731
0.667	0.142402566	0.00264	-0.01845
0.677	0.152203021	0.00219	-0.01969
0.686	0.162500845	0.00180	-0.02107
0.696	0.173312588	0.00147	-0.02260
0.706	0.184655071	0.00118	-0.02432
0.716	0.196545384	0.00094	-0.02624
0.725	0.209000889	0.00074	-0.02843
0.735	0.222039220	0.00057	-0.03092
0.745	0.235678280	0.00043	-0.03379
0.754	0.249936244	0.00032	-0.03713
0.764	0.264831557	0.00023	-0.04106
0.774	0.280382937	0.00016	-0.04575

0.783	0.296609369	0.00011	-0.05144
0.793	0.313530113	0.00007	-0.05846
0.803	0.331164697	0.00005	-0.06735
0.812	0.349532920	0.00003	-0.07894
0.822	0.368654855	0.00001	-0.09462
0.832	0.388550842	0.00001	-0.11698
0.841	0.409241493	0.00000	-0.15125
0.851	0.430747693	0.00000	-0.20991
0.880	0.500000000	0.00000	-0.26857 /

table above is repeated here (no misicibility)

- -Oil-Wet table (Corresponds to SURFNUM number)

Sw	Krw	Kro	Pc(atm)
0.090	0.000000000	0.50000	-0.000759
0.096	0.000000001	0.48545	-0.0007641
0.105	0.000000074	0.46192	-0.00081
0.115	0.000000516	0.43925	-0.0008395
0.125	0.000001896	0.41742	-0.0009168
0.135	0.000005053	0.39642	-0.0009964
0.144	0.000011099	0.37622	-0.0010782
0.154	0.000021415	0.35680	-0.0011624
0.164	0.000037652	0.33815	-0.0012491
0.173	0.000061734	0.32023	-0.0013384
0.183	0.000095856	0.30304	-0.0014303
0.193	0.000142481	0.28655	-0.0015251
0.202	0.000204345	0.27074	-0.0016229
0.212	0.000284456	0.25559	-0.0017237
0.222	0.000386090	0.24109	-0.0018278
0.231	0.000512795	0.22722	-0.0019352
0.241	0.000668392	0.21395	-0.0020462
0.251	0.000856969	0.20127	-0.0021609
0.260	0.001082888	0.18916	-0.0022795
0.270	0.001350780	0.17761	-0.0024021
0.280	0.001665548	0.16660	-0.0025291
0.289	0.002032365	0.15611	-0.0026605
0.299	0.002456675	0.14612	-0.0027968
0.309	0.002944195	0.13661	-0.002938

0.319	0.003500909	0.12758	-0.0030845
0.328	0.004133074	0.11901	-0.0032365
0.338	0.004847219	0.11087	-0.0033944
0.348	0.005650141	0.10316	-0.0035586
0.357	0.006548911	0.09586	-0.0037293
0.367	0.007550869	0.08895	-0.0039069
0.377	0.008663624	0.08242	-0.0040919
0.386	0.009895061	0.07626	-0.0042848
0.396	0.011253331	0.07045	-0.0044859
0.406	0.012746859	0.06498	-0.004696
0.415	0.014384338	0.05983	-0.0049154
0.425	0.016174735	0.05500	-0.0051449
0.435	0.018127285	0.05047	-0.0053851
0.444	0.020251496	0.04622	-0.0056368
0.454	0.022557146	0.04224	-0.0059009
0.464	0.025054284	0.03853	-0.0061781
0.473	0.027753229	0.03507	-0.0064694
0.483	0.030664572	0.03184	-0.0067761
0.493	0.033799175	0.02885	-0.0070992
0.503	0.037168169	0.02607	-0.0074401
0.512	0.040782959	0.02349	-0.0078002
0.522	0.044655218	0.02112	-0.0081811
0.532	0.048796890	0.01892	-0.0085847
0.541	0.053220193	0.01691	-0.009013
0.551	0.057937611	0.01505	-0.0094683
0.561	0.062961904	0.01336	-0.0099531
0.570	0.068306099	0.01181	-0.0104703
0.580	0.073983495	0.01040	-0.0110231
0.590	0.080007663	0.00912	-0.01162
0.599	0.086392442	0.00797	-0.01225
0.609	0.093151947	0.00692	-0.01294
0.619	0.100300557	0.00598	-0.01367
0.628	0.107852929	0.00515	-0.01447
0.638	0.115823984	0.00440	-0.01534
0.648	0.124228920	0.00373	-0.01628
0.657	0.133083202	0.00315	-0.01731
0.667	0.142402566	0.00264	-0.01845

0.677	0.152203021	0.00219	-0.01969
0.686	0.162500845	0.00180	-0.02107
0.696	0.173312588	0.00147	-0.02260
0.706	0.184655071	0.00118	-0.02432
0.716	0.196545384	0.00094	-0.02624
0.725	0.209000889	0.00074	-0.02843
0.735	0.222039220	0.00057	-0.03092
0.745	0.235678280	0.00043	-0.03379
0.754	0.249936244	0.00032	-0.03713
0.764	0.264831557	0.00023	-0.04106
0.774	0.280382937	0.00016	-0.04575
0.783	0.296609369	0.00011	-0.05144
0.793	0.313530113	0.00007	-0.05846
0.803	0.331164697	0.00005	-0.06735
0.812	0.349532920	0.00003	-0.07894
0.822	0.368654855	0.00001	-0.09462
0.832	0.388550842	0.00001	-0.11698
0.841	0.409241493	0.00000	-0.15125
0.851	0.430747693	0.00000	-0.20991
0.880	0.500000000	0.00000	-0.26857 /

- -Oil-Wet table (Corresponds to SURFWNUM number)

Sw	Krw	Kro	Pc(atm)
0.090	0.0000000000	0.70000	24.37791
0.096	0.0000000004	0.67963	1.599039
0.105	0.0000000222	0.64668	0.461709
0.115	0.0000001547	0.61494	0.241595
0.125	0.0000005687	0.58439	0.155423
0.135	0.0000015160	0.55498	0.111188
0.144	0.0000033297	0.52671	0.084873
0.154	0.0000064244	0.49952	0.067685
0.164	0.0000112956	0.47340	0.055707
0.173	0.0000185203	0.44832	0.046954
0.183	0.0000287567	0.42425	0.04032
0.193	0.0000427442	0.40116	0.035145
0.202	0.0000613036	0.37903	0.031012
0.212	0.0000853368	0.35783	0.027648

0.222	0.0001158270	0.33753	0.024865
0.231	0.0001538386	0.31810	0.02253
0.241	0.0002005176	0.29953	0.020546
0.251	0.0002570907	0.28178	0.018845
0.260	0.0003248663	0.26483	0.017371
0.270	0.0004052339	0.24866	0.016085
0.280	0.0004996643	0.23324	0.014954
0.289	0.0006097094	0.21855	0.013952
0.299	0.0007370026	0.20456	0.01306
0.309	0.0008832584	0.19126	0.012262
0.319	0.0010502726	0.17861	0.011544
0.328	0.0012399223	0.16661	0.010895
0.338	0.0014541657	0.15522	0.010306
0.348	0.0016950424	0.14442	0.00977
0.357	0.0019646734	0.13420	0.00928
0.367	0.0022652606	0.12453	0.00883
0.377	0.0025990873	0.11539	0.008417
0.386	0.0029685183	0.10676	0.008035
0.396	0.0033759994	0.09863	0.007683
0.406	0.0038240576	0.09097	0.007356
0.415	0.0043153015	0.08377	0.007052
0.425	0.0048524205	0.07700	0.006769
0.435	0.0054381856	0.07065	0.006505
0.444	0.0060754489	0.06470	0.006258
0.454	0.0067671439	0.05914	0.006027
0.464	0.0075162852	0.05394	0.00581
0.473	0.0083259687	0.04909	0.005606
0.483	0.0091993717	0.04458	0.005415
0.493	0.0101397525	0.04039	0.005234
0.503	0.0111504508	0.03650	0.005063
0.512	0.0122348877	0.03289	0.004901
0.522	0.0133965653	0.02956	0.004749
0.532	0.0146390671	0.02649	0.004604
0.541	0.0159660578	0.02367	0.004466
0.551	0.0173812834	0.02108	0.004336
0.561	0.0188885712	0.01870	0.004212
0.570	0.0204918296	0.01654	0.004094

0.580	0.0221950485	0.01456	0.003981
0.590	0.0240022988	0.01277	0.003874
0.599	0.0259177327	0.01115	0.003771
0.609	0.0279455840	0.00969	0.003673
0.619	0.0300901672	0.00838	0.003579
0.628	0.0323558786	0.00720	0.00349
0.638	0.0347471953	0.00616	0.003404
0.648	0.0372686760	0.00523	0.003322
0.657	0.0399249605	0.00441	0.003243
0.667	0.0427207698	0.00369	0.003167
0.677	0.0456609063	0.00306	0.003094
0.686	0.0487502536	0.00252	0.003024
0.696	0.0519937765	0.00205	0.002957
0.706	0.0553965213	0.00165	0.002892
0.716	0.0589636151	0.00131	0.00283
0.725	0.0627002667	0.00103	0.00277
0.735	0.0666117659	0.00080	0.002712
0.745	0.0707034839	0.00060	0.002656
0.754	0.0749808731	0.00045	0.002602
0.764	0.0794494672	0.00033	0.00255
0.774	0.0841148810	0.00023	0.002499
0.783	0.0889828107	0.00016	0.002451
0.793	0.0940590338	0.00010	0.002404
0.803	0.0993494090	0.00006	0.002358
0.812	0.1048598761	0.00004	0.002314
0.822	0.1105964565	0.00002	0.002271
0.832	0.1165652526	0.00001	0.00223
0.841	0.1227724480	0.00000	0.00219
0.851	0.1292243079	0.00000	0.002151
0.880	0.1500000000	0.00000	0 /

- - Outermost blocks

0.00000	0.00000	1.0000	0.00000
1.00000	1.00000	0.0000	0.00000 /
0.00000	0.00000	1.0000	0.00000
1.00000	1.00000	0.0000	0.00000/
0.00000	0.00000	1.0000	0.00000
1.00000	1.00000	0.0000	0.00000 /

/

(THIS IS A TWO COLUMN PAGE)

```
RSCONST                                  0.00691632     0.000104397
0 0.1 /                                  0.00922176     0.000139196/
PVTW
10 1 4.4D-5 0.35 0 /                     0.00000000     0.000000000
/                                        0.00230544     0.000034799
ROCK                                     0.00461088     0.000069598
10 4.2D-5 /                              0.00691632     0.000104397
/                                        0.00922176     0.000139196/
DENSITY
0.7834 0.9847 0.0097 /                   0.00000000     0.000000000
/ PVDO                                   0.00230544     0.000034799
1.0 1.0 0.65                             0.00461088     0.000069598
10 0.9 0.65 /                            0.00691632     0.000104397
/                                        0.00922176     0.000139196/
SURFST
0.00000000 20                            0.00000000     0.000000000
0.00230544 20                            0.00230544     0.000034799
0.00268968 20                            0.00461088     0.000069598
0.00691632 20                            0.00691632     0.000104397
0.00922176 20 /                          0.00922176     0.000139196/
/
SURFVISC                                 0.00000000     0.000000000
0.00000000 0.35                          0.00230544     0.000034799
0.00230544 0.35                          0.00461088     0.000069598
0.00268968 0.35                          0.00691632     0.000104397
0.00691632 0.35                          0.00922176     0.000139196/
0.00922176 0.35/
/                                        0.00000000     0.000000000
SURFADS                                  0.00230544     0.000034799
0.00000000     0.000000000               0.00461088     0.000069598
0.00230544     0.000034799               0.00691632     0.000104397
0.00461088     0.000069598               0.00922176     0.000139196/
```

```
                                0.000069598     1
SURFADDW                        0.000104397     1
0.000000000     1               0.000139196     1/
0.000034799     1
0.000069598     1               0.000000000     0.875
0.000104397     1               0.000034799     0.27
0.000139196     1/              0.000069598     0.265
                                0.000104397     0.22
0.000000000     1               0.000139196     0.19/
0.000034799     1

0.000000000     1               -7      0
0.000034799     1               -6      0
0.000069598     1               -5.09       0
0.000104397     1               -4.74       0
0.000139196     1/              -4.16       0
                                -3.9        0 /
0.000000000     1               -8      0
0.000034799     1               -7      0
0.000069598     1               -6      0
0.000104397     1               -5.09       0
0.000139196     1/              -4.74       0
                                -4.16       0
0.000000000     1               -3.9        0 /
0.000034799     1               -8      0
0.000069598     1               -7      0
0.000104397     1               -6      0
0.000139196     1/              -5.09       0
                                -4.74       0
SURFCAPD                        -4.16       0
-8      0                       -3.9        0 /
-7      0                       -8      0
-6      0                       -7      0
-5.09       0                   -6      0
-4.74       0                   -5.09       0
-4.16       0                   -4.74       0
-3.9        0 /                 -4.16       0
-8      0                       -3.9        0 /
```

```
-8      0
-7      0
-6      0
-5.09       0
-4.74       0
-4.16       0
-3.9        0 /
EQUALS
FIPNUM 1 1 40 1 20 19 58 /
SATNUM 1 1 40 1 20 19 58 /
SURFNUM 2 1 40 1 20 19 58 /
SURFWNUM 3 1 40 1 20 19 58 /
FIPNUM 2 1 60 1 20 1 18 /
FIPNUM 2 1 60 1 20 59 80 /
FIPNUM 2 41 60 1 20 19 58 /
SATNUM 4 1 60 1 20 1 18 /
SATNUM 4 1 60 1 20 59 80 /
SATNUM 4 41 60 1 20 19 58 /
SURFNUM 5 1 60 1 20 1 18 /
SURFNUM 5 1 60 1 20 59 80 /
SURFNUM 5 41 60 1 20 19 58 /
SURFWNUM 6 1 60 1 20 1 18 /
SURFWNUM 6 1 60 1 20 59 80 /
SURFWNUM 6 41 60 1 20 19 58 /
/

SOLUTION ==============
RESTART
BASE 501 /
RPTSOL
RESTART=2 SOIL SWAT PRESSURE
/
RPTRST
BASIC=3 FREQ=5 PCOW /
ENDBOX
PRESSURE
96000*10.00 /
RPTSOL
RESTART=2 SOIL SWAT PRESSURE
/
RPTRST
BASIC=3 FREQ=5 PCOW /
SUMMARY ==============
ROEIW
1 /
ROE
1 /
ROFT
1 2 /
/
RWFT
1 2 /
/
FPR
FWIR
FWIT
FWPR
FWPT
FOPR
FOPT
FTPRSUR
FTPTSUR
FTIRSUR
FTITSUR
FTADSUR
FTIPTSUR
WTPRSUR
/
WTPTSUR
/
WTIRSUR
/
WTITSUR
/
```

```
RUNSUM                                TSTEP
EXCEL                                 50*0.01 /
SCHEDULE ==============               TSTEP
RPTRST                                50*0.01 /
BASIC=2 /                             TSTEP
MESSAGES                              50*0.1 /
9* 10000 2* /                         TSTEP
TUNING                                50*0.1 /
0.001 0.25 0.005 0.005 /              TSTEP
/                                     50*0.1 /
50 1* 400 /                           TSTEP
MESSAGES                              50*1 /
9* 100000 100000 100000 /             TSTEP
TSTEP                                 50*1 /
50*0.01 /                             - - long TSTEP not included here END
TSTEP
50*0.01 /
```

END OF THE BASE_RST FILE

Appendix B

Saturation and Pc tables generated using WF

Table B.1: *Relative permeability and Pc generated using WF in history matching section-0S, 1S*

		0S			1S	
Sw	Krw	Kro	Pc(atm)	Krw	Kro	Pc(atm)
0.09	0	0.524	2.92468107	0	0.646	17.7956681
0.09580991	1.3398E-09	0.50875458	0.19121233	7.1523E-10	0.62720507	1.1670925
0.10549308	6.775E-08	0.48408779	0.05469223	3.6168E-08	0.59679526	0.33682857
0.11517626	4.7241E-07	0.46032904	0.02825258	2.5219E-07	0.56750488	0.17613737
0.12485943	1.7364E-06	0.43745576	0.01784388	9.2694E-07	0.53930614	0.11321091
0.13454261	4.6287E-06	0.41544566	0.0124658	2.471E-06	0.51217156	0.0808985
0.14422578	1.0167E-05	0.39427677	0.009236	5.4274E-06	0.48607403	0.06166648
0.15390896	1.9616E-05	0.37392736	0.00709928	1.0472E-05	0.46098678	0.04909612
0.16359213	3.4489E-05	0.35437601	0.00558565	1.8412E-05	0.4368834	0.04032883
0.17327531	5.6549E-05	0.33560157	0.00445669	3.0188E-05	0.41373782	0.03391482
0.18295848	8.7804E-05	0.31758319	0.00357966	4.6873E-05	0.39152432	0.02904711
0.19264166	0.00013051	0.30030029	0.00287524	6.9673E-05	0.37021754	0.02524381
0.20232483	0.00018718	0.28373258	0.00229336	9.9925E-05	0.34979246	0.02220092
0.21200801	0.00026056	0.26786005	0.00180095	0.0001391	0.33022442	0.01971799
0.22169118	0.00035366	0.25266298	0.00137535	0.0001888	0.31148909	0.01765792
0.23137436	0.00046972	0.23812192	0.00100056	0.00025076	0.29356252	0.01592405
0.24105753	0.00061225	0.22421773	0.00066493	0.00032684	0.27642109	0.01444644
0.25074071	0.00078498	0.21093152	0.00035981	0.00041906	0.26004153	0.01317333

0.26042388	0.00099193	0.19824471	7.8641E-05	0.00052953	0.24440092	0.01206564
0.27010706	0.00123731	0.18613899	-0.0001837	0.00066053	0.2294767	0.0110934
0.27979023	0.00152564	0.17459635	-0.0004312	0.00081445	0.21524664	0.01023323
0.28947341	0.00186165	0.16359904	-0.000667	0.00099383	0.2016889	0.00946665
0.29915658	0.00225031	0.15312962	-0.0008939	0.00120131	0.18878194	0.00877889
0.30883976	0.00269688	0.14317092	-0.001114	0.00143971	0.1765046	0.00815798
0.31852293	0.00320683	0.13370604	-0.0013291	0.00171194	0.16483607	0.00759417
0.32820611	0.0037859	0.12471839	-0.0015407	0.00202107	0.15375587	0.00707937
0.33788928	0.00444005	0.11619164	-0.0017504	0.00237029	0.1432439	0.00660688
0.34757246	0.00517553	0.10810978	-0.0019592	0.00276292	0.13328038	0.00617106
0.35725563	0.0059988	0.10045704	-0.0021682	0.00320242	0.12384589	0.00576714
0.36693881	0.0069166	0.09321796	-0.0023785	0.00369237	0.11492138	0.00539105
0.37662198	0.00793588	0.08637736	-0.0025909	0.00423651	0.10648811	0.00503931
0.38630516	0.00906388	0.07992033	-0.0028064	0.00483868	0.09852774	0.00470889
0.39598833	0.01030805	0.07383227	-0.0030257	0.00550288	0.09102223	0.00439716
0.40567151	0.01167612	0.06809885	-0.0032497	0.00623321	0.08395393	0.00410182
0.41535468	0.01317605	0.06270601	-0.0034793	0.00703394	0.0773055	0.00382083
0.42503786	0.01481606	0.05764	-0.0037152	0.00790945	0.07106	0.00355237
0.43472103	0.01660459	0.05288733	-0.0039583	0.00886424	0.06520079	0.00329482
0.44440421	0.01855037	0.04843481	-0.0042094	0.00990298	0.05971162	0.00304669
0.45408738	0.02066235	0.04426953	-0.0044695	0.01103044	0.05457656	0.00280666
0.46377056	0.02294972	0.04037887	-0.0047395	0.01225154	0.04978005	0.00257347
0.47345373	0.02542196	0.03675046	-0.0050203	0.01357133	0.04530687	0.00234597
0.48313691	0.02808875	0.03337227	-0.0053132	0.01499498	0.04114215	0.00212309
0.49282008	0.03096004	0.03023251	-0.0056192	0.0165278	0.03727138	0.0019038
0.50250326	0.03404604	0.02731969	-0.0059397	0.01817523	0.03368038	0.00168709
0.51218643	0.03735719	0.0246226	-0.006276	0.01994287	0.03035534	0.001472
0.52186961	0.04090418	0.02213032	-0.0066295	0.0218364	0.0272828	0.00125758
0.53155278	0.04469795	0.0198322	-0.0070021	0.02386168	0.02444962	0.00104288
0.54123596	0.0487497	0.0177179	-0.0073955	0.02602467	0.02184305	0.00082691
0.55091913	0.05307085	0.01577733	-0.0078118	0.02833149	0.01945068	0.0006087
0.56060231	0.0576731	0.01400071	-0.0082533	0.03078837	0.01726042	0.0003872
0.57028548	0.06256839	0.01237853	-0.0087226	0.03340168	0.01526056	0.0001613
0.57996866	0.06776888	0.01090158	-0.0092226	0.03617793	0.01343973	-7.015E-05
0.58965183	0.07328702	0.00956091	-0.0097566	0.03912375	0.01178692	-0.0003084
0.59933501	0.07913548	0.00834787	-0.0103284	0.0422459	0.01029146	-0.0005549
0.60901818	0.08532718	0.0072541	-0.0109423	0.0455513	0.00894303	-0.0008112

0.61870136	0.09187531	0.0062715	-0.0116033	0.04904697	0.00773166	-0.0010789
0.62838453	0.09879328	0.00539228	-0.0123171	0.05274008	0.00664773	-0.00136
0.63806771	0.10609477	0.00460891	-0.0130903	0.05663793	0.00568198	-0.0016568
0.64775088	0.11379369	0.00391417	-0.0139309	0.06074794	0.00482548	-0.0019718
0.65743406	0.12190421	0.00330109	-0.014848	0.06507769	0.00406967	-0.0023079
0.66711723	0.13044075	0.00276303	-0.0158525	0.06963485	0.00340633	-0.0026686
0.67680041	0.13941797	0.00229358	-0.0169576	0.07442728	0.00282758	-0.0030581
0.68648358	0.14885077	0.00188666	-0.018179	0.07946291	0.00232592	-0.0034814
0.69616676	0.15875433	0.00153645	-0.0195358	0.08474986	0.00189418	-0.0039443
0.70584993	0.16914404	0.00123742	-0.0210516	0.09029633	0.00152552	-0.0044543
0.71553311	0.18003557	0.00098432	-0.0227556	0.09611069	0.0012135	-0.0050204
0.72521628	0.19144481	0.00077219	-0.0246847	0.10220143	0.00095197	-0.0056539
0.73489946	0.20338793	0.00059635	-0.0268856	0.10857718	0.00073519	-0.0063694
0.74458264	0.2158813	0.0004524	-0.029419	0.11524668	0.00055773	-0.0071854
0.75426581	0.2289416	0.00033623	-0.0323649	0.12221882	0.00041451	-0.0081267
0.76394899	0.24258571	0.00024402	-0.0358304	0.12950263	0.00030083	-0.0092261
0.77363216	0.25683077	0.00017221	-0.0399632	0.13710726	0.00021231	-0.010529
0.78331534	0.27169418	0.00011756	-0.0449715	0.14504198	0.00014493	-0.0120994
0.79299851	0.28719358	7.7078E-05	-0.0511592	0.15331623	9.5023E-05	-0.0140305
0.80268169	0.30334686	4.8079E-05	-0.058987	0.16193954	5.9273E-05	-0.0164638
0.81236486	0.32017216	2.8152E-05	-0.0691872	0.1709216	3.4707E-05	-0.0196239
0.82204804	0.33768785	1.5174E-05	-0.082997	0.18027222	1.8707E-05	-0.0238906
0.83173121	0.35591257	7.3028E-06	-0.1026776	0.19000136	9.0031E-06	-0.0299577
0.84141439	0.37486521	2.9821E-06	-0.132835	0.20011909	3.6764E-06	-0.0392382
0.85109756	0.39456489	9.3877E-07	-0.1844605	0.21063562	1.1573E-06	-0.0551048
0.88	0.458	0	-0.2363395	0.2445	0	-0.0725132

Table B.2: *Relative permeability and Pc generated using WF in history matching section - 2S, 3S*

		2S			3S	
Sw	Krw	Kro	Pc(atm)	Krw	Kro	Pc(atm)
0.09	0	0.647	17.9175615	0	0.586	16.5768107
0.09581	7.1011E-10	0.62817598	1.17509152	6.2016E-10	0.56895073	1.08717874
0.105493	3.5909E-08	0.59771909	0.33914116	3.136E-08	0.54136536	0.31378364
0.115176	2.5039E-07	0.56838337	0.17734954	2.1867E-07	0.51479545	0.16409962
0.124859	9.2031E-07	0.54014098	0.11399261	8.0373E-07	0.48921579	0.10548563
0.134543	2.4533E-06	0.5129644	0.08145943	2.1425E-06	0.46460145	0.0753889
0.144226	5.3886E-06	0.48682647	0.06209623	4.706E-06	0.44092784	0.05747672
0.153909	1.0397E-05	0.46170038	0.04944036	9.0798E-06	0.41817067	0.04577
0.163592	1.828E-05	0.43755969	0.04061361	1.5964E-05	0.39630599	0.03760593
0.173275	2.9972E-05	0.41437828	0.03415628	2.6175E-05	0.37531016	0.03163405
0.182958	4.6538E-05	0.39213039	0.02925586	4.0643E-05	0.35515983	0.02710264
0.192642	6.9174E-05	0.37079063	0.02542715	6.0412E-05	0.33583201	0.02356283
0.202325	9.921E-05	0.35033393	0.0223641	8.6642E-05	0.317304	0.02073144
0.212008	0.0001381	0.3307356	0.01986485	0.00012061	0.29955342	0.01842175
0.221691	0.00018745	0.31197128	0.01779138	0.0001637	0.28255822	0.01650606
0.231374	0.00024896	0.29401695	0.01604637	0.00021743	0.26629665	0.01489433
0.241058	0.0003245	0.27684899	0.0145594	0.0002834	0.2507473	0.01352143
0.250741	0.00041606	0.26044407	0.01327835	0.00036335	0.23588906	0.01233913
0.260424	0.00052574	0.24477925	0.01216389	0.00045914	0.22170114	0.01131105
0.270107	0.0006558	0.22983192	0.01118583	0.00057273	0.20816307	0.01040926
0.27979	0.00080862	0.21557984	0.01032064	0.00070619	0.1952547	0.009612
0.289473	0.00098671	0.20200111	0.00954971	0.00086172	0.18295618	0.00890207
0.299157	0.00119272	0.18907417	0.00885817	0.00104163	0.17124801	0.00826571
0.30884	0.00142941	0.17677783	0.00823398	0.00124834	0.16011099	0.00769178
0.318523	0.00169969	0.16509123	0.00766731	0.00148439	0.14952622	0.0071712
0.328206	0.00200661	0.15399388	0.00715003	0.00175242	0.13947514	0.00669646
0.337889	0.00235332	0.14346564	0.00667538	0.00205522	0.12993951	0.0062613
0.347572	0.00274314	0.13348669	0.0062377	0.00239566	0.12090139	0.0058605
0.357256	0.0031795	0.1240376	0.00583218	0.00277674	0.11234318	0.00548963
0.366939	0.00366595	0.11509927	0.00545474	0.00320157	0.10424756	0.0051449
0.376622	0.00420619	0.10665296	0.00510185	0.00367338	0.09659758	0.00482307
0.386305	0.00480405	0.09868026	0.00477049	0.00419551	0.08937656	0.00452136
0.395988	0.00546349	0.09116313	0.004458	0.00477141	0.08256815	0.00423732

0.405672	0.0061886	0.08408388	0.00416208	0.00540467	0.07615635	0.00396883
0.415355	0.0069836	0.07742517	0.00388067	0.00609896	0.07012543	0.003714
0.425038	0.00785283	0.07117	0.00361194	0.00685809	0.06446	0.00347116
0.434721	0.0088008	0.06530172	0.00335427	0.00768597	0.05914499	0.00323881
0.444404	0.0098321	0.05980405	0.00310617	0.00858663	0.05416565	0.00301561
0.454087	0.01095149	0.05466105	0.0028663	0.00956423	0.04950753	0.00280034
0.463771	0.01216385	0.04985711	0.00263341	0.01062302	0.04515652	0.00259185
0.473454	0.01347419	0.045377	0.00240635	0.01176737	0.0410988	0.00238912
0.483137	0.01488765	0.04120584	0.00218405	0.01300178	0.0373209	0.00219117
0.49282	0.0164095	0.03732907	0.00196546	0.01433085	0.03380964	0.00199707
0.502503	0.01804515	0.03373252	0.0017496	0.0157593	0.03055217	0.00180594
0.512186	0.01980013	0.03040233	0.00153551	0.01729197	0.02753596	0.00161694
0.52187	0.02168011	0.02732503	0.00132223	0.01893381	0.02474879	0.00142921
0.531553	0.02369089	0.02448747	0.00110882	0.02068988	0.02217876	0.00124192
0.541236	0.0258384	0.02187687	0.00089431	0.02256536	0.01981429	0.00105425
0.550919	0.02812871	0.01948078	0.00067772	0.02456555	0.01764411	0.00086533
0.560602	0.030568	0.01728713	0.00045802	0.02669585	0.01565728	0.00067427
0.570285	0.03316261	0.01528418	0.00023412	0.02896179	0.01384317	0.00048014
0.579969	0.03591899	0.01346054	4.8701E-06	0.031369	0.01219146	0.00028196
0.589652	0.03884372	0.01180517	-0.000231	0.03392325	0.01069216	7.8656E-05
0.599335	0.04194353	0.01030739	-0.0004748	0.0366304	0.0093356	-0.0001309
0.609018	0.04522527	0.00895687	-0.0007281	0.03949643	0.00811241	-0.0003481
0.618701	0.04869592	0.00774363	-0.0009926	0.04252744	0.00701355	-0.0005742
0.628385	0.0523626	0.00665802	-0.0012702	0.04572964	0.0060303	-0.0008109
0.638068	0.05623254	0.00569077	-0.0015631	0.04910937	0.00515424	-0.00106
0.647751	0.06031314	0.00483295	-0.0018737	0.05267306	0.00437729	-0.0013237
0.657434	0.06461189	0.00407597	-0.0022051	0.05642728	0.00369168	-0.0016043
0.667117	0.06913645	0.0034116	-0.0025606	0.06037869	0.00308995	-0.0019047
0.6768	0.07389457	0.00283196	-0.0029442	0.06453408	0.00256496	-0.0022282
0.686484	0.07889416	0.00232952	-0.0033609	0.06890036	0.00210989	-0.0025791
0.696167	0.08414326	0.00189711	-0.0038165	0.07348454	0.00171825	-0.002962
0.70585	0.08965004	0.00152788	-0.0043183	0.07829375	0.00138383	-0.0033831
0.715533	0.09542278	0.00121537	-0.004875	0.08333524	0.00110079	-0.0038496
0.725216	0.10146993	0.00095345	-0.0054979	0.08861638	0.00086356	-0.004371
0.734899	0.10780004	0.00073633	-0.0062012	0.09414463	0.00066691	-0.0049589
0.744583	0.1144218	0.00055859	-0.0070032	0.09992759	0.00050593	-0.0056286
0.754266	0.12134405	0.00041515	-0.007928	0.10597297	0.00037601	-0.0064001

0.763949	0.12857572	0.00030129	-0.009008	0.11228858	0.00027289	-0.0073004
0.773632	0.13612592	0.00021264	-0.0102877	0.11888237	0.00019259	-0.0083663
0.783315	0.14400385	0.00014515	-0.0118299	0.12576237	0.00013147	-0.00965
0.792999	0.15221887	9.5171E-05	-0.0137262	0.13293677	8.6198E-05	-0.0112275
0.802682	0.16078046	5.9364E-05	-0.0161152	0.14041383	5.3767E-05	-0.013214
0.812365	0.16969823	3.476E-05	-0.0192177	0.14820196	3.1483E-05	-0.0157927
0.822048	0.17898193	1.8736E-05	-0.0234061	0.15630966	1.6969E-05	-0.0192729
0.831731	0.18864143	9.017E-06	-0.0293616	0.16474556	8.1669E-06	-0.02422
0.841414	0.19868675	3.6821E-06	-0.0384711	0.17351839	3.335E-06	-0.0317854
0.851098	0.209128	1.1591E-06	-0.0540445	0.18263702	1.0498E-06	-0.044717
0.88	0.24275	0	-0.0711704	0.212	0	-0.0590849

Table B.3: *Relative permeability and Pc generated using WF in history matching section-4S*

		4S	
Sw	Krw	Kro	Pc(atm)
0.09	0	0.586	16.5768107
0.09580991	6.2016E-10	0.56895073	1.08717874
0.10549308	3.136E-08	0.54136536	0.31378364
0.11517626	2.1867E-07	0.51479545	0.16409962
0.12485943	8.0373E-07	0.48921579	0.10548563
0.13454261	2.1425E-06	0.46460145	0.0753889
0.14422578	4.706E-06	0.44092784	0.05747672
0.15390896	9.0798E-06	0.41817067	0.04577
0.16359213	1.5964E-05	0.39630599	0.03760593
0.17327531	2.6175E-05	0.37531016	0.03163405
0.18295848	4.0643E-05	0.35515983	0.02710264
0.19264166	6.0412E-05	0.33583201	0.02356283
0.20232483	8.6642E-05	0.317304	0.02073144
0.21200801	0.00012061	0.29955342	0.01842175
0.22169118	0.0001637	0.28255822	0.01650606
0.23137436	0.00021743	0.26629665	0.01489433
0.24105753	0.0002834	0.2507473	0.01352143
0.25074071	0.00036335	0.23588906	0.01233913
0.26042388	0.00045914	0.22170114	0.01131105
0.27010706	0.00057273	0.20816307	0.01040926
0.27979023	0.00070619	0.1952547	0.009612
0.28947341	0.00086172	0.18295618	0.00890207
0.29915658	0.00104163	0.17124801	0.00826571
0.30883976	0.00124834	0.16011099	0.00769178
0.31852293	0.00148439	0.14952622	0.0071712
0.32820611	0.00175242	0.13947514	0.00669646
0.33788928	0.00205522	0.12993951	0.0062613
0.34757246	0.00239566	0.12090139	0.0058605
0.35725563	0.00277674	0.11234318	0.00548963
0.36693881	0.00320157	0.10424756	0.0051449
0.37662198	0.00367338	0.09659758	0.00482307
0.38630516	0.00419551	0.08937656	0.00452136
0.39598833	0.00477141	0.08256815	0.00423732

0.40567151	0.00540467	0.07615635	0.00396883
0.41535468	0.00609896	0.07012543	0.003714
0.42503786	0.00685809	0.06446	0.00347116
0.43472103	0.00768597	0.05914499	0.00323881
0.44440421	0.00858663	0.05416565	0.00301561
0.45408738	0.00956423	0.04950753	0.00280034
0.46377056	0.01062302	0.04515652	0.00259185
0.47345373	0.01176737	0.0410988	0.00238912
0.48313691	0.01300178	0.0373209	0.00219117
0.49282008	0.01433085	0.03380964	0.00199707
0.50250326	0.0157593	0.03055217	0.00180594
0.51218643	0.01729197	0.02753596	0.00161694
0.52186961	0.01893381	0.02474879	0.00142921
0.53155278	0.02068988	0.02217876	0.00124192
0.54123596	0.02256536	0.01981429	0.00105425
0.55091913	0.02456555	0.01764411	0.00086533
0.56060231	0.02669585	0.01565728	0.00067427
0.57028548	0.02896179	0.01384317	0.00048014
0.57996866	0.031369	0.01219146	0.00028196
0.58965183	0.03392325	0.01069216	7.8656E-05
0.59933501	0.0366304	0.0093356	-0.0001309
0.60901818	0.03949643	0.00811241	-0.0003481
0.61870136	0.04252744	0.00701355	-0.0005742
0.62838453	0.04572964	0.0060303	-0.0008109
0.63806771	0.04910937	0.00515424	-0.00106
0.64775088	0.05267306	0.00437729	-0.0013237
0.65743406	0.05642728	0.00369168	-0.0016043
0.66711723	0.06037869	0.00308995	-0.0019047
0.67680041	0.06453408	0.00256496	-0.0022282
0.68648358	0.06890036	0.00210989	-0.0025791
0.69616676	0.07348454	0.00171825	-0.002962
0.70584993	0.07829375	0.00138383	-0.0033831
0.71553311	0.08333524	0.00110079	-0.0038496
0.72521628	0.08861638	0.00086356	-0.004371
0.73489946	0.09414463	0.00066691	-0.0049589
0.74458264	0.09992759	0.00050593	-0.0056286
0.75426581	0.10597297	0.00037601	-0.0064001

0.76394899	0.11228858	0.00027289	-0.0073004
0.77363216	0.11888237	0.00019259	-0.0083663
0.78331534	0.12576237	0.00013147	-0.00965
0.79299851	0.13293677	8.6198E-05	-0.0112275
0.80268169	0.14041383	5.3767E-05	-0.013214
0.81236486	0.14820196	3.1483E-05	-0.0157927
0.82204804	0.15630966	1.6969E-05	-0.0192729
0.83173121	0.16474556	8.1669E-06	-0.02422
0.84141439	0.17351839	3.335E-06	-0.0317854
0.85109756	0.18263702	1.0498E-06	-0.044717
0.88	0.212	0	-0.0590849

Appendix C

ECLIPSE 100 KEYWORDS

Table C.1: *Relavant ECLIPSE 100 Kewords*

Keyword	Description
RUNSPEC	
SURFACT	Activates the Surfactant Model
SURFACTW	Activates the Surfactant Model and enables modeling of changes of wettability
GRID	
RPTGRID	Controls output from the GRID section. Argument KOVERD outputs the K/D values used in the calculation of the capillary number
PROPS	
HWSWL, HWSWLPC, HWSWCR, HWSWU, HWSOWCR, HWSOGCR, HWKRW, HWKRWR, HWKRO, HWKRORW, HWKRORG and HWPCW	Immiscible water-wet saturation end-points.
RPTPROPS	Controls output from the PROPS section. Arguments SURFVISC and so on output surfactant properties.
SURFADDW	Defines weighting between oil-wet and water-wet relative permeabilities as a function of the adsorbed surfactant mass.
SURFADS	Surfactant adsorption isotherm.

ADSORP	Analytical adsorption isotherm with salinity dependence.
SURFCAPD	Surfactant capillary de-saturation data.
SURFROCK	Surfactant-rock properties and adsorption model indicator.
SURFST	Water-oil surface tension in the presence of surfactant.
SURFSTES	Water-oil surface tension as a function of surfactant and salt concentrations.
SURFVISC	Modified water viscosity.
SWL, SWLPC, SWCR, SWU, SGL,SGLPC, SGCR, SGU, SOWCR,SOGCR, KRW, KRWR,KRG, KRGR, KRO, KRORW, KRORG,PCW and PCG	Immiscible oil-wet saturation end-points.
REGIONS	
SATNUM	Defines the region number for oil-wet immiscible saturation function table.
SURFNUM	Surfactant miscible region numbers.
SURFWNUM	Defines the region number for water-wet immiscible saturation function tables and additionally the table describing the wettability as a function of surfactant adsorption (SURFADDW).
SOLUTION	
RPTSOL	Controls output from the SOLUTION sectio. • SOCR outputs the critical oil saturations following a surfactant flood. • SUFRBLK outputs the surfactant concentration as well as water-oil surface tension (both for salinity dependent and salinity independent surface tension).
SURF	Initial surfactant concentrations.

SUMMARY	
ROEIW	(OIP(initial) - OIP(now)) / Initial Mobile Oil with respect to Water
ROE	(OIP(initial) - OIP(now)) / OIP(initial)
ROFT	Inter-region oil flow total (in liquid and wet gas phases)
RWFT	Inter-region water flow total
FPR	Pressure average value
FWIR	Field water injection rate
FWIT	Field water injection rate total
FWPR	Field water production rate
FWPT	Field water production cumulative total
FOPR	Field oil production rate
FOPT	Field oil production total
FTPTSUR	Production Total
FTIRSUR	Injection Rate
FTITSUR	Injection Total
SCHEDULE	
RPTSCHED	Controls output from the SCHEDULE section. Arguments: • FIPSURF: surfactant in place. • SURFADS: adsorbed surfactant concentration. • SURFBLK: surfactant concentrations and the capillary number as well as water-oil surface tension.
RPTRST	Controls output to the restart file. • SURFACT: surfactant concentration. • SURFADS: adsorbed surfactant concentration. • SURFMAX: maximum adsorbed surfactant concentration. • SURFST or (SURFSTES): water-oil surface tension
TUNING	Sets simulator control parameters. Item 11 of Record 2 (TRGSFT) sets the target surfactant change.
WSURFACT	Specifies the surfactant concentration of a water injector.

Appendix D

Grid Images

Figure D.1: *Grid*

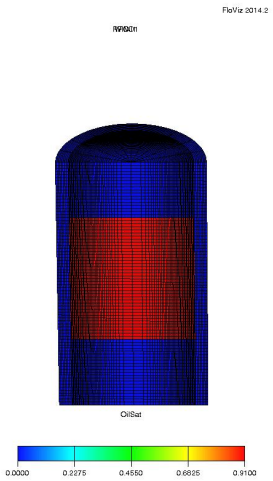

Figure D.2: *Outermost blocks and Core sample*

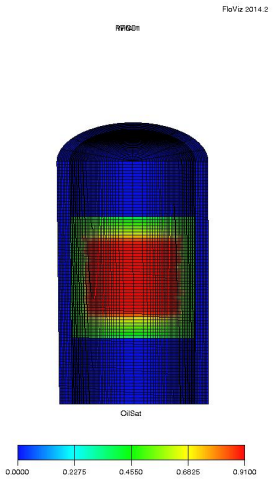

Figure D.3: *SI*

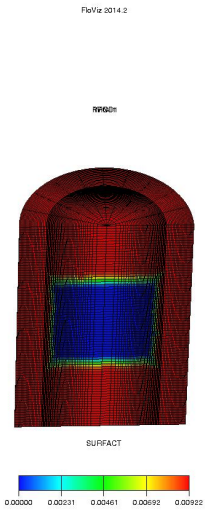

Figure D.4: *Surfactant adsroption*